

## Effect of ATF2 transcription factor on DLL4 gene expression in angiogenesis

Item Type	Thesis or dissertation
Authors	Kalyanakrishnan, Krithika
Publisher	University of Wolverhampton
Rights	Attribution-NonCommercial-NoDerivatives 4.0 International
Download date	2026-03-16 12:33:32
License	<a href="http://creativecommons.org/licenses/by-nc-nd/4.0/">http://creativecommons.org/licenses/by-nc-nd/4.0/</a>
Link to Item	<a href="http://hdl.handle.net/2436/624703">http://hdl.handle.net/2436/624703</a>



**EFFECT OF ATF2 TRANSCRIPTION FACTOR ON *DLL4* GENE  
EXPRESSION IN ANGIOGENESIS**

**KRITHIKA KALYANAKRISHNAN**

**(Student number:1828826)**

A thesis submitted in partial fulfilment of the requirements of the

University of Wolverhampton for the degree of

Master of Philosophy

Research Institute in Healthcare Science

Faculty of Science and Engineering

University of Wolverhampton

November 2021

## **DECLARATION**

This work or any part thereof has not previously been presented in any form to the University or to any other body whether for the purposes of assessment, publication or for any other purpose (unless otherwise indicated). Save for any express acknowledgments, references and/or bibliographies cited in the work, I confirm that the intellectual content of the work is the result of my own efforts and of no other person.

The right of Krithika Kalyanakrishnan to be identified as author of this work is asserted in accordance with ss.77 and 78 of the Copyright, Designs and Patents Act 1988. At this date copyright is owned by the author.

**Signature: KRITHIKA KALYANAKRISHNAN**

**Date: 25/11/2021**

# **ABSTRACT**

**INTRODUCTION:** ATF2 belongs to the AP1 transcription factor family that homodimerize or heterodimerize with other members of the bZIP family and regulates the transcriptional activation of target genes. Previous studies have shown that ATF2 mediates VEGF-induced angiogenic processes but the molecular mechanisms implicating ATF2 as a regulator of angiogenesis and its effect on other angiogenic related genes are largely unknown.

**METHODS:** The sequences of the enhancers and the promoter of the *DLL4*, which is an angiogenic-related gene, were obtained from the ensembl website and using the ConTraV3 R software, the putative binding sites of ATF2 on the regulatory regions of *DLL4* were identified. Among the four enhancers and the promoter regions identified, it was attempted to clone one enhancer sequence in a luciferase-based reporter plasmid. ATF2 functionality was suppressed by infecting HUVEC with an adenovirus expressing a phosphorylation-mutant, dominant-negative version of ATF2 (Ad-ATF2AA). HUVEC infection with an adenovirus encoding GFP (Ad-GFP) was used as a control. Alternatively, ATF2 expression in HUVEC was suppressed by siRNA-mediated knockdown. qPCR was performed to determine the effect of ATF2 functional suppression on the expression of *DLL4*-target genes and other genes related to angiogenesis. A colony of ATF2<sup>flox/flox</sup> mice was established by crossing ATF2<sup>flox/flox</sup> breeders with the intention of a future development of an endothelial-specific ATF2 knockout mice for future *in vivo* studies.

**RESULTS:** *In silico* analysis revealed that ATF2 has potential binding sites on the regulatory regions of the *DLL4* locus suggesting its involvement in the regulation of *DLL4*. HUVEC deficient in ATF2, achieved by overexpression of a mutant protein or knockdown of ATF2, showed a significant increase in the

expression of the Notch ligand *DLL4* in basal and VEGF-stimulated conditions. The gene expression of angiogenic related genes *HEY1* and *NRARP* were also altered, suggesting ATF2 involvement in the regulation of these proteins.

**CONCLUSION:** This study shows that activation of ATF2 is essential for the negative regulation of *DLL4*, *HEY1* and *NRARP*. Interestingly, activation of these Notch-related genes has been reported to have an inhibitory effect on angiogenesis. These results indicate that the negative effect of ATF2 suppression observed in angiogenesis might implicate upregulation of *DLL4*, *HEY1* and *NRARP*.

# CONTENTS

<b>ABSTRACT</b> .....	i
<b>LIST OF FIGURES</b> .....	vii
<b>LIST OF TABLES</b> .....	x
<b>LIST OF ABBREVIATIONS</b> .....	x
<b>ACKNOWLEDGMENTS</b> .....	xiv
<b>1 INTRODUCTION</b> .....	xv
<b>1.1 ANGIOGENESIS</b> .....	1
<b>1.2 CELLULAR BIOLOGY OF ANGIOGENESIS</b> .....	3
<b>1.3 MOLECULAR BIOLOGY OF ANGIOGENESIS</b> .....	5
<b>1.4 ANTI-ANGIOGENIC THERAPY</b> .....	8
<b>1.5 ENDOTHELIAL SIGNAL TRANSDUCTION PATHWAYS ACTIVATED BY VEGF-A</b> .....	9
<b>1.6 ROLE OF ATF2 IN ANGIOGENESIS</b> .....	10
<b>2 HYPOTHESIS AND AIMS</b> .....	13
<b>3 MATERIALS AND METHODS</b> .....	18
<b>3.1 CELL CULTURE</b> .....	19
<b>3.1.1 Tissue culture of HUVEC</b> .....	19
<b>3.1.2 Subculture of adherent cells</b> .....	19
<b>3.1.3 Tissue culture of Human Embryonic Kidney cells (HEK293A)</b> .....	20
<b>3.1.4 Freezing cells</b> .....	20
<b>3.1.5 Recovering cells from liquid nitrogen</b> .....	21
<b>3.1.6 Counting cells</b> .....	21
<b>3.2 TRANSFECTION OF HUVEC USING REPLICATION DEFICIENT ADENOVIRUS VECTORS</b> .....	22
<b>3.2.1 Adenovirus used in this study</b> .....	22
<b>3.2.2 Amplification and purification of adenovirus by infection with HEK293A cells</b> .....	23
<b>3.2.3 HUVEC infection with adenoviral vectors</b> .....	25
<b>3.3 QUANTIFICATION OF GENE EXPRESSION OF RNA LEVEL</b> .....	25
<b>3.3.1 Total RNA isolation</b> .....	25

3.3.2	RNA quantification .....	26
3.3.3	Reverse transcription .....	26
3.3.4	Quantitative real time PCR .....	28
3.4	PROTEIN ISOLATION .....	29
3.5	WESTERN BLOT .....	30
3.5.1	Polyacrylamide gel electrophoresis .....	30
3.5.2	Sample loading.....	31
3.5.3	Transfer of protein to membrane.....	32
3.5.4	Reduction of unspecific binding.....	32
3.5.5	Protein detection using specific antibody .....	32
3.5.6	Image development.....	33
3.6	ISOLATION OF DNA FROM CULTURED CELLS.....	33
3.6.1	Harvesting adherent cells by scraping.....	33
3.6.2	Lysis and RNA removal .....	34
3.6.3	Protein precipitation .....	34
3.6.4	DNA precipitation .....	35
3.7	CLONING .....	35
3.7.1	Primer Preparation .....	35
3.7.2	Precipitation .....	37
3.7.3	Digestion.....	37
3.7.4	DNA gel purification.....	37
3.7.5	Ligation .....	38
3.8	Transformation.....	38
3.9	DNA Maxipreparation .....	39
3.10	METHOD FOR ISOLATION OF GENOMIC DNA FROM MOUSE TAIL .....	40
3.11	PCR CONDITIONS TO GENOTYPE ATF2 FLOXED AND ATF2 WILD TYPE MICE .....	41
3.12	STATISTICAL ANALYSIS.....	42
4	RESULTS .....	43
4.1	WESTERN BLOT ANALYSIS FOR ADENOVIRUS INFECTED CELLS ..	44
4.2	ROLE OF DLL4 IN ANGIOGENESIS.....	45
4.3	BIOINFORMATIC ANALYSIS OF THE DLL4 LOCUS.....	49

<b>4.4 PCR AMPLICAION OF -16 KB, -12 KB AND +14 KB ENHANCER REGION OF THE DLL4 LOCUS .....</b>	<b>55</b>
<b>4.4.1 Preparation of pGL2 promotor for cloning.....</b>	<b>57</b>
<b>4.4.2 Optimisation of PCR reactions to amplify DLL4 enhancer regions .</b>	<b>59</b>
<b>4.5 EFFECT OF ATF2 SILENCING ON GENES DOWNSTREAM TO DLL4 .</b>	<b>62</b>
<b>4.6 EFFECT OF BLOCKAGE OF ATF2 FUNCTIONALITY ON THE EXPRESSION OF DOWNSTREAM TARGET OF DLL4.....</b>	<b>68</b>
<b>4.7 GENOTYPING OF MICE EAR SNIPS SAMPLES.....</b>	<b>74</b>
<b>5 DISCUSSION.....</b>	<b>76</b>
<b>6 CONCLUSIONS .....</b>	<b>85</b>
<b>REFERENCES .....</b>	<b>87</b>

## LIST OF FIGURES

Figure 1.1: Different proangiogenic and antiangiogenic factors .....	2
Figure 1.2: Cellular biology of angiogenesis .....	4
Figure 1.3: Detailed description of the VEGF ligand and its receptors.....	7
Figure 1.4: Calcineurin-NFAT pathway, ERK pathway and MAPK pathway .....	9
Figure 1.5: ATF2 protein structure indicating its phosphorylation sites .....	11
Figure 2.1: Western blot for ATF2 protein with cells stimulated with pro-angiogenic factors.....	14
Figure 2.2: Hypothesis that various pro-angiogenic factors induces the phosphorylation of the ATF2 protein .....	15
Figure 2.3: DLL4 gene expression with overexpression of mutant ATF2 protein .....	16
Figure 3.1: Changes in HUVEC morphology induced by detachment from the tissue culture flask .....	20
Figure 3.2: Cell counting using a haemocytometer .....	22
Figure 3.3: Vectors containing control Ad-GFP and mutant Ad-ATF2AA.....	23
Figure 4.1: Analysis of recombinant protein expression in HUVEC cells infected with adenoviruses Ad-GFP and Ad-ATF2AA.....	45
Figure 4.2: Knockdown of <i>ATF2</i> by siRNA mediated silencing in endothelial cells .....	46
Figure 4.3: Knockdown of <i>ATF2</i> leads to an increase in the VEGF-induced upregulation of <i>DLL4</i> in endothelial cells.....	47
Figure 4.4: Two potential mechanisms (direct or indirect) implicated in the negative regulatory effect exerted by ATF2 in the expression of <i>DLL4</i> .....	48
Figure 4.5: Enhancers of <i>DLL4</i> gene located by (Shah, A., 2017) - previously published data.....	49
Figure 4.6: Putative ATF-2 binding sites identified in the regulatory regions of the <i>DLL4</i> locus .....	50

Figure 4.7: The above 12 predicted binding sites contain the consensus sequence of ATF2.....	55
Figure 4.8: A) Flow diagram of steps involved in the cloning process. B) The cloning procedure of -16 kb enhancer which would serve as the control as it does not contain any putative ATF2 binding site .....	56
Figure 4.9: pGL2 promotor vector image obtained from the 'Promega pGL2 Luciferase reporter vectors manual' .....	57
Figure 4.10: Agarose gel electrophoresis of the digested pGL2 promotor vector	58
Figure 4.11: Agarose gel electrophoresis of the digested -16 kb enhancer insert .....	60
Figure 4.12: Agarose gel electrophoresis of the digested -12 kb enhancer insert .....	62
Figure 4.13: Functional suppression of ATF2 results to no significant change in the VEGF-induced upregulation of <i>Hey1</i> in endothelial cells .....	63
Figure 4.14: Functional suppression of ATF2 results to no significant change in the VEGF-induced upregulation of <i>ID1</i> in endothelial cells .....	64
Figure 4.15: Functional suppression of ATF2 results to no significant change in the VEGF-induced upregulation of <i>NRARP</i> in endothelial cells .....	64
Figure 4.16: Functional suppression of ATF2 results to significant change in the VEGF-induced upregulation of <i>JAG1</i> in endothelial cells.....	65
Figure 4.17: Functional suppression of ATF2 results to no significant change in the VEGF-induced upregulation of <i>LRP1</i> in endothelial cells.....	66
Figure 4.18: Functional suppression of ATF2 results to no significant change in the VEGF-induced upregulation of <i>NPR1</i> in endothelial cells .....	66

Figure 4.19: Functional suppression of ATF2 results to significant change in the VEGF-induced upregulation of <i>VEGFR1</i> in endothelial cells .....	67
Figure 4.20: Functional suppression of ATF2 results to significant change in the VEGF-induced upregulation of <i>VEGFR2</i> in endothelial cells .....	68
Figure 4.21: Functional suppression of ATF2 leads to an increase in the VEGF-induced upregulation of <i>Hey1</i> in endothelial cells .....	69
Figure 4.22: Functional suppression of ATF2 does not alter the VEGF-induced upregulation of <i>ID1</i> in endothelial cells .....	69
Figure 4.23: Functional suppression of ATF2 leads to an increase in the VEGF-induced upregulation of <i>NRARP</i> in endothelial cells .....	70
Figure 4.24: Functional suppression of ATF2 does not alter the VEGF-induced upregulation of <i>JAG1</i> in endothelial cells .....	71
Figure 4.25: Functional suppression of ATF2 does not alter the VEGF-induced upregulation of <i>LRP1</i> in endothelial cells .....	71
Figure 4.26: Functional suppression of ATF2 does not alter the VEGF-induced upregulation of <i>VEGFR1</i> in endothelial cells.....	72
Figure 4.27: Functional suppression of ATF2 does not alter the VEGF-induced upregulation of <i>VEGFR2</i> in endothelial cells.....	73
Figure 4.28: Functional suppression of ATF2 does not alter the VEGF-induced upregulation of <i>NRP1</i> in endothelial cells .....	73
Figure 4.29: Agarose gel electrophoresis performed using the PCR products obtained from mice ear snips .....	75
Figure 5.1: Hypothetical model of the regulation of the c-jun gene expression by	

transcription factor complex containing activated ATF2 by Jin C (2002).....	78
Figure 5.2: Functional suppression of ATF2 results to no significant change in the VEGF-induced upregulation of <i>ATF7</i> in endothelial cells.....	82
Figure 5.3: Functional suppression of ATF2 leads to a decrease in both control VEGF stimulated RNA expression of <i>E-Selectin</i> in endothelial cells .....	83

## LIST OF TABLES

Table 1.1: Diseases caused by abnormal angiogenesis .....	3
Table 3.1. Reagents required for the preparation of retro transcription master mix .....	27
Table 3.2. Reagents required for the preparation of qRT-PCR master mix.....	28
Table 3.3: TaqMan gene expression assays analysed using qRT-PCR .....	29
Table 3.4. Reagents and their respective volumes to prepare resolving gel for western blot using different antibodies.....	30
Table 3.5: Reagents and their respective volumes to prepare stacking gel for western blot using different antibodies.....	31

## ABBREVIATION

- µg- microgram**
- ADP - Adenosine Diphosphate**
- ANG2- Angiopoietin 2**
- ANOVA- Analysis of Variance**
- APS- Ammonium Per Sulphate**
- ATP- Adenosine Triphosphate**
- ATPase- Adenosine Triphosphatase**

**bFGF- basic Fibroblast Growth Factor**  
**BSA- Bovine Serum Albumin**  
**Ca<sup>2+</sup>- Calcium**  
**CAM- Calmodulin**  
**cDNA- Complementary Deoxyribonucleic Acid**  
**CO<sub>2</sub>- carbon dioxide**  
**C<sub>t</sub>- Cycle Threshold**  
**DLL- Delta like ligand**  
**DMEM- Dulbecco's Modified Eagle Medium**  
**DMSO- Dimethyl Sulfoxide**  
**DNA- Deoxyribonucleic acid**  
**DSL- Delta/Serrate/Lag2**  
**EC- Endothelial Cell**  
**ECGM- Endothelial Cell Growth Medium**  
**ECM- Extracellular Matrix Components**  
**EGF- Epidermal Growth Factor**  
**EGFR - Epidermal Growth Factor Receptor**  
**ERK- Extracellular Signal Regulated Kinase**  
**EXP- Experiment**  
**FBS- Fetal Bovine Serum**  
**FGF- Fibroblast Growth factor**  
**GFP- Green Fluorescent Protein**  
**HEY1- Hes-related family bHLH TF**  
**HGF- Hepatocyte Growth Factor**  
**HPRT1- Hypoxanthine Phosphoribosyl transferase 1**  
**HUVECs- Human Umbilical Vein Endothelial Cells**  
**ID1- Inhibitor of DNA binding 1**  
**Ig- Immunoglobulin**  
**IGF-1 - Insulin-like Growth Factor 1**  
**IP<sub>3</sub>- Phosphatidylinositol 3 phosphate**  
**JAG1- Jagged 1**  
**JNK- Jun N-terminal Kinase**  
**kDa- Kilo Dalton**  
**KO- Knock-out**

**LRP1- LDL receptor related protein 1**  
**MAPK- Mitogen Activated Protein Kinase**  
**MAPKK- MAP Kinase Kinase**  
**MAPKKK- MAP Kinase Kinase Kinase**  
**mg- milligram**  
**mL- Millilitre**  
**MMPs- Matrix Metalloproteinases**  
**MOI- multiplicity of infection**  
**mRNA- Messenger Ribonucleic Acid**  
**MW- Molecular Weight**  
**Na<sup>2+</sup>/K<sup>+</sup> ATPase- Sodium Potassium ATPase**  
**NES- Nuclear Export Signal**  
**NFAT- Nuclear Factor of Activated T-Cells**  
**ng- nanogram**  
**NICD- Notch Intra Cellular Domain**  
**NLS- Nuclear Localization Signal**  
**NO- Nitric Oxide**  
**NRARP- NOTCH regulated ankyrin repeat protein a**  
**NRP1- Neuropilin 1**  
**ns- non-significant**  
**PAGE- Polyacrylamide gel electrophoresis**  
**PBS- Phosphate Buffered Saline**  
**PCR- Polymerase Chain Reaction**  
**PDGF- Platelet Derived Growth factor**  
**PDGFR – Platelet Derived Growth Factor Receptor**  
**PECAM-1 -Platelet Endothelial Cell Adhesion Molecule 1**  
**PEDF – Pigment epithelial-derived Factor**  
**PI3K- Phosphatidylinositol-3 Kinase**  
**PIP<sub>2</sub>- Phosphatidylinositol 4,5- bisphosphate**  
**PKC- Protein Kinase C**  
**PLC $\gamma$ - Phospholipase C gamma**  
**PIGF- Placental Growth Factor**  
**qPCR- Quantitative Polymerase Chain Reaction**  
**RPM- Rotations per minute**

**RT PCR- Real time Polymerase Chain Reaction**  
**RTK- Receptor Tyrosine Kinase**  
**SD- Standard Deviation**  
**SDS- Sodium Dodecyl Sulphate**  
**SE- Standard Error of Mean**  
**SELE- Selectin E**  
**siRNA- Small Interfering RNA**  
**TBS- Tris Buffered Saline**  
**TC- Tip cell**  
**TEMED- N,N,N,N'-Tetramethylethylenediamine**  
**TGF $\alpha$ - Transforming Growth Factor alpha**  
**TIMP3- Tissue inhibitor of Metalloproteinase 3**  
**TM- transmembrane**  
**TNF $\alpha$ - Tumour Necrosis Factor alpha**  
**TSP-1- Thrombospondin-1**  
**VCAM-1- Vascular Cell Adhesion Molecule- 1**  
**VEGF- Vascular Endothelial Growth Factor**  
**VE Cadherin- Vascular Endothelial Cadherin**  
**VEGFR- Vascular Endothelial Growth Factor Receptor**  
**VMSC- Vascular smooth muscle cells**  
**WB- Western Blot**  
**WT- Wildtype**

## ACKNOWLEDGEMENTS

I would first and foremost like to thank my supervisor Prof. Angel Armesilla, for his invaluable support and motivation throughout the project. Special thanks for formulating such an inspiring project and methodology. I would like to express my gratitude to Dr. Vinodh Kannappan and Prof. James Cotton for giving me an opportunity to work under the supervision of Prof. Angel Armesilla. I would also like to thank Dr Wolfgang Breitwieser (CRUK-Manchester Institute) for providing the Ad-GFP, Ad-ATF2AA and the ATF2<sup>flox/flox</sup> mice that were used in this study.

I would like to acknowledge my colleagues Reshma Ranjit Immanual, Suhail Ahmed, Kinza Khan, Shervin Najafi, Miebaka L. Ian-Gobo and Jude Flier Ihugba for assisting me in the lab for the entire duration of my project.

I would also like to extend my gratitude to all my colleagues Dr. Sathishkumar Kurusamy, Samna Sagadevan and Gowtham Rajendran for helping me throughout my stay at Wolverhampton.

However, completion of my project would not have been possible without the kind support and help of many individuals and organizations. I would like to extend my sincere thanks to all of them.

Appreciation is due to my friends at University of Wolverhampton and my family members for their constant support and encouragement.

Finally, I would like to thank the almighty for the opportunity to work in my area of interest.

## **1. INTRODUCTION**

## 1.1 ANGIOGENESIS

During the development of an embryo, angioblasts differentiate into endothelial cells resulting in the formation of a primary network of blood vessels. The formation of this primary vascular network is called vasculogenesis. Further, to fulfil the needs of the growing embryo, the vascular network forms new blood vessels to deliver oxygen and nutrients. Reorganisation of the vascular plexus is essential for embryo development. This process of development of new blood vessels from pre-existing vasculature is called angiogenesis. Angiogenesis occurs in various other processes like menstruation, wound healing or in pathological conditions like cancer (Potente M. et al., 2011).

In physiological conditions, excessive or insufficient angiogenesis is prevented by maintaining an equilibrium in the expression of pro- and anti-angiogenic factors respectively (Figure 1.1). Angiogenesis is triggered in the presence of proangiogenic stimuli produced by conditions like a wound, inflammation, hypoxic or ischemic conditions.

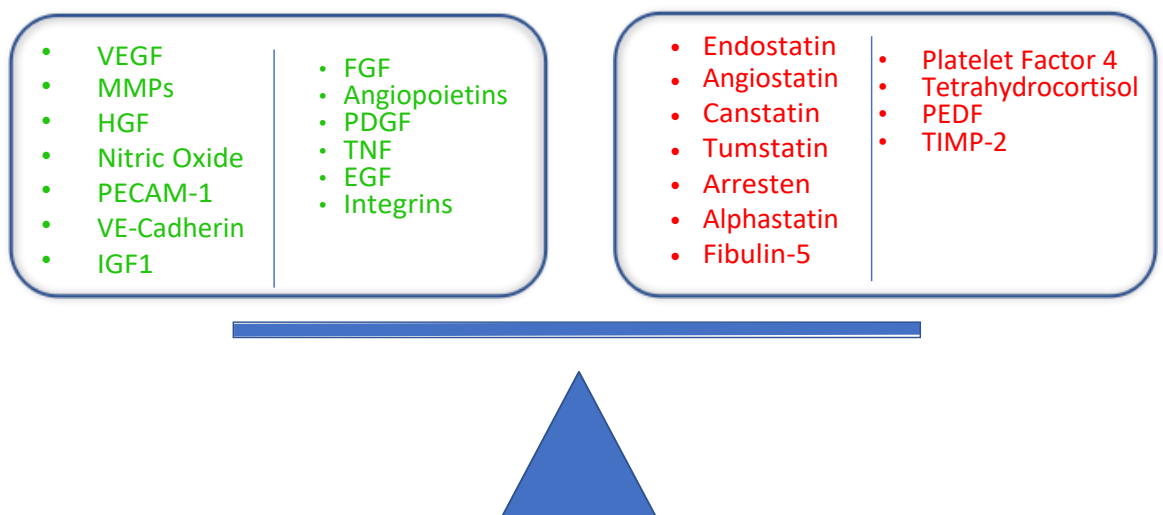


**Figure 1.1: Different proangiogenic and antiangiogenic factors.** Balance between pro- and anti- angiogenic factors is essential in maintaining proper angiogenesis. Here, the pro-angiogenic factors are highlighted in green and the anti-angiogenic factors are indicated in red.

Disruption in this equilibrium of angiogenic factors leads to the development of diseases. The table 1.1 shows a list of diseases associated with abnormal angiogenesis caused by an imbalance between pro- and anti-angiogenic factors.

**Table 1.1:** List of diseases caused by abnormal angiogenesis adapted from Carmeliet (2003) and Carmeliet, P., & Jain, R. K. (2011)

<b>Diseases caused due to excessive angiogenesis</b>	<b>Diseases caused due to insufficient angiogenesis</b>
<ul style="list-style-type: none"> <li>• Vascular malformation</li> <li>• Pulmonary hypertension</li> <li>• Arthritis</li> <li>• Diabetic retinopathy</li> <li>• Obesity</li> <li>• Tumour growth, metastasis</li> <li>• Psoriasis</li> <li>• Ocular neovascularisation</li> <li>• Endometriosis</li> </ul>	<ul style="list-style-type: none"> <li>• Alzheimer’s disease</li> <li>• Hypertension</li> <li>• Atherosclerosis</li> <li>• Stroke</li> <li>• Pulmonary fibrosis</li> <li>• Restenosis</li> <li>• Gastric ulcerations</li> <li>• Myocardial infraction</li> <li>• Peripheral ischemia</li> </ul>

During cancer progression, tumour cells proliferate at an unusual rate. These tumour cells acquire nutrients and oxygen from the adjoining blood vessels. The tumour core becomes hypoxic when the diameter of the tumour increases beyond 2-3 mm. (Forster J.C. et al., 2017). Due to the lack of oxygen, the tumour cells would not survive. To overcome the hypoxic conditions, the cells at the core of the tumour release pro-angiogenic factors like VEGF, bFGF, HGF, etc. that induce endothelial cells to initiate angiogenesis and promote the formation of new blood vessels (Lugano R., 2020). These newly formed vasculature provides oxygen and nutrients to the cancer cells and hence the tumour continues to grow.

## **1.2 CELLULAR BIOLOGY OF ANGIOGENESIS**

Angiogenesis is initiated when there are pro-angiogenic factors in the microenvironment. The presence of these factors induces the endothelial cells to produce molecules that disintegrate the extracellular matrix. This allows the endothelial cells to migrate and proliferate. Two endothelial cells from either end undergo anastomosis to form a mature three-dimensional tube. This suggests that pro-angiogenic factors have a major contribution in the induction of angiogenesis (Jacobs J., 2007). The first step towards the formation of new blood vessels in the presence of pro-angiogenic factors is the initiation process.

This process involves detachment of the pericytes and other mural cells (Figure 1.2). This detachment is stimulated by angiopoietin-2 (ANG2) (Carmeliet, P., & Jain, R. K., (2011). Following the detachment of the pericytes, to facilitate the proliferation of endothelial cells, matrix metalloproteases (MMPs) such as MMP1 are produced which degrade the extracellular matrix. (Huang H., 2010). Altogether, these processes destabilize the tube enabling the endothelial cells to migrate towards the pro-angiogenic factors.

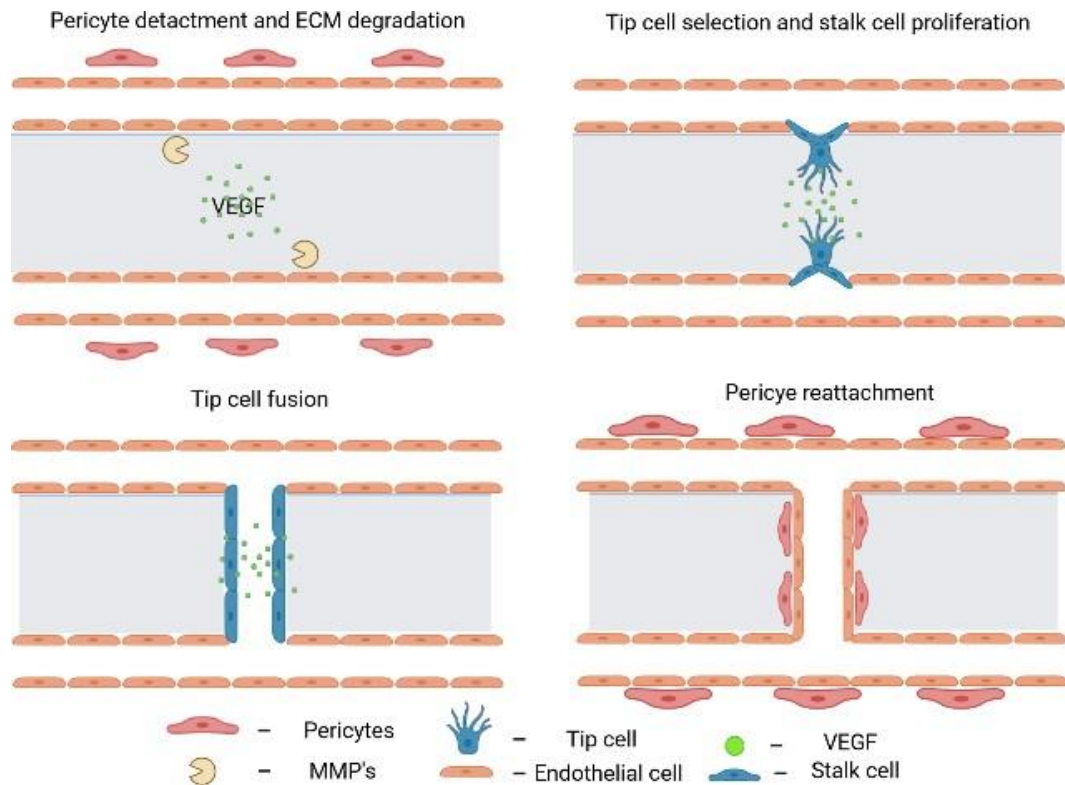


**Figure 1.2: Cellular biology of angiogenesis.** When VEGF is produced in the microenvironment, the cells produce MMPs to digest the ECM and pave a way for the tip cell migration. The stalk cells proliferate and follow the lead of the tip cell. When the two tip cells fuse, they form a lumen.

As a result of the process of initiation, one of the endothelial cells differentiate to form the tip cell while the other cells are called stalk cells. The tip cell selection occurs via the Notch signalling pathway and migrates towards the pro-angiogenic stimuli. The stalk cells proliferate and follow the lead of the tip cell, forming the lumen. When two tip cells come in contact, they undergo anastomosis forming a new vessel (Potente M. et al., 2011). This tube formation is followed by the reattachment of the pericytes to the endothelial cells and the re-establishment of the extracellular matrix around the vessel endothelium (Figure 1.2).

### 1.3 MOLECULAR BIOLOGY OF ANGIOGENESIS

Development of blood vessels through angiogenesis is essential for biological processes like wound healing, embryonic development etc. There are various positive regulators of angiogenesis such as VEGF, bFGF, TGF $\alpha$ , TNF $\alpha$ , HGF etc (Xu L., 2012). Among these, the pro-angiogenic stimulus that play a prominent role in both physiological conditions and in tumour angiogenesis, and that has been intensively studied in the last two decades is VEGF. Previously published data have shown that deletion of a single allele of *Vegf* leads to embryonic death during mice development (Ferrara N. et al., 1996). Similarly, previously published results prove that when VEGF binds to soluble Flt receptors in oxygen induced retinopathic mice models, it results in significantly reduced vascularization (Liu C.H. et al., 2017). This is due to the fact that when VEGF ligand binds to soluble Flt receptors, there is a reduced number of ligands available to bind to the cell surface receptors. This suggests a prominent role for VEGF in the onset and progression of angiogenesis. Hence it is essential to understand in detail the molecular regulation of this molecule (Ferrara N. et al., 2003).

VEGF belongs to the PDGF supergene family which contains seven proteins namely VEGF-A, VEGF-B, VEGF-C, VEGF-D, PlGF, VEGF-E and VEGF-F (Shibuya M., 2011), of which VEGF-A plays a major role in angiogenesis. VEGF-A contains 8 exons separated by 7 introns. Splicing of the VEGF-A gene results in the formation of various isoforms of the ligands such as VEGF-A<sub>206</sub>, VEGF-A<sub>189</sub>, VEGF-A<sub>183</sub>, VEGF-A<sub>165</sub>, VEGF-A<sub>148</sub>, VEGF-A<sub>145</sub> and VEGF-A<sub>121</sub> are generated (Figure 1.3) (Harper S. J., & Bates D. O., 2008). All the above isoforms contain the same region encoded by exon 1-5 and exon 8 contains the region responsible to promote endothelial cell proliferation. The difference in these isoforms is mainly present in exon 6 and 7 which determines their ability to bind

to heparan or heparan sulphate proteoglycans present in the extracellular matrix (Melincovici C.S. et al., 2018). VEGF-A<sub>165</sub> is only partially bound to the ECM as it does not contain exon 6 whereas VEGF-A<sub>121</sub> is acidic and is freely diffusible in the bloodstream. The isoforms VEGF-A<sub>189</sub> and VEGF-A<sub>206</sub> bind to the ECM with higher affinity and hence are less common (Takahashi H., & Shibuya M; 2005). Among the isoforms, VEGF-A<sub>165</sub> is proved to initiate pro-angiogenic pathways resulting in the induction of high levels of angiogenic related genes (Herbert S.P., & Stainier D.Y.; 2011).

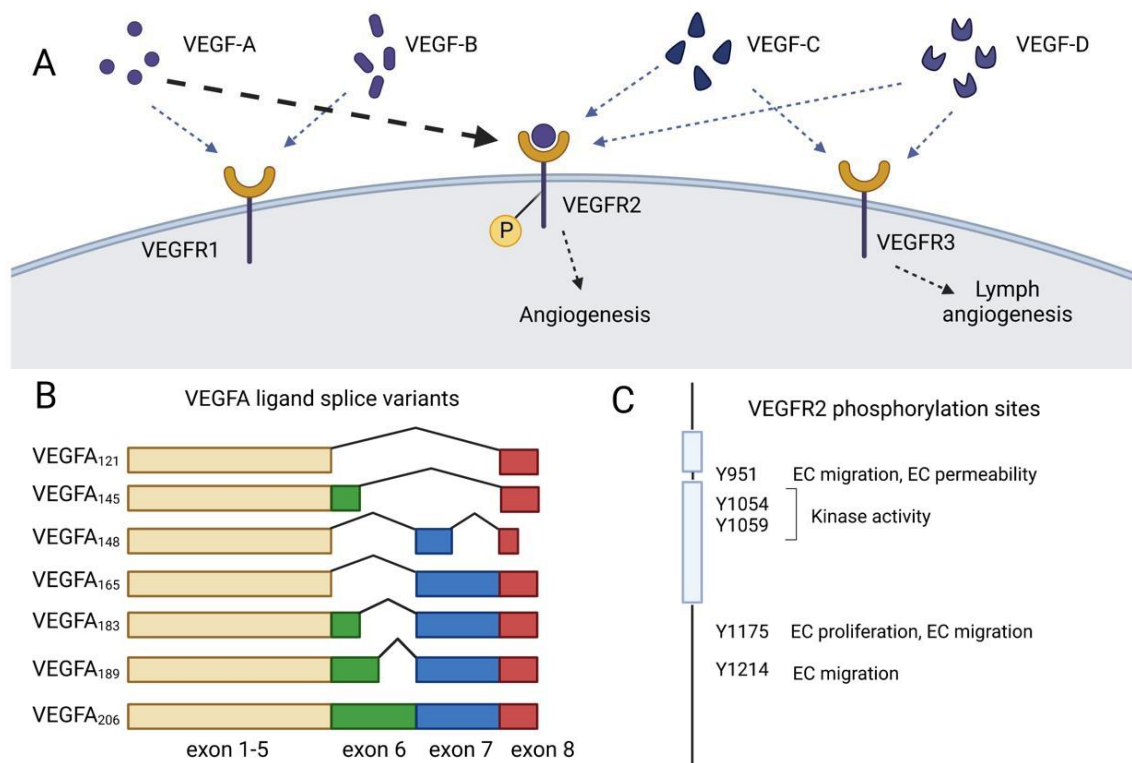


**Figure 1.3: Detailed description of the VEGF ligand and its receptors.** A) Summary of all the VEGF ligands indicating binding to all the possible receptors. The heavy black arrow indicates the highly expressed VEGF ligand in pathological conditions binding to a VEGFR2 that influences angiogenesis. B) The splice variants of VEGF-A ligand as it plays a major role in angiogenesis. C) VEGF -Receptor2 protein indicating the major phosphorylation sites that is essential for process related to angiogenesis.

The VEGF-A ligand and its isoforms shown in Figure 1.3-B bind to one of the type III receptor tyrosine kinases (RTKs) VEGFR-1, VEGFR-2 and VEGFR-3 (Cébe-Suarez et al., 2006). VEGFR1 is considered to be a decoy receptor. The main function of VEGFR1 is to modulate the activation of VEGFR2 by acting as a decoy receptor. VEGFR2 activation is achieved by binding of various VEGF ligands. VEGFR3 activation is achieved by binding VEGF-C and this pathway is important for maintaining the lymph system. Among all the above interactions, binding of VEGF-A<sub>165</sub> to VEGFR2 has been shown to be the main mediator of angiogenesis through activation of downstream signalling cascades such as MAP kinases or the calcineurin/NFAT pathway, among others (Figure 1.4) (Claesson-Welsh L., 2013; Armesilla A.L. et al, 1999).

## 1.4 ANTI-ANGIOGENIC THERAPY

Previously published data show that angiogenesis is essential for tumour growth and metastasis. Hence anti-angiogenic therapy was developed to reduce tumour growth in pathological conditions. Since the most extensively studied pro-angiogenic factor is VEGF, anti-angiogenic drugs namely, sorafenib, sunitinib, pazopanib, axitinib, bevacizumab, etc. were developed. Majority of these drugs target either VEGF ligands or receptors. A humanized monoclonal antibody was developed against VEGF-A ligand which was shown to be efficient when administered with chemotherapy. This drug was named bevacizumab. (Botrel T. et al., 2016). For better efficiency, later bevacizumab was altered which led to the development of ranibizumab, a smaller version of the monoclonal antibody with improved penetration in the tissue. Sorafenib is a multi-kinase inhibitor that either acts on the VEGF or PDGF receptor's phosphorylation or interferes with the activation of MAPKs in the Raf/MEK/ERK pathway. Sunitinib is a small, multitargeted RTK inhibitor that blocks the activation of the receptors of VEGF and PDGF ligands (Gridelli C. et al., 2007). When anti-VEGF drugs like bevacizumab and ranibizumab were administered to patients, the tumours produced other pro-angiogenic factors resulting in the recurrence of tumours. Hence developing and administering drugs targeting individual pro-angiogenic factors is necessary, (Rajabi M., & Mousa S. A.; 2017) but would be a tedious process. In this sense, the identification of an intracellular effector common to signalling pathways activated by several pro-angiogenic factors would constitute an excellent molecular target to design more efficient drugs. Thus, a full characterization of the molecular pathways activated by pro-angiogenic signalling in endothelial cells is an essential pre-requisite to improve anti-angiogenic therapies.

## 1.5 ENDOTHELIAL SIGNAL TRANSDUCTION PATHWAYS ACTIVATED BY VEGF-A

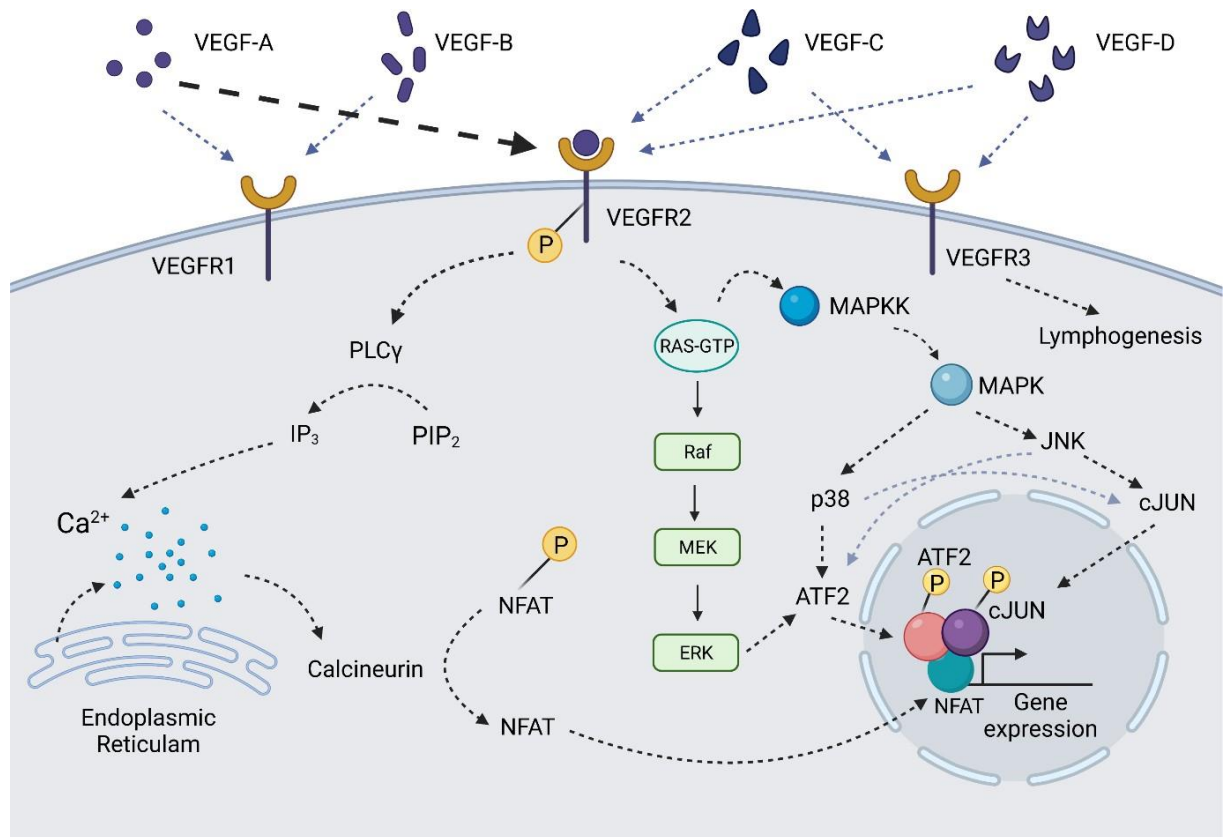


**Figure 1.4: Calcineurin-NFAT pathway, ERK pathway and MAPK pathway.** Activation of various genes related to angiogenesis by the formation of a transcription factor complex. This requires the activation of NFAT pathway, Raf/MEK/ERK pathway and the MAPK pathway to activate NFAT, ATF2 and c-Jun.

Angiogenic signalling involves activation of several effector molecules such as the Activating Transcription Factor 2 (ATF2) and NFAT (Figure 1.4). These molecules are activated when VEGFA binds to VEGFR2. The intracellular domain of the VEGFR2 is phosphorylated at Y1175 which activates Phospholipase Cy (PLCγ). This kinase phosphorylates Phosphatidylinositol 4,5- bisphosphate (PIP<sub>2</sub>) to Inositol 1,4,5-triphosphate (IP<sub>3</sub>). Continuing the signalling cascade, IP<sub>3</sub> induces calcium (Ca<sup>2+</sup>) to be released from the endoplasmic reticulum. Then, the signalling phosphatase calcineurin is activated by increase

in the amount of calcium in the cytoplasm. Activated calcineurin dephosphorylates the Nuclear Factor of Activated T-cells (NFAT). NFAT dephosphorylation promotes translocation to the nucleus and binding to NFAT-binding sites, independently or together with the AP-1 transcription factor complex and regulate NFAT-target genes (Armesilla et al, 1999). Another major pathway activated by the VEGFA/VEGFR2 is the Mitogen Activated Protein Kinase (MAPK) pathway. The MAP3K activates MAPKK, which in turn activates MAPK. The downstream target of this molecule is the p38 and c-JUN N-terminal Kinase (JNK) (Ferrara N et al., 2003). These molecules subsequently activate ATF2 or c-JUN respectively which is phosphorylated and translocated to the nucleus followed by heterodimerization to form the AP-1 transcription factor (TF) complex. Simultaneously, the ATF2 molecule can also be activated by the Raf/MEK/ERK (Rapidly Accelerated Fibrosarcoma/ Mitogen activated protein kinase kinase/ Extracellular signal related kinase) pathway where the Raf is the MAP3K, MEK is the MAPKK and ERK is the MAPK (Ouwens D.M., 2002). This AP-1 transcription factor complex binds to the NFAT molecule and activate various genes (RCAN1.4, COX-2) (Baggott RR,2014) that regulate angiogenesis.

## **1.6 ROLE OF ATF2 IN ANGIOGENESIS**

The ATF2 is a member of the AP-1 transcription factor superfamily. The gene encoding for this protein is located on human chromosome 2 (2q32) (<http://www.ncbi.nlm.nih.gov/gene/1386>). ATF2 plays a major role as a transcription factor. It is ubiquitously present and contributes to DNA damage repair (Lau E. et al., 2012). The homodimerization or heterodimerization of ATF2 with other transcription factors like Jun, Fos or Maf activates a transcription factor

complex (van Dam H., 2001; Papavassiliou et al., 1995). The heterodimerization of ATF2 with other transcription factors occurs as a result of phosphorylation of ATF2 at the Ser121 residue by the protein kinase C (PKC) (Yamasaki T. et al., 2009). ATF2 has a nuclear export sequence (NES) and a bipartite nuclear localization signal (NLS) that facilitate the translocation of ATF2 between the cytoplasm and the nucleus (Figure 1.5). Nuclear export is mainly aided by leucine zipper-NES and a small region at the N-terminus which also contributes to nuclear export (N-NES), although the precise mechanism is unclear (Hsu C. C, 2012). ATF2 molecule is translocated from the nucleus to the cytoplasm and vice versa at a regular basis. Cytoplasmic retention of the ATF2 occurs in disease conditions (Hsu C. C, 2012). Phosphorylation at the Thr52 amino acid by the PKC $\epsilon$  promotes nuclear localization of ATF2 molecule (Watson G. et al, 2017). This promotes dimerization with cofactors resulting in the transcriptional activity of its targets (Lau E., 2012). An auto inhibitory interaction between the zinc finger domain (ZnF) and the leucine zip region (bZip) is generally present in the inactive state of ATF2. Phosphorylation of two threonine residues at the trans-activating domain, Thr 69 by the Ral–RalGDS–Src–p38 pathway and Thr 71 by the Raf- MEK-ERK pathway (Ouwens D.M., 2002) near the N terminal (Figure 1.5) disrupts the auto inhibitory interaction, activating the protein (Watson G. et al, 2017).

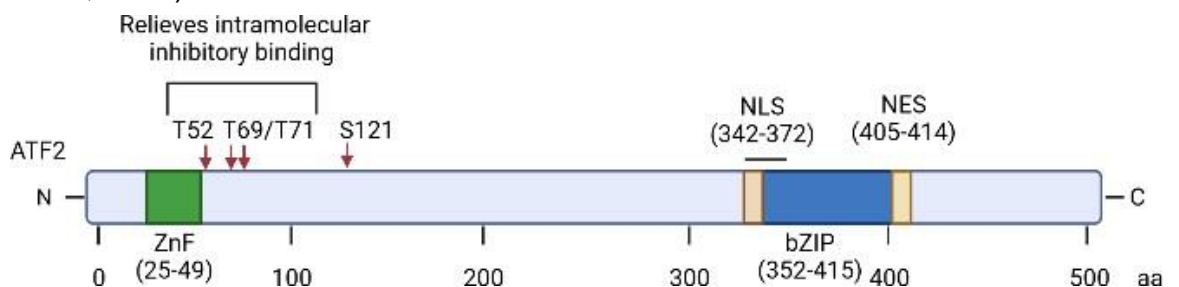


**Figure 1.5: ATF2 protein structure indicating its phosphorylation sites.** (Watson G et al., 2017). The zinc finger domain (indicated in green) is present near the N-terminal and the bZIP domain (indicated in blue) close to the C-terminal. The activation sites Thr69 and Thr71 are present near the ZnF domain.

ATF2 is known to act as a transcription factor that regulates the expression of matrix metalloprotease (MMP-2) (Song H. et al, 2006). Work by Quintero-Fabián S et al, 2019 shows that MMPs are essential in the process of initiation in angiogenesis as they degrade the extracellular matrix, paving the way for migration of the endothelial cells. This suggests that ATF2 might play an important role in regulating the expression of genes related to angiogenesis. In fact, Fearnley G.W. et al (2014) have recently demonstrated that ATF-2 silencing in endothelial cells leads to a significant decrease in VEGF-induced tubular morphogenesis (Fearnley G.W. et al., 2014). Hence, targeting the transcription factor ATF2 could be used therapeutically to decrease VEGF-mediated angiogenesis progression.

## **2. HYPOTHESIS AND AIMS**

Interestingly, preliminary results obtained in Prof Armesilla's laboratory indicate that endothelial ATF2 is activated not only by VEGF but also by other pro-angiogenic factors such as basic Fibroblast Growth Factor (bFGF), Epidermal Growth Factor (EGF) and Hepatocyte Growth Factor (HGF) (Figure 2.1, unpublished results).

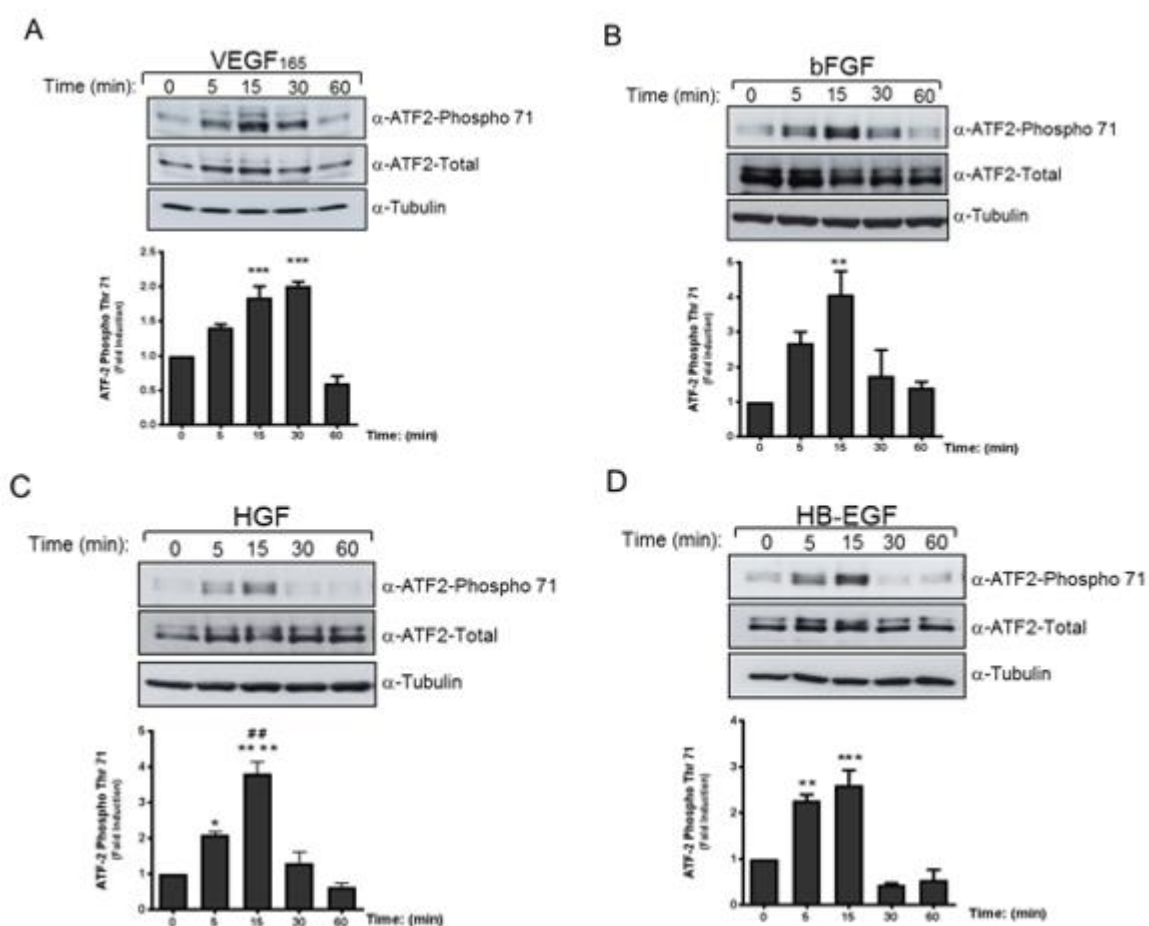


**Figure 2.1: Western blot for ATF2 protein with cells stimulated with pro-angiogenic factors.** HUVEC cells were stimulated with pro-angiogenic factors for various time intervals. Western blot analysis was performed with three different antibodies. Western blot with tubulin antibody was used as the loading control. The total ATF2 antibody and the ATF2-p71 antibody was used to investigate if pro-angiogenic factors influence the activation of ATF2 protein. \*\*-  $p < 0.01$ , \*\*\*-  $p < 0.001$  and \*\*\*\*-  $p < 0.0001$  indicates statistical significance when comparing cells stimulated with pro-angiogenic factors for up to 3 hours.

This finding suggests that ATF2 might act as a common effector shared by several intracellular signalling pathways activated by a variety of pro-angiogenic factors. It was hypothesized that ATF2 might represent an ideal molecular target

to block intracellular signalling activated by several pro-angiogenic factors and to avoid the evasion problems currently observed when treating cancer patients with bevacizumab and other anti-VEGF drugs (Figure 2.2).

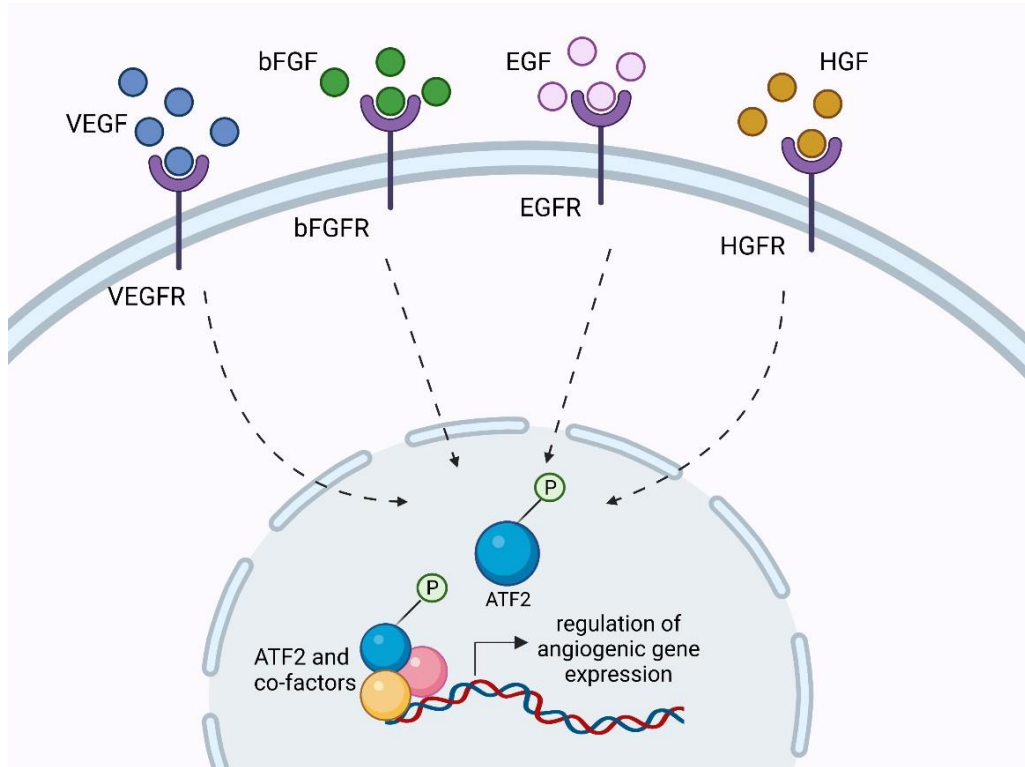


**Figure 2.2: Hypothesis that various pro-angiogenic factors induces the phosphorylation of the ATF2 protein and other co activators which further influence angiogenic related genes.**

In this sense, one of the lines of research currently carried out in Professor Armesilla's laboratory at the University of Wolverhampton is focused on the characterisation of the ATF2-target genes upregulated by pro-angiogenic stimuli in endothelial cells. Previous unpublished results in Armesilla's laboratory have shown that overexpression of an activation-deficient mutant of ATF2 in endothelial cells results in a significant enhancement of the VEGF-induced expression of *DLL4* (Figure 2.3, Suhail Ahmed and Prof. Angel Armesilla, unpublished observations).

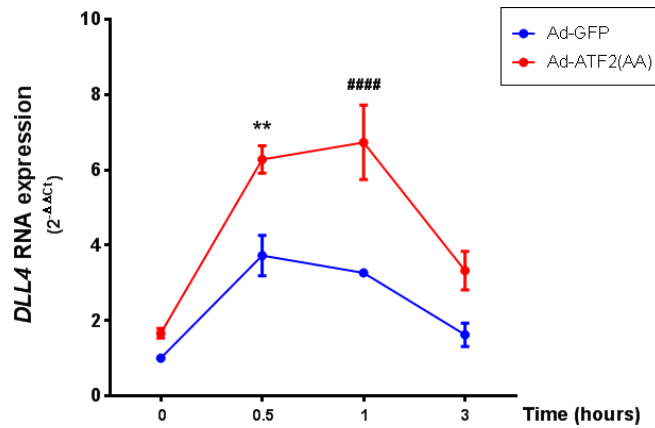


**Figure 2.3: DLL4 gene expression with overexpression of mutant ATF2 protein.** HUVEC cells were infected with Ad-ATF2AA, a dominant negative mutant of ATF2 where Ad-GFP infected cells were maintained as control. These cells were stimulated with VEGF (25 ng/mL) for up to 3 hours. The statistical method used to determine the significance is the Tukey test. \*\* -  $p < 0.01$  and #### -  $p < 0.0001$  indicates statistical significance when comparing cells transfected with Ad-GFP or Ad-ATF2AA and stimulated with VEGF of up to 3 hours.

DLL4 is a key member of the Notch signalling pathway. This pathway plays a major role during the differentiation of endothelial tip cells from stalk cells. The Notch signalling family is formed by five DSL ligands (DLL1, 3, 4, Jagged 1, 2) which bind to four Notch receptors (Notch1, 2, 3 and 4). DLL4 is one of the notch ligands expressed in the endothelial cells of vertebrates (Kuhnert F., 2011). Knockout of *DLL4* in mice results in embryonic lethality or severe vascular defects in a small percentage of mice that are born (Krebs, L. T., 2004). The vascular defect in these mice is characterised by excessive angiogenesis. This, and other studies, have identified DLL4 as an inhibitor of angiogenesis (Ridgway J et al., 2006).

Given the prominent role of DLL4 in the regulation of angiogenesis, in this project, the overall aim was to further investigate the role of ATF2 in the expression of *DLL4* and *DLL4*-target genes during the angiogenic process. For this purpose, the following objectives have been established for this study:

- To express a phosphorylation mutant, inactive version of ATF2 in primary human umbilical vein endothelial cells (HUVEC) using replication-incompetent adenoviral vectors.
- To knockdown the expression of *ATF2* in primary HUVEC by siRNA-mediated silencing.
- To investigate the functional consequences of blocking ATF2 function in the expression of DLL4-target genes in HUVEC stimulated with VEGF.
- To identify putative ATF2-binding sites in the regulatory regions of *DLL4* gene by bioinformatic analysis of the promoter and enhancer sequences.

### **3. MATERIALS AND METHODS**

## **3.1 CELL CULTURE**

### **3.1.1 Tissue culture of HUVEC**

Human Umbilical Vein Endothelial Cells (HUVEC) were purchased from Cellworks Ltd. and grown in Endothelial Cell Growth Medium (ECGM) (PromoCell, Heidelberg, Germany) supplemented with 2% FBS, 0.4% endothelial cell growth supplement, 0.1 ng/ml epidermal growth factor (recombinant human), 1 ng/ml basic fibroblast growth factor (recombinant human), 90 µg/ml heparin, 1 µg/ml hydrocortisone, and 1% penicillin/streptomycin/amphotericin B (Sigma-Aldrich, UK). ECGM medium supplemented as described will be hereafter called ECGM complete.

### **3.1.2 Subculture of adherent cells**

Cells were generally cultured in T175 tissue culture flasks. When cells reached confluency, they were detached from the flask and split equally into two different flasks. For this procedure, two T175 flasks were coated with 10 ml of 0.1% gelatin which would act as a replacement for extracellular matrix for the cells to adhere in *in-vitro* conditions. The media from the confluent culture was aspirated and the cells were washed with 1X PBS to remove the excess media between the cells. 3 ml of a 0.25% trypsin-EDTA solution (Sigma-Aldrich) was added to the cells and the flask was tapped gently to aid the cells to detach. Attached endothelial cells show a cobblestone-like morphology (Figure 3.1, left panel) whereas detached cells become round (Figure 3.1, right panel). To nullify the effect of trypsin after the cells have detached, 7 ml of ECGM complete was added to the cell solution so that the serum inactivates the trypsin. The cells were transferred to a falcon tube and centrifuged at 1310 g for 5 mins. The supernatant was discarded and the pellet was resuspended in fresh ECGM complete media that was split between two flasks pre-coated with 0.1% gelatin in a final volume of 30

ml of ECGM complete. Cells were incubated at 37°C, 5% CO<sub>2</sub> in a humidified incubator until reaching confluency.

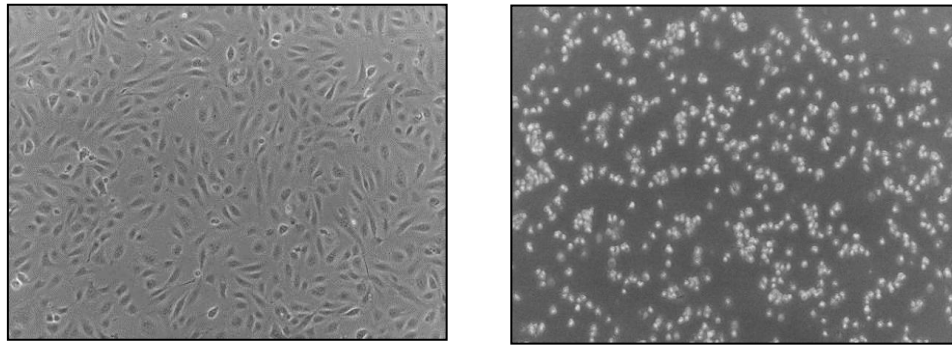


**Figure 3.1: Changes in HUVEC morphology induced by detachment from the tissue culture flask.** Microscopy images of HUVEC before (left panel) and after detachment (right panel) from the flask by incubation in a 0.25% Trypsin-EDTA solution. Images were recorded using a Nikon DSFi1 digital camera coupled to a Nikon ECLIPSE TS100 microscope at 10x magnification.

### **3.1.3 Tissue culture of Human Embryonic Kidney 293A Cells (HEK293A)**

Human Embryonic Kidney 293A cells were purchased from Cellworks and cultured in Dulbecco's modified Eagle's medium (DMEM) which is supplemented with 10% FBS and 1% penicillin/streptomycin/amphotericin B (Sigma-Aldrich). The media is referred to as DMEM complete. This cell line has a stably integrated copy of the E1 proteins which is required to amplify deactivated adenoviral vectors.

### **3.1.4 Freezing cells**

Cells can be frozen for later use with the help of freezing solution. This solution is prepared by adding 10% DMSO in FBS. After the cells are trypsinised from the flask, the cell suspension is centrifuged. 1ml of the freezing solution is added to the cell pellet. The Eppendorf is carefully wrapped in tissue and stored in -80°C. For long term storage, the Eppendorf tube is transferred and stored in liquid nitrogen.

### **3.1.5 Recovering cells from liquid nitrogen**

When cells are recovered from the liquid nitrogen, only 40% of the cells will be viable. The solution is thawed and then transferred to 10 ml of media. This media is then transferred to the respective flask, dropwise. The flask is incubated at 37°C overnight. The media is replaced the following day to remove the damaging effects of DMSO.

### **3.1.6 Counting cells**

To conduct experiments, a specified number of cells are required according to the size of the plate. To plate a required number of cells, a haemocytometer was used to count the number of cells in a given volume of tissue culture media. After the cells were detached using trypsin, as described above, the cell pellet was resuspended in 10 ml of fresh tissue culture media and a small aliquot is taken in an Eppendorf tube. The cell solution was placed in the chamber formed by the coverslip and the haemocytometer slide, and the number of cells in one of the grids formed by 16 squares (Figure 3.2) was counted. To increase accuracy, counting was repeated in another 16-square grid and the average calculated. The number of cells in the cell suspension was determined as following:

$$\text{Number of cells in a 16-square grid} \times 10^4 = \text{Number of cells/ml of cell suspension}$$

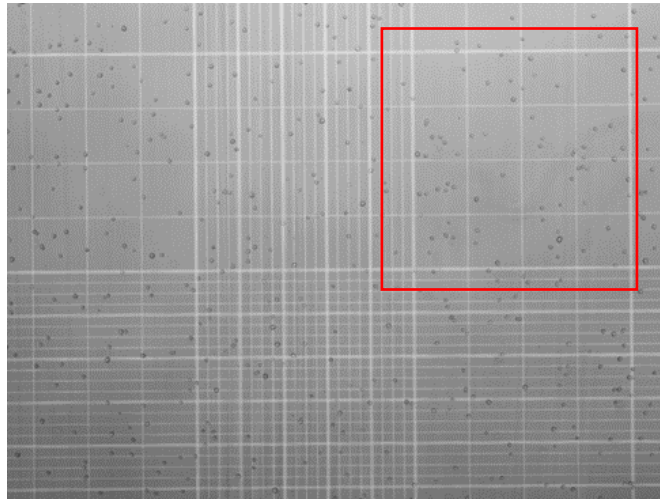


**Figure 3.2: Cell counting using a haemocytometer.** The red outlined square indicates the 16-square grid area where number of cells were counted. Image was recorded using a Nikon DSFi1 digital camera coupled to a Nikon ECLIPSE TS100 microscope at 10x magnification.

## **3.2 TRANSFECTION OF HUVEC USING REPLICATION-DEFICIENT ADENOVIRAL VECTORS**

### **3.2.1 Adenovirus used in this study**

Recombinant-deficient adenoviruses used in this study (Figure 3.3); Ad-GFP (encoding the Green Fluoresce Protein) and Ad-ATF2AA (encoding a mutant version of ATF2 where amino acids threonine 69 and threonine 71 have been mutated to alanine) have been previously described (Gozdecka M et al, 2014) and were a generous gift by Dr Wolfgang Breitwieser (CRUK-Manchester Institute).

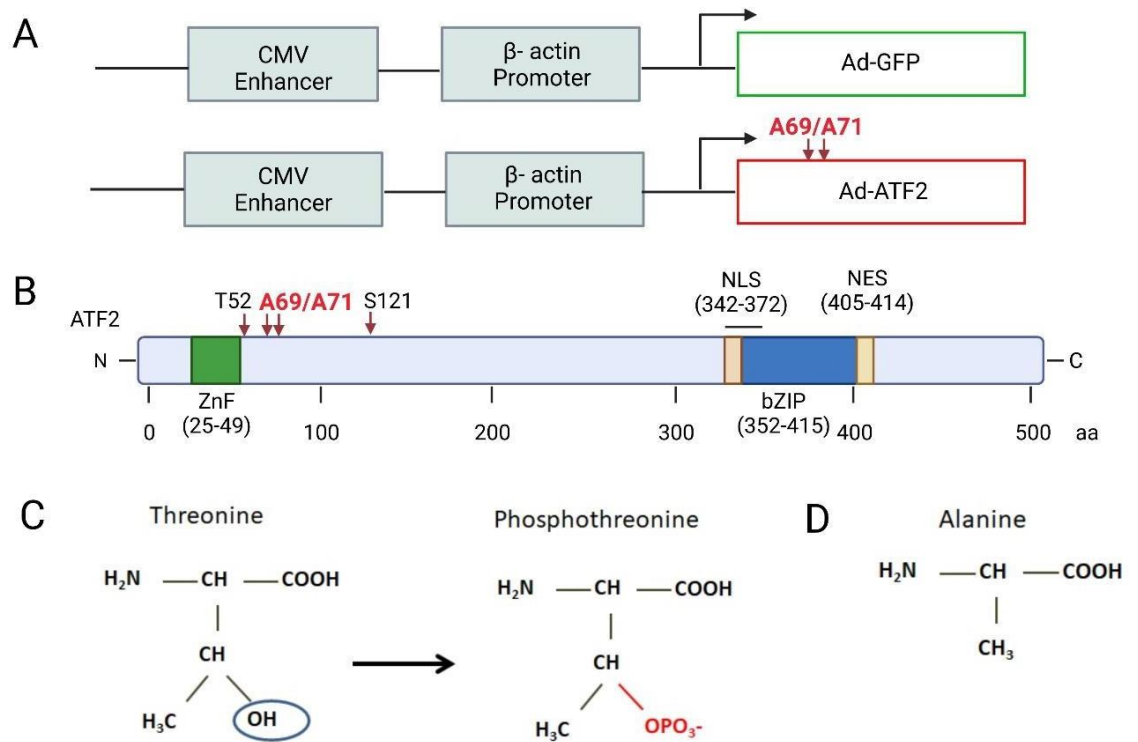


**Figure 3.3: Vectors containing control Ad-GFP and mutant Ad-ATF2AA.** A) Recombinant adenovirus such as Ad-GFP and Ad-ATF2AA. B) The mutant version of ATF2 present in the Ad-ATF2AA where the 69 and the 71 base pairs containing threonine are replaced with alanine. C) Phosphorylation of the threonine occurs at the hydroxyl group at 69 and 71 position in the wild type ATF2 protein. D) Alanine contains no hydroxyl group and hence cannot be phosphorylated in the mutant form of the ATF2 protein (ATF2AA)

### 3.2.2 Amplification and purification of adenovirus by infection of HEK293A cells

Adenoviral amplification was carried out by infecting HEK293A cells with secondary adenoviral stock. Usually, for large scale amplification, 12 tissue culture T175 flasks of HEK293A cells at 80-90% confluency were infected with 50  $\mu$ l/flask of secondary stock. Secondary stock was originally prepared by Dr Breitwieser following the instructions of the Dual Adenovirus Expression System (Takara). One additional T175 flask of HEK293A was left uninfected as negative control.

The flasks were checked regularly to see if HEK293 cells showed cytotoxic signs of viral infection. Detachment of cells is an indication that the cells are infected with virus. The infected cells also differ in morphology from the triangular-shape attached cells as they appeared under the microscope as refringent, round-shape cells. Flaks were maintained in incubation without changing the medium until 80% of the cells were floating (indication that most of the cells were infected). The culture medium was then transferred to a 50 ml tube and centrifuged at 1638 g for 5 minutes at room temperature to collect the cells harbouring multiple copies of viral particles inside. The supernatant was discarded and 5 ml of 1X PBS was added without resuspended the pellet to avoid damaging the cells and losing viral particles. The cell pellet was washed in 1X PBS by gently tapping the bottom of the tube to float the pellet. The solution was centrifuged at 1638 g for 5 minutes, and the PBS discarded. The pellet was resuspended with 0.5 ml 1X PBS per flask. The cell suspension was then transferred to a Falcon tube and an equal volume of chloroform is added. The solutions were gently mixed by tube inversion for 5 minutes and then centrifuged at 3276 g for 15 minutes. After centrifugation, three layers can be seen in the falcon tube; the bottom layer contains the chloroform, the middle layer contains cell debris, and the top layer is the aqueous phase containing the viral particles. The top aqueous phase with the virus was gently collected, aliquoted in cryogenic vials, and stored in -80°C until further use. Titration to calculate the number of infectious particles was determined using the "Tissue culture infection method" as described by Pickard, A (Pickard 2007). In brief, HEK293-A cells were infected with serial dilutions of the viral solution and titre calculated by identifying the end point viral dilution inducing cytotoxic effect in at least 50% of the cells.

### **3.2.3 HUVEC infection with adenoviral vectors**

Low passage HUVEC were plated on a 6-well tissue culture plate at a density of  $3 \times 10^5$  cells/well and cultured overnight. The following day, cells were infected with adenoviral vectors at a multiplicity of infection (MOI) of 200 by incubation in the presence of adenoviral particles for 72 hours at 37°C, 5% CO<sub>2</sub> in a humidified incubator.

## **3.3 QUANTIFICATION OF GENE EXPRESSION AT RNA LEVEL**

### **3.3.1 Total RNA isolation**

Media was removed from the HUVEC cells cultured on a 6-well plate, and cells were washed with 1X PBS. The plate was tilted a few times and the PBS removed completely. Total RNA was isolated using a “Total RNA Purification Plus Kit” (Norgene) according to the manufacturer’s recommendations. In brief, cells were lysed in 300 µl of “RL Buffer”. The lysis solution was added to release the contents of the cell including RNA, DNA, proteins etc. The plates were tilted from side to side to cover the entire well and the lysate containing the components of the cell along with the cell debris was completely transferred to an Eppendorf tube. These samples can be stored at -80°C for RNA isolation.

To eliminate genomic DNA, the lysate was added into gDNA Columns provided in the kit and passed throughout the columns by centrifugation for 1 minute at 14197 g. Once the DNA was eliminated, the solution was treated with 200 µl of 100% ethanol and vortexed briefly for approximately 10 seconds. Once vortexed, the solution was transferred to a “RNA purification column” placed inside 2 ml collection tubes and passed throughout the column by centrifugation for 1 minute at 14197 g, at room temperature. After centrifugation, the waste was discarded from the collection tubes and the column washed with 400 µl of “PE Wash Buffer”

by centrifugation at 14197 g for 1 minute at room temperature. The waste from the collection tube was discarded. Washing was repeated twice more. Finally, the columns were centrifuged another time to remove the washing buffer completely from the column.

The column was transferred to a new, nuclease-free Eppendorf tube and 40 µl of RNA elution buffer was added on top of the resin. After incubation for 1 minute at room temperature, the columns were centrifuged at 2184 g for 2 minutes, and again at 14197 g for 1 minute. The extracted RNA was transferred to a fresh nuclease-free Eppendorf tube and stored at -80°C until further use.

### **2.3.2 RNA quantification**

The purified RNA was quantified using a NanoDrop 2000 spectrophotometer (Thermo Scientific, UK). The elution buffer from the RNA isolation kit (see above) was used as blank. RNA concentration was calculated considering that 1 optical density unit of absorbance corresponds to 40 µg/µl of RNA. RNA purity was determined by calculating the ratio of absorbance at 260nm and 280nm.

### **2.3.3 Reverse transcription**

Reverse transcription is a process to convert the isolated RNA to cDNA. For retro-transcription, 500 ng of RNA were diluted in nuclease-free water to final volume of 10 µl.

Reverse transcription was performed using a “High-capacity cDNA reverse transcription kit” (Applied Biosystems, UK). Briefly, a master mix was prepared using the following reagents provided in the kit; retro-transcription RT buffer which maintains the pH, 25x dNTP mix which contains dATP, dTTP, dCTP and dGTP,

Random primers, RNase inhibitor, and Multiscribe Reverse Transcriptase according to the conditions shown in Table 3.1

**Table 3.1.** Reagents required for the preparation of retro transcription master mix

Solutions in the Master mix	Volume for one sample
10x RT buffer	2 $\mu$ l
25x dNTP mix (100mM)	0.8 $\mu$ l
10x RT Random primer	2 $\mu$ l
Multiscribe Reverse Transcriptase	1 $\mu$ l
RNase Inhibitor	1 $\mu$ l
Nuclease free water	3.2 $\mu$ l
<b>Total Volume</b>	<b>10<math>\mu</math>l</b>

After preparing the master mix, it was placed on ice and mixed gently. 10  $\mu$ l of the master mix was added to 10  $\mu$ l of the RNA sample in a fresh Eppendorf tube. The Eppendorf tube was briefly centrifuged to bring down the contents and to eliminate the air bubbles.

The samples were then loaded on a thermal cycle programmed to alter the temperature at the following time intervals

- 25°C for 10 minutes
- 37°C for 120 minutes
- 85°C for 5 minutes
- 4°C until the samples are collected

cDNA samples were diluted with 80  $\mu$ l of nuclease-free water and stored at -20°C until further use in qPCR reactions.

### 3.3.4 Quantitative Real-Time PCR (qRT-PCR)

RNA levels of each gene were determined by qPCR using TaqMan Gene Expression Assays (Thermofisher, UK) with FAM reporter. For each gene to be analysed, a master mix was prepared as described in Table 3.2.

**Table 3.2.** Reagents required for the preparation of qRT-PCR master mix

				1x
Taqman Primers	Gene	Expression	Assay	1µl
Polymerase mix				10µl
dH <sub>2</sub> O				3.4µl

14.4 µl/well of qPCR master mix were added to a Microamp fast optical 96-well reaction plate (Applied biosystems, UK) followed by 5.6 µl of the cDNA sample. PCR plate was sealed with MicroAmp® Optical Adhesive Film (Thermofisher, UK) and then centrifuged at 900 rpm for 1 minute to bring down all the contents. The plate was placed on ice until loaded on a 7500 Fast Real-Time PCR System (Applied Biosystems, UK). Reactions were run at the following conditions:

- Initial enzyme activation step at 95°C for 10 minutes
- 40 cycles of denaturation at 95°C for 15 seconds and anneal/extension at 60°C for 60 seconds.

Results were analysed using the comparative cycle threshold  $2^{-\Delta\Delta C_t}$  method using *HPRT1* as an endogenous control gene.

TaqMan Gene Expression Assays used in this study are detailed in Table 3.3

**Table 3.3:** TaqMan gene expression assays analysed using qRT-PCR

Taqman Primers	ID Assays
<b>DLL4 (Delta like ligand 4)</b>	<i>Hs00184092_m1</i>
<b>HEY1 (Hes-related family bHLH TF)</b>	<i>Hs05047713_s1</i>
<b>ID1 (Inhibitor of DNA binding 1)</b>	<i>Hs03676575_s1</i>
<b>NRARP (NOTCH regulated ankyrin repeat protein a)</b>	<i>Hs04183811_s1</i>
<b>JAG1 (Jagged 1)</b>	<i>Hs01070032_m1</i>
<b>LRP1 (LDL receptor related protein 1)</b>	<i>Hs00233856_m1</i>
<b>VEGFR1 (fms related tyrosine kinase 1)</b>	<i>Hs01052961_m1</i>
<b>VEGFR2 (Kinase insert Domain Receptor)</b>	<i>Hs00911700_m1</i>
<b>NRP1 (Neuropilin 1)</b>	<i>Hs00826128_m1</i>
<b>ATF2 (Activating Transcription Factor 2)</b>	<i>Hs01095345_m1</i>
<b>ATF7 (Activating Transcription Factor 7)</b>	<i>Hs00232499_m1</i>
<b>HPRT1(hypoxanthine phosphoribosyltransferase 1)</b>	<i>Hs99999909_m1</i>

### 3.4 PROTEIN ISOLATION

Experiments for western blot analysis were carried out by culturing cells in 6 well plates. The cells were subjected to appropriate stimulation and then lysed using 100 µl of 1x NuPAGE protein loading buffer (Novex). The protein loading buffer disrupts the cell membrane and solubilises the protein. Lysate was then transferred to a sterile Eppendorf tube which is heated at 100°C for 10 minutes to denature and disrupt the DNA. Lysates were stored at -80°C for further use.

### 3.5 WESTERN BLOT ANALYSIS

Western Blotting is a technique used to separate and identify proteins from a mixture, based on their molecular weight. The protein mixture is loaded on a polyacrylamide gel along with pre-stained protein markers and then proteins are separated by electrophoresis.

#### 3.5.1 Polyacrylamide Gel Electrophoresis (PAGE)

The polyacrylamide gel contains two parts, a lower part that separates the proteins (resolving gel) and an upper part that concentrates the samples (stacking gel) to obtain sharp bands of proteins during subsequent separation.

The percentage of acrylamide/bis-acrylamide used to prepare the resolving gel depends on the length of the protein. If the protein is large the percentage of the gel used decreases. For instance, the protein Green Fluorescent Protein (GFP) is about 28 kDa and hence 12% concentration gel was prepared whereas the Activating Transcription Factor 2 (ATF2) is about 69 kDa and hence 8% concentration gel was used. Ammonium Persulfate (APS) is a compound used along with TEMED (Tetramethylethylenediamine) to catalyse the polymerisation of acrylamide to form the gel. Resolving gel was prepared as shown in Table 2.4

**Table 3.4.** Reagents and their respective volumes to prepare resolving gel for Western Blot analysis using different antibodies.

	Resolving gel %		
	12% (GFP)	10% (Tubulin)	8% (ATF2)
<b>Distilled water</b>	4.525ml	5.5ml	6.5ml
<b>Acrylamide/Bis-acrylamide (30% stock solution)</b>	5.6ml	4.7ml	3.75ml
<b>Resolving buffer (Geneflow Limited)</b>	3.75ml	3.75ml	3.75ml
<b>Ammonium Persulfate (10% stock)</b>	100µl	100µl	100µl
<b>N,N,N,N-Tetramethylethylenediamin (TEMED)</b>	80µl	80µl	80µl

After addition of TEMED, the solution was immediately transferred between 2 glass plates using a standard twin-plate mini gel unit system (SCIE-PLAS). Then, butanol was used to remove the bubbles and level the surface of the resolving gel. Once the resolving gel polymerised, the butanol layer was removed and the surface of the gel washed with water several times to remove any traces of butanol. Finally, the water was removed completely using filter paper. The resolving gel was allowed to polymerize while the stacking gel is prepared. Stacking gel was prepared as shown in Table 3.5

**Table 3.5:** Reagents and their respective volumes to prepare stacking gel for Western Blot using different antibodies

<b>Distilled water</b>	6.1ml
<b>Acrylamide/ Bis-acrylamide (30% stock solution)</b>	1.4ml
<b>Stacking gel buffer (Geneflow Limited)</b>	2.5ml
<b>Ammonium Persulfate (0.1% stock)</b>	100µl
<b>N,N,N,N-tetramethylethylenediamine(TEMED)</b>	80µl

Stacking gel solution is quickly transferred between the plates and placed on top of the resolving gel. A comb is placed in the stacking gel solution to form wells. Once the stacking gel solution has polymerized, the comb is quickly and carefully removed without damaging the wells. If the wells were disfigured, a small piece of vertical filter paper is used to re-shape the wells.

### 3.5.2 Sample Loading

Before loading the samples, they are heated at 100°C for 2 minutes and cooled down on ice to denature the proteins. To remove the condensation caused by the heat shock, samples were briefly centrifuged before loading. 15 µl of BLUeye

protein ladder (GeneFlow, UK) and 15 µl of SeeBlue® pre-stained protein ladder (Thermofisher) was loaded as markers of protein molecular weight. Gels were run in a container immersed in “running buffer” (0.025M Tris, 0.192M Glycine, 0.1% SDS) at 150V until the mixture of protein markers was clearly separated.

### **3.5.3 Transfer of the Proteins to Membrane**

Once the proteins were separated on the gel based on the molecular weight, the proteins were transferred to a membrane. A PDVF membrane was cut to the required size and briefly placed in methanol to hydrate it. The methanol was then removed by washing the membrane several times with deionised water. For the transfer process, the membrane was placed on top of the gel, and gel and membrane were sandwiched between four layers of Whatman 3 MM chromatography paper and sponges on either side of the gel and placed in a transfer apparatus immersed in transfer buffer (0.025M Tris, 0.192M Glycine, 20% methanol). Transfer of proteins to the membrane took place at 35 volts for 90 minutes.

### **3.5.4 Reduction of Unspecific Binding**

Once the proteins had been transferred to the membrane, the membrane was carefully removed from the transfer apparatus and incubated for one hour in 5% skimmed milk solution in TBS-T (TBS-0.05% Tween 20) to prevent binding of antibody to unspecific regions and thereby reduce the background.

### **3.5.5 Protein Detection using Specific Antibodies**

To identify ATF2, GFP or tubulin, an anti-ATF2 rabbit polyclonal antibody (New England Biolabs), an anti-GFP (D5.1) XP rabbit monoclonal antibody (Cell Signalling) or an anti-tubulin mouse monoclonal antibody (Sigma) respectively, were dissolved in TBS-T at 1:1000 concentration and the membrane was incubated in this solution overnight on a shaker at 4°C. After incubation, the

membrane was thoroughly washed four times with TBS-T for five minutes. Primary antibodies raised in rabbit were detected using a 1:5000 solution of HRP-conjugated anti-rabbit immunoglobulin secondary antibody prepared in TBS-T. Primary antibodies raised in mouse were detected using a 1:5000 solution of HRP-conjugated anti-mouse immunoglobulin secondary antibody prepared in TBS-T. The membrane was incubated with the solution containing the secondary antibody for three hours at room temperature on a shaker. Then, the membrane was thoroughly washed with TBS-T five times for five minutes.

### **3.5.6 Image Development**

The PVDF membrane was placed on a cling film (Bacofilm Pvc) and the loading markers were marked to identify the protein size. For antibody detection using the ECL method, the membrane was incubated in 2 ml of ECL solution for 1 minute at room temperature. ECL solution was prepared by mixing 1 ml of solution A and 1 ml of solution B from an EZ-ECL chemiluminescence detection kit (GeneFlow, UK). After incubation, solution was drained off, and signal detected by exposing the membrane in the dark to a Kodak BioMax MS auto-radiographic film (Sigma-Aldrich, UK) for different times, and subsequent film development.

## **3.6 ISOLATION OF DNA FROM CULTURED CELLS**

### **3.6.1 Harvesting adherent cells by scraping**

The cells were cultured in a T175 flask until they were completely confluent. A minimum of  $1 \times 10^7$  cells were required to isolate DNA. The media was gently aspirated, and the cells were rinsed with 8 ml of cold 1X PBS. The PBS was removed and 3 ml per  $1 \times 10^7$  cells of Cellular Lysis Buffer from a "DNA isolation

kit for cells and tissue" (Roche, Germany) was added. The monolayer of cells was immersed in Cellular Lysis Buffer and a cell scraper was used to scrape the cells to the bottom of the flask. The lysis buffer containing the cells was transferred to a centrifuge tube.

### **3.6.2 Lysis and RNA removal**

The buffer containing the cells was then homogenised using a Dounce glass homogenizer, and then, 2µl of Proteinase K solution from "DNA isolation kit for cells and tissue" (Roche, Germany) was added to remove the contaminating proteins. The sample was vortexed for 2-3 seconds to mix the Proteinase K in the suspension. The solution was then placed at 65°C in a water bath for 2 hours as the optimal temperature for the highest activity of Proteinase K is 65°C. The sample was removed, and the cap loosened to release the pressure. 100 µl of RNase solution from a "DNA isolation kit for cells and tissue" (Roche, Germany) was added to the sample to degrade the RNA. The sample was vortexed for 2-3 seconds to mix the RNase solution into the suspension. Then, it was placed at 37°C for 15 minutes which can be extended up to 1 hour.

### **3.6.3 Protein Precipitation**

After incubation, 1.2 ml of protein precipitation solution from a "DNA isolation kit for cells and tissue" (Roche, Germany) was added and vortexed for 5-10 seconds. The sample was then placed on ice for 5 minutes to help the precipitation of the protein followed by centrifugation at 16381 g for a minimum of 20 minutes at room temperature. Lower centrifugation speeds results in loose protein pellets. Then, the supernatant containing the DNA was transferred to a new centrifuge tube.

### 3.6.4 DNA Precipitation

For DNA precipitation, 0.7x volumes of isopropanol was added to the samples. The tubes were gently inverted to mix the upper and lower phases. The sample was then centrifuged at 16381 g for 10 minutes. Then the supernatant was discarded and 250 µl of TE buffer was added. The samples were stored at 4°C for later use.

## 3.7 CLONING

### 3.7.1 Primer preparation

Oligonucleotides specific for the target sequence to be cloned were purchased and resuspended in nuclease free water. The regions of the *DLL4* gene to be cloned were amplified by PCR using the following conditions:

Reagents used for amplification of -16 kb enhancer insert:

10 µl of 10.12 ng/µl concentrated human gDNA isolated as described above

1 µl of 100 ng/µl solution forward primer (For -16 kb enhancer) –

CTTCGCGGTACCCTCAACCTCCAGCCCCCTCCC

1 µl of 100 ng/µl solution reverse primer (For -16 kb enhancer) –

CTTCGCCTCGAGCCGGAGCACCTGAGCCAATGG

10 µl of 5X GC enhancer (ThermoFisher)

3 µl of nuclease free water

25 µl of PCR 2X SuperFi master mix

Reagents used for amplification of -12 kb enhancer insert:

10 µl of 10.12 ng/µl concentrated human gDNA isolated as described above

1 µl of 100 ng/µl solution forward primer (For -12 kb enhancer) –

CTTCGCGGTACCCCTGGGGCTTCTCTCAAGCTG

1 µl of 100 ng/µl solution reverse primer (For -12 kb enhancer) –

CTTCGCCTCGAGAGCAGCCAGGGTGAGGCCGCC

10 µl of 5X GC enhancer (ThermoFisher)

3 µl of nuclease free water

25 µl of PCR 2X SuperFi master mix

The 5X GC enhancer buffer was only added since the target sequence has high GC island content.

Oligonucleotide  $T_m$  was calculated according to the following formula

$$T_m = [(A+T) \times 2] + [(G+C) \times 3]$$

Hence the following conditions were used for PCR amplification of the -16 kb enhancer of the human *DLL4* gene

98°C for 2 minutes

35 cycles of 98°C for 30 seconds

52°C for 1 minute

72°C for 2 minutes

72°C for 10 minutes

For -12 kb enhancer amplification, I used the following conditions

98°C for 2 minutes

35 cycles of 98°C for 30 seconds

51°C for 1 minute

72°C for 2 minutes

72°C for 10 minutes

20% of the PCR product was analysed by DNA gel agarose electrophoresis after adding DNA loading buffer (Sigma). The electrophoresis gel prepared depends on the length of the cloned product. Since -16kb enhancer is short (400bp) 1% agarose gel was used and for -12 kb enhancer (1500 bp), a 0.7% agarose gel.

### **3.7.2 Precipitation**

To the PCR product obtained earlier, 10% of Sodium acetate solution was added along with 2.5x volumes of 100% Ethanol. This solution was incubated overnight at -20°C. The following morning the solution was centrifuged at 14197 g at 4°C to pellet the precipitated DNA.

### **3.7.3 Digestion**

The pellet obtained after precipitation was resuspended in the following solution:

64µl of nuclease free water

10µl of Buffer A (Promega)

10µl of 10X Bovine Serum Albumin (BSA)

6µl of restriction enzyme KpnI (Promega)

10µl of restriction enzyme XhoI (Promega)

The above mixture was incubated overnight in a water bath at 37°C. The following day, 1% agarose gel was prepared to perform electrophoresis. Using UV light, the bands were identified, cut out and gel purified.

### **3.7.4 DNA Gel Purification**

The gel containing the band was placed in an Eppendorf tube. 600 µl of solubilization buffer was added and the mixture placed at 50°C for 10 minutes to

solubilise agarose. The solution was vortexed for 2 minutes until the gel liquifies. Then, 200µl of isopropanol was added and mixed by inversion. The entire solution is transferred to a gDNA column and centrifuged for 1 minute at 14197 g. 500µl of solubilization buffer was added again and centrifuged at 14197 g for 1 minute. To wash the column containing the DNA, 750µl of was buffer was added and the column centrifuged at 14197 g for 1 min (twice). The column was then placed in a separate Eppendorf tube and 20µl of elution buffer was added. DNA eluted from the column was recovered by centrifugation at 14197 g for 1 minute.

### **3.7.5 Ligation**

Ligation reactions were set up as follows: vector, insert, distilled Nuclease-free water, ligase buffer 1X (New England Biolabs), T4 DNA Ligase ( $2 \times 10^6$ U/ml) (New England Biolabs) to a final volume of 20µl. Samples were incubated at 15°C overnight in a thermal cycler.

## **3.8 TRANSFORMATION**

Luria-Broth was prepared by adding 2.5% LB powder to distilled water. To prepare LB-agar plates, 1.5% of agar was then added to the broth. The previously prepared LB agar was heated in the microwave until it melts and placed in a hot water bath for 10 minutes at 50°C. The concentration of ampicillin in the agar was 100 µg/ml. 25 ml of media was added to each plate and allowed to solidify. Later, its placed in the incubator at 37°C, inverted to prevent condensation. For transformation of a ligated plasmid in bacteria using the “heat-shock” method, the plasmid of interest was added to competent E.coli JM109 cells (transformation efficiency  $10^8$  cfu/µg) (Promega, UK) and cooled down on ice for 30 minutes. Then, the solution was heated in a water bath at 42 for exactly 2 minutes. The

solution containing the bacteria and the plasmid was supplemented with 0.3 ml of LB and placed in a 37°C incubator with shaking for 1 hour. L-rod was prepared using a Pasteur pipette. 100 or 400 µl of the solution with transformed bacteria were spread onto LB-ampicillin agar plates and incubated at 37°C overnight. The next day, an individual colony was used to inoculate 10 ml of LB broth, and the culture incubated at 37°C overnight. Grown cultures were used for DNA miniprep to verify the presence of plasmid containing the insert in the isolated bacterial colony.

### **3.9 DNA MAXIPREPARATION**

Maxiprep is performed for one bacterial colony at a time. A colony is picked up from the LB agar plate and inoculated in a new Falcon tube containing 9ml of LB broth and 1ml of 100 ng/µl ampicillin for 2 hours until the bacteria reach log phase. The bacterial suspension was transferred to 400 ml LB broth and incubated in a shaker at 37°C, overnight. The following day, the suspension was centrifuged at 3500 rpm for 10 minutes. The supernatant was discarded and the pellet suspended in 10 ml of Resuspension buffer (P1, Qiagen Plasmid Maxi kit). The P1 buffer containing the cells was transferred to a new, smaller centrifuge tube. 10ml of Lysis buffer (P2, Qiagen Plasmid Maxi kit) was added to lyse the cells and mixed by inversion. Following buffer P2, Neutralization buffer (P3, Qiagen Plasmid Maxi kit) was added to neutralise the effect of P2 and mixed by inversion. The tubes were centrifuged at 4500 rpm for 10 minutes to precipitate the chromosomal DNA. A Qiagen column was equilibrated by 10ml of equilibration buffer. The supernatant containing the plasmid, after precipitation of chromosomal DNA, was added to the column. The plasmid DNA is retained by

the resin in the column. The column was washed with washing buffer, twice. Then, 15ml of elution buffer was added to elute the plasmid DNA from the resin into a new centrifuge tube. The plasmid DNA was precipitated from the elution buffer by adding 10.6ml isopropanol, mixed by inversion and centrifuged at 9600 rpm for 1 hour. The supernatant was discarded swiftly from the centrifuge tube and the pellet re-suspended in 300µl of nuclease free water. Finally, the concentration of the plasmid DNA was measured by nanodrop.

### **3.10 METHOD FOR ISOLATION OF GENOMIC DNA FROM MOUSE TAIL**

The mice ear snip samples were collected and placed in an Eppendorf tube in 200µl of lysis buffer (50mM Tris, 100mM EDTA, 0.5% SDS). To this, 10µl of 10 mg/ml solution of Proteinase K (DNA isolation kit for cells and tissue, Roche, Germany) was added and the mixture was incubated at 56°C overnight. The following day, samples were centrifuged at 14197 g for 10 minutes. The supernatant, containing the cell lysis products, was transferred to another Eppendorf tube. 300 µl of isopropanol was added to precipitate the DNA and the sample inverted multiple times (approximately 30 times) and incubated on ice for 30 minutes. After incubation on ice, the sample was centrifuged at 14197 g for 5 minutes to pellet the DNA. The DNA pellet was washed with 100 µl of 70% ethanol and centrifuged. The ethanol was discarded and the pellet was air dried. Depending on the size of the pellet (the amount of DNA present), the pellet was resuspended in 50 – 500 µl of TE buffer (10mM Tris pH 7.5, 1mM EDTA pH=8).

### **3.11 PCR CONDITIONS TO GENOTYPE ATF2-FLOX OR ATF2-WILD TYPE MICE**

The mice ear snip samples were obtained from our collaborators from the University of Manchester. The PCR product of the fragment amplified from genomic DNA isolated from wild type mice was 195 bp in length, whereas the fragment amplified from DNA isolated from mutant ATF2-floxed mice was 230bp in length.

The sequences of the forward and the reverse primer used for mouse genotyping were:

The following products were used to perform the PCR:

10 µl of isolated genomic DNA from mice tail

Master mix - 1 µl of 100 ng/µl solution forward primer  
(TCAGATAAAGCCAAGTCGAATCTGG)

1 µl of 100 ng/µl solution reverse primer  
(TCTGGTACAACACTGTAGGACT)

13 µl of nuclease free water

25 µl of Polymerase mix (MyTaq HS Red mix, Bioline)

This PCR mixture was then placed in the Thermo Fisher thermal cycler and programmed to alter the temperatures at the following intervals:

95°C for 1 minute

For 35 cycles - 95°C for 30 seconds

46°C for 30 seconds

72°C for 30 seconds

72°C for 5 minutes

4°C until the samples are removed

These samples were then stored at -20°C and then used for further experiments.

### **3.12 STATISTICAL ANALYSIS**

The results for the qRT-PCR were shown as mean  $\pm$  SE. Two-way Anova with post-hoc Tukey test was used to analyse samples with more than two groups and two independent variables. The post-hot Tukey test is used to compare the means of various groups.  $P < 0.05$  was set as statistically significant.

## **4. RESULTS**

## **4.1 WESTERN BLOT ANALYSIS FOR ADENOVIRUS INFECTED CELLS**

A Western Blot experiment was performed to determine the infection efficiency of adenovirus in HUVEC cells. In the following experiments, HUVEC cells were infected with Ad-GFP containing the green fluorescent protein and Ad-ATF2AA which produces the dominant negative mutant form of the ATF2 protein. Cells were incubated for two days in the presence of the virus and then lysed directly using protein lysis buffer. Protein analysis by Western Blot showed significant expression of recombinant ATF2-AA protein in the Ad-ATF2AA infected cells when compared to cells infected with control Ad-GFP (Figure 4.1). This is because the Ad-GFP infected cells express only the endogenous wild type ATF2 protein whereas the Ad-ATF2AA infected cells also express large amounts of the functionally mutated form of the ATF2 protein along with the wild type ATF2. To demonstrate infection by control Ad-GFP, expression of the GFP protein was also analysed in the protein lysates. As expected, GFP could be detected in control samples but not in lysates isolated from cells infected with Ad-ATF2AA (Figure 4.1).

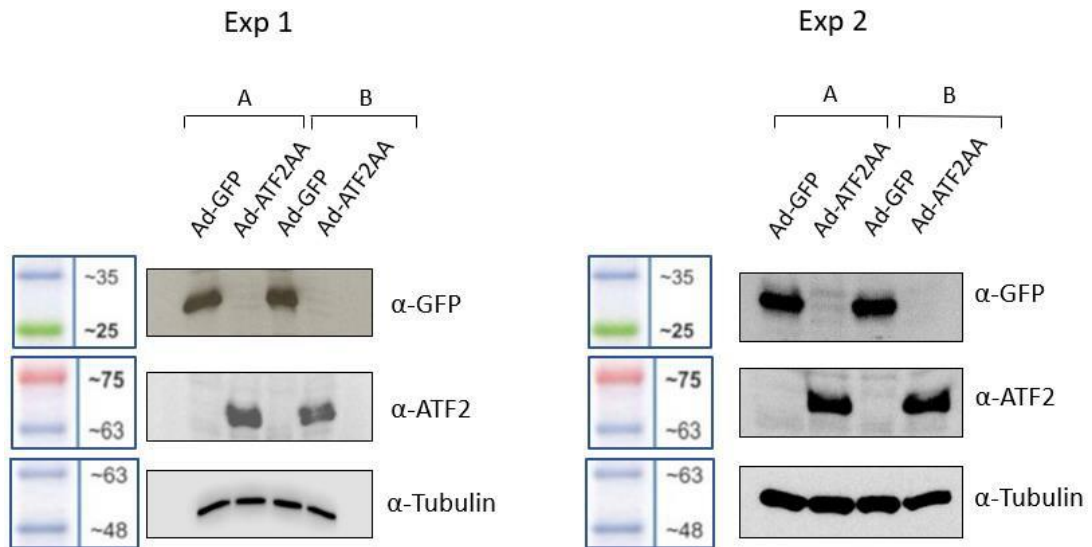


**Figure 4.1: Analysis of recombinant protein expression in HUVEC cells infected with adenoviruses Ad-GFP and Ad-ATF2AA.** Western blot analysis of GFP ( $\alpha$ -GFP), ATF2AA ( $\alpha$ -ATF2) and tubulin ( $\alpha$ -tubulin) expression in HUVEC cells infected with adenovirus as indicated. Infection with Ad-ATF2AA results in overexpression of the ATF2-AA protein compared to endogenous wild type ATF2 present in control Ad-GFP infected cells. Western blot for tubulin was performed as a loading control. The above results were obtained from two independent experiments performed in duplicate (set A and set B) in each experiment. Blueye pre-stained protein ladder markers (GeneFlow) were used for molecular weight identification.

## 4.2 ROLE OF DLL4 IN ANGIOGENESIS

As highlighted in the introduction (page 19), previous results in Prof Armesilla's laboratory have shown that expression of ATF2AA, a function-defective mutant of ATF2, results in an increase of *DLL4* gene expression (Figure 2.3). The DLL4-Notch signalling pathway helps in differentiation of the tip cell from the stalk cells. There are five DSL ligands (*DLL1*, 3, 4, *Jagged 1*, 2) which bind to four Notch receptors (Notch 1, 2, 3 and 4). DLL4 is one of the Notch ligands expressed in the endothelial cells of vertebrates (Kuhnert F., 2011). Earlier studies have reported that knockout of *dll4* in mouse animal models leads to severe vascular defects and, in many cases, death of embryos during development (Krebs, L. T., 2004). Reports from several groups have shown that DLL4 deletion leads to excessive angiogenesis, suggesting that DLL4 plays a key role as an inhibitor of angiogenesis which is necessary for proper branching of blood vessels and

perfect development of the vascular plexus. Therefore, it could be assumed that the altered expression of *DLL4* in endothelial cells lacking functional ATF2, might be one of the reasons of the decrease in angiogenesis observed by Fearnly G.W. et al (2014).

Fearnly G.W. et al. used siRNA-mediated technology to eliminate ATF2 functionality in endothelial cells. Whereas, experiments in our laboratory demonstrate an enhancement of *DLL4* gene expression in cells expressing the ATF2AA dominant negative. Therefore, to confirm that enhancement of *DLL4* expression could be related to the observations described in Fearnly G.W. et al., expression of the *DLL4* gene in HUVEC cells transfected with an siRNA specific for human ATF2 (siATF2) and stimulated with VEGF was analysed. Expression of ATF2 was significantly silenced in siATF2-transfected cells when compared to that in control cells transfected with a control siRNA, siNon-Target (siNT), that does not target any mammalian known genes (Figure 4.2).

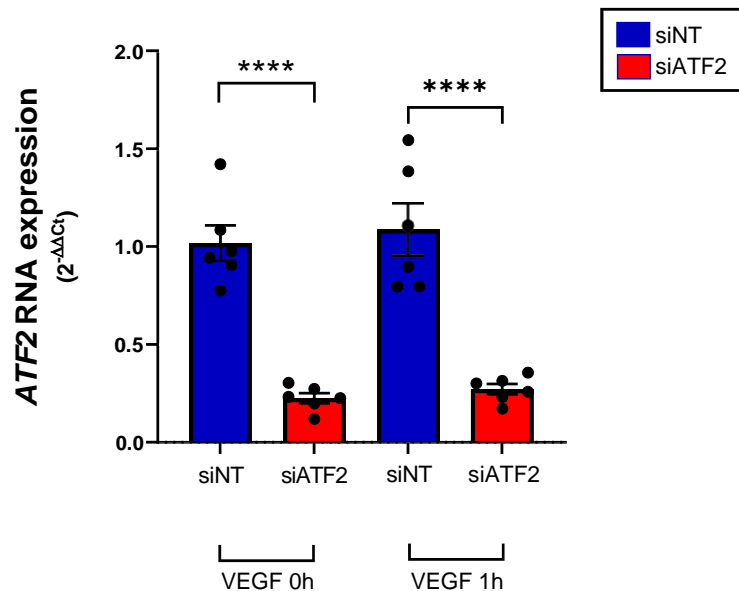


**Figure 4.2. Knockdown of ATF2 by siRNA mediated silencing in endothelial cells.** HUVEC were transfected with siRNA targeting ATF2 gene (siATF2) and non-specific siRNA (siNT). Transfected cells were left unstimulated (control) or stimulated with VEGF (25 ng/mL) for 1 hour. qPCR analysis of ATF2 RNA expression is shown. Values are expressed using the  $2^{-\Delta\Delta C_t}$  method referred to unstimulated HUVEC transfected with siNT. Histograms represent mean  $\pm$  SEM (n=6). Differences in gene expression were evaluated using Two-way ANOVA with Tukey's multiple comparisons post-hoc test. \*\*\*\* $p < 0.0001$  indicates statistical significance when comparing cells transfected with siNT or siATF2 in control or VEGF-stimulated conditions.

Further analysis confirmed that, similar to the results obtained using ATF2AA overexpression, ATF2 silencing also led to a significant enhancement in the expression of *DLL4* in VEGF-stimulated HUVEC cells (Figure 4.3).

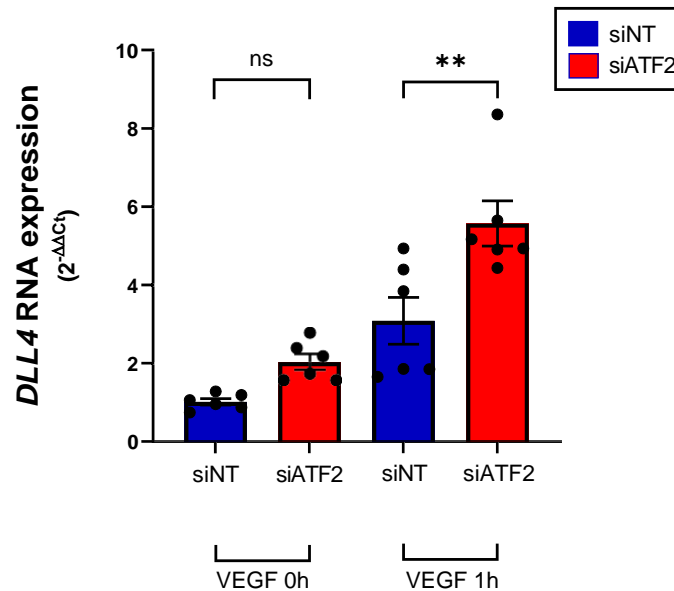


**Figure 4.3: Knockdown of *ATF2* leads to an increase in the VEGF-induced upregulation of *DLL4* in endothelial cells.** HUVEC were transfected with siRNA targeting *ATF2* gene (siATF2) and non-specific siRNA (siNT). Transfected cells were left unstimulated (0 hours) or stimulated with VEGF (25 ng/mL) for 1 hour. qPCR analysis of *DLL4* RNA expression is shown. Values are expressed using the  $2^{-\Delta\Delta C_t}$  method referred to unstimulated HUVEC transfected with siNT. Histograms represent mean  $\pm$  SEM (n=6). Differences in gene expression were evaluated using Two-Way ANOVA with Tukey's multiple comparisons post-hoc test. \*\* $p < 0.01$  indicates statistical significance when comparing cells transfected with siNT or siATF2, and stimulated with VEGF of upto 1 hours. ns = non-significant.

These results suggest that lack of functional *ATF2* activity in endothelial cells alters *DLL4* expression leading to a decrease in angiogenesis. However, the mechanism underlying regulation of the *DLL4* gene by *ATF2* is not clear currently. It is uncertain if the negative effect of *ATF2* in *DLL4* expression is due to direct binding of *ATF2* to the regulatory regions of the *DLL4* locus, or if it is caused by an indirect effect due to *ATF2* triggering the expression of a repressor factor that in turn binds to the regulatory regions of the *DLL4* gene (Figure 4.4).

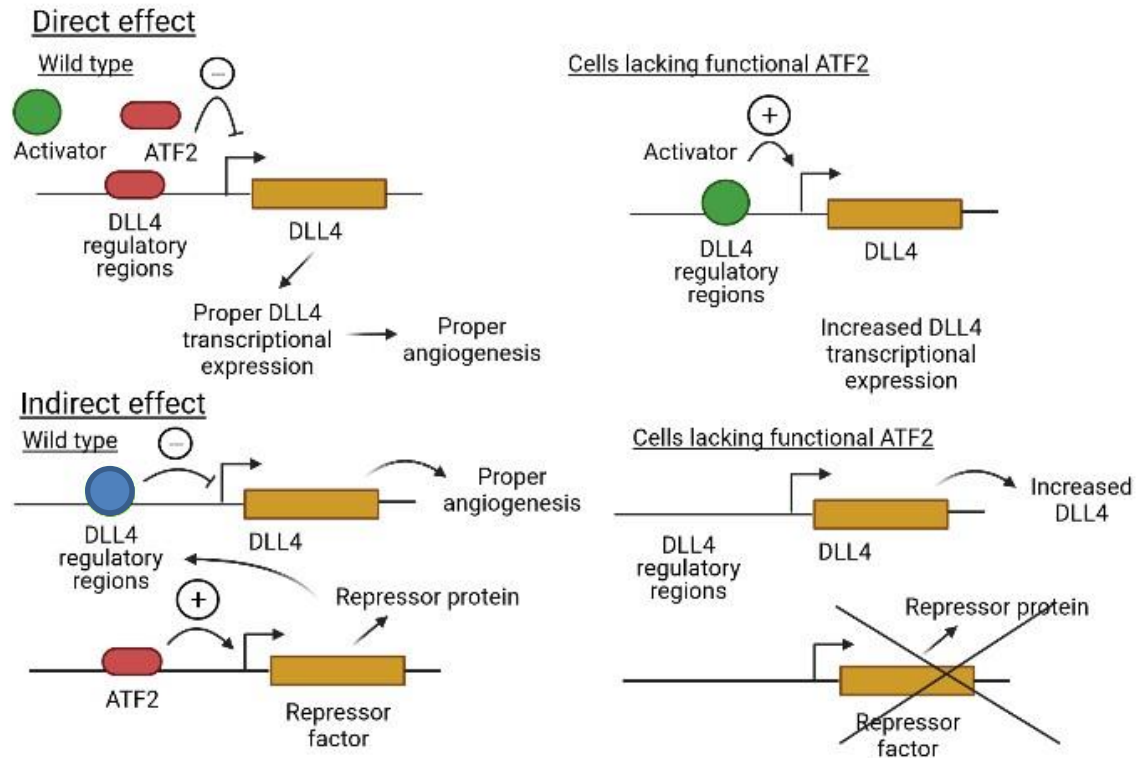


**Figure 4.4: Two potential mechanisms (direct or indirect) implicated in the negative regulatory effect exerted by ATF2 in the expression of *DLL4*.** The green molecule indicates an activator, the blue molecule indicates a repressor protein and the red molecule shows the ATF2 protein. ATF2 protein has either a direct or indirect influence on *DLL4* gene which is depicted by the yellow rectangle region.

As a first step to characterise in detail the role of ATF2 in the expression of *DLL4*, an *in-silico* analysis was performed in the regulatory regions of the gene to identify potential binding sites for ATF2. Five different regulatory regions have been reported in the *DLL4* gene (Sacilotto N, 2013); 4 enhancers (named -16 kb, -12 kb, intron 3 and +14 kb), and a promoter region located immediately upstream of the transcriptional start site (Figure 4.5) (Shah, A., 2017).

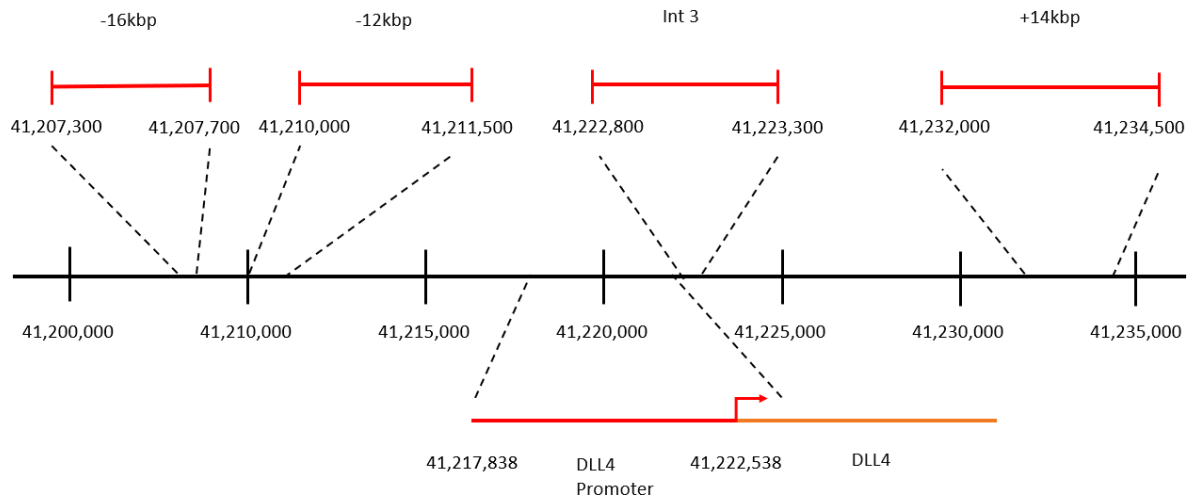


**Figure 4.5: Enhancers of DLL4 gene located by (Shah, A., 2017) - previously published data.** The DLL4 promoter (red line upstream to the arrow) is located before the transcription start site (red arrow) of the DLL4 gene (orange line). The region before and after the DLL4 gene and promoter, contains the enhancers. The numbers below this region represent the location of the enhancer in the DLL4 locus.

### 4.3 BIOINFORMATIC ANALYSIS OF THE *DLL4* LOCUS

The sequences of the enhancers and the promoter were downloaded from the ensemble website (<https://www.ensembl.org/index.html>). These sequences were uploaded in the ConTraV3 R database software to identify sequence motifs that match the consensus sequence recognised by ATF2. Only potential ATF2-binding motifs conserved in several species (human, primates, mouse, rat, dog and cat) were further considered in the analysis. These analyses revealed 12 putative ATF2 binding sites (Figure 4.6) located in the -12 kb enhancer (sites 1-5), the promoter region (sites 6-9) and the +14 kb enhancer (sites 10-12) (Figure 4.5, 4.6). No evolutionarily conserved ATF2-binding sites were found in -16 kb enhancer or intron 3 enhancer (Figure 4.6).

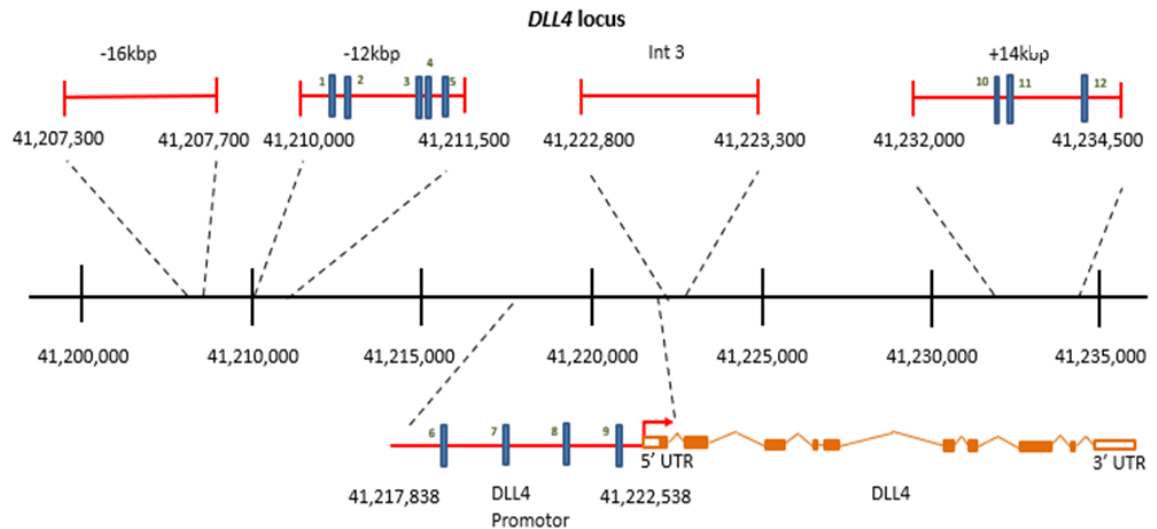


**Figure 4.6: Putative ATF-2 binding sites identified in the regulatory regions of the *DLL4* locus.** *DLL4* gene is indicated in orange, containing exons (orange blocks) and introns (diagonal lines). The red arrow indicates the transcription start site and the sequence adjacent to the arrow is the *DLL4* promoter. The four enhancers of the *DLL4* gene (-16kbp, -12kbp, Int 3 and +14kbp) are all within 35,000 bp and hence they are collectively called as super enhancer. The ATF2 putative binding sites are indicated by blue boxes, approximately close to the sequence position (not to scale)

### Site 1

<b>Human</b>	a a a g g c t g g t g a t g t c a c c a g t c g
<b>Baboon</b>	a a a g g c t g g t g a t g t c a c c a g t c g
<b>Orangutan</b>	a a a g g c t g g t g a t g t c a c c a g t c g
<b>Gorilla</b>	a a a g g c t g g t g a t g t c a c c a g t c g
<b>Chimp</b>	a a a g g c t a g t g a t g t c a c c a g t c g
<b>Mouse</b>	a a a g g c c g g t g a t g t c a c c a g t c g
<b>Rat</b>	a a a g g c c g g t g a t g t c a c c a g t c g
<b>Dog</b>	a a a g g c c g g t g a t g t c a c c a g t c g
<b>Cat</b>	a a a g g c c g g t g a t g t c a c c a g t c g

## Site 2

<b>Human</b>	g a a a c g c t g t g a t g t c c t g - - - - -
<b>Baboon</b>	g a a a c g c t g t g a t g t c c t g - - - - -
<b>Orangutan</b>	g a a a c g c t g t g a t g t c c t g - - - - -
<b>Gorilla</b>	g a a a c g c t g t g a t g t c c t g - - - - -
<b>Chimp</b>	g a a a c g c t g t g a t g t c c t g - - - - -
<b>Mouse</b>	g a a a c g c t g t g a t g t c c t g t c g t g
<b>Rat</b>	g a a a c g c t g t g a t g t c c t g t c g t g
<b>Dog</b>	g a a a c g c a g t g a t g t c c t g - - - - -
<b>Cat</b>	g a a a c g c c g t g a t g t c c t g - - - - -

## Site 3

<b>Human</b>	g c a g c c a c c t c a g a a t g g a c g
<b>Baboon</b>	g c a g c c a c c t c a g a a t g g a c g
<b>Orangutan</b>	g c a g c c a c c t c a g a a t g g a c g
<b>Gorilla</b>	g c a g c c a c c t c a g a a t g g a c g
<b>Chimp</b>	g c a g c c a c c t c a g a a t g g a c g
<b>Mouse</b>	g t a g c c a c c t c a g a a t g g a c g
<b>Rat</b>	g c a g c c a c c t c a g a a t g g a c g
<b>Dog</b>	g c a g c c a c c t c a g a a t g g a c g
<b>Cat</b>	g c a g c c a c c t c a g a a t g g a c g

## Site 4

<b>Human</b>	a g a c a g g g t g a c g a c a t t g t t g t
<b>Baboon</b>	a g a c a g g g t g a c g a c a t t g t t g t
<b>Orangutan</b>	a g a c a g g g t g a c g a c a t t g t t g t
<b>Gorilla</b>	a g a c a g g g t g a c g a c a t t g t t g t
<b>Chimp</b>	a g a c a g g g t g a c g a c a t t g t t g t
<b>Mouse</b>	a g a c a g g g t g a c g a c a t t g t t g t
<b>Rat</b>	a g a c a g g g t g a c g a c a t t g t t g t
<b>Dog</b>	a g a c a g g g t g a c g a c a t t g t t g t
<b>Cat</b>	a g a c a g g g t g a c g a c a t t g t t g t

### Site 5

Human	a c - a a c a c g a c c t c a c t c t t c c t g
Baboon	a c - a a c a c g a c c t c a c t c t t c c t g
Orangutan	a c - a a c a c g a c c t c a c t c t t c c t g
Gorilla	a c - a a c a c g a c c t c a c t c t t c c t g
Chimp	a c - a a c a c g a c c t c a c t c t t c c t g
Mouse	a c - a a c a c g a c c t c a c t c t t c c t g
Rat	a c - a a c a c g a c c t c a c t c t t c c t g
Dog	a c - a a c a c g a c c t c a c t c t t c c t g
Cat	a c - a a c a c g a c c t c a c t c t t c c t g

### Site 6

Human	a a g g c a a g a t g a c g a g g c t c c c a t
Baboon	a a g g c a a g a t g a c g a g g c t c c c a t
Orangutan	a a g g c a a g a t g a c g a g g c t c c c a t
Gorilla	a a g g c a a g a t g a c g a g g c t c c c a t
Chimp	a a g g c a a g a t g a c g a g g c t c c c a t
Mouse	a a g g c a a g a t g a c g a g g c t c c c a t
Rat	a a g g c a a g a t g a c g a g g c t c c c a t
Dog	a a g g c a a g a t g a c g a g g c t c c c a t
Cat	a a g g c a a g a t g a c g a g g c t c c c a t

### Site 7

Human	a c - t c a c - - - - t g t g a g g t g - - - - c c t t c c
Baboon	a c - t c a c - - - - t g t g a g g t g - - - - c c t t c c
Orangutan	a c - t c a c - - - - t g t g a g g t g - - - - c c t t c c
Gorilla	a c - t c a c - - - - t g t g a g g t g - - - - c c t t c c
Chimp	a c - t c a c - - - t t g t g a g g t g - - - - c c t t c c
Mouse	a c - t c a c - - - - t g t g a a g t g - - - - c c t t c c
Rat	a c - t c a c - - - - t g t g a g g t g - - - - c c t t c c
Dog	a c - t c a c - - - - t g t g a g g t g - - - - c c t t c c
Cat	a c - t c a c - - - - t g g g a a a t g - - - - c c t t c c

### Site 8

Human      - - - - - - - - - c c t - - - - - - - - - - - - - g a g g a c a g  
Baboon     - - - - - - - - - c c t - - - - - - - - - - - - - g a g g a c a g  
Orangutan - - - - - - - - - c c t - - - - - - - - - - - - - g a g g a c a g  
Gorilla    - - - - - - - - - c c t - - - - - - - - - - - - - g a g g a c a g  
Chimp      - - - - - - - - - c c t - - - - - - - - - - - - - g a g g a c a g  
Mouse      c c t t c g g g c c t - - - - - - - - - - - - - g a g g a c a g  
Rat        c c t t c g g g c c t - - - - - - - - - - - - - g a g g a c a g  
Dog        c c t c c a g c t c t - - - - - - - - - - - - - g a g g a c a g  
Cat        c c t c c a g c t c t - - - - - - - - - - - - - g a g g a c a g

### Site 9

Human      g g g c c g g g c t g a c g c g t g g c a g  
Baboon     g g g c c g g g c t g a c g c g t g g c a g  
Orangutan g g g c c g g g c t g a c g c g t g g c a g  
Gorilla    g g g c c g g g c t g a c g c g t g g c a g  
Chimp      g g g c c g g g c t g a c g c g t g g c a g  
Mouse      g g g c c g g g c t g a c g c g t g g c a g  
Rat        g g g c c g g g c t g a c g c g t g g c a g  
Dog        g g g c c g g g c t g a c g c g t g g c a g  
Cat        g g g c c g g g c t g a c g c g t g g c a g

### Site 10

Human      g a g c c c - g t c t c c t c a c c t c g c c c c  
Baboon     g a g c c c - g t c t c c t c a c c t c g c c c c  
Orangutan g a g c c c - g t c t c c t c a c c t c g c c c c  
Gorilla    g a g c c c - g t c t c c t c a c c t c g c c c c  
Chimp      g a g c c c - g t c t c c t c a c c t c g c c c c  
Mouse      g a g c c c - g t c t c c t c a c c t c a c c c c  
Rat        g a g c c c - g t c t c c t c a c c t c a c c c c  
Dog        a a g c c c - g t c t c c t c a c c t c g c c c c  
Cat        a a g c c c - g t c t c c t c a c c t c g c c c c

### Site 11

Human	g g g g c c a g a a c - - - - - c t c a t t a c c a t a
Baboon	g g g g c c a g a a c - - - - - c t c a t t a c c a t a
Orangutan	g g g g c c g g a a c - - - - - c t c a t t a c c a t a
Gorilla	g g g g c c a g a a c - - - - - c t c a t t a c c a t a
Chimp	g g g g c c a g a a c - - - - - c t c a t t a c c a t a
Mouse	a a g a c t a g a a c - - - - - c t c a t t a c c a t a
Rat	a c g a c t a g a a c - - - - - c t c a t t a c c a t a
Dog	g g g g t c a g a a c t - - - - - c t t a t t a c c a t a
Cat	g g g g c c a g g c c - - - - - c t c a t t a c c a t a

### Site 12

Human	t c t c t g a a g a t a a t a a
Baboon	t c t c t g a a g a t a a t a a
Orangutan	t c t c t g a a g a t a a t a a
Gorilla	t c t c t g a a g a t a a t a a
Chimp	t c t c t g a a g a t a a t a a
Mouse	t t t c t g a g g a a a a t g g
Rat	t t t c t g a g g a a a a t g g
Dog	t c c c t g a g g a t a - - - a
Cat	t c t c t g a g g a t a - - - a

**Figure 4.7: The above 12 predicted binding sites contain the consensus sequence of ATF2** that were identified on the DLL4 locus. These conserved sites were identified using ConTra V3 R software. The amino acids containing the ATF2 consensus sequence 'TGACGTCA' is highlighted in yellow and represented in some of the mammals.

Confirmation of physical ATF2 binding onto the putative sites found in the regulatory regions of the *DLL4* locus could be done by performing ChIP (chromatin immunoprecipitation) experiments. However, disruption in laboratory access due to COVID-19 pandemic made it impossible to set up the conditions for these experiments.

In addition to performing ChIP experiments, a functional analysis of the potential ATF2-binding sites could be performed by cloning *DLL4* regulatory regions in luciferase-based reporter vectors and investigate their activity in cells containing ATF2, or those where ATF2 has been silenced by siRNA transfection. To this end, cloning of the *DLL4* -12 Kb enhancer, the +14 Kb enhancer, and the -16 Kb enhancer (that does not contain any ATF2-binding sites and will be used as negative control) in pGL2-Promoter luciferase reporter vector (Promega) was performed. Additionally, a luciferase reporter vector containing the *Dll4* promoter region was provided as a generous gift by Professor Tsutomu Kume (Feinberg Cardiovascular and Renal Research Institute, Northwestern University School of Medicine, Chicago, USA) and it was transformed in bacteria and amplified to be used in these functional experiments.

#### **4.4 PCR AMPLIFICATION OF THE -16 Kb, -12 Kb, AND +14 Kb ENHANCER REGIONS OF THE *DLL4* LOCUS**

The enhancers of the *DLL4* gene were to be cloned to quantitatively determine which ATF2 putative binding site influences *DLL4* gene expression. As it is shown in the figure on page 53, the -12 kb enhancer, the +14 kb enhancer and the *DLL4* promoter contain putative binding sites. It was decided to clone -16 kb enhancer which is 400 bp in length and it would serve as a negative control (Figure 4.7B).

# Cloning of the DLL4 -16 enhancer

- A** Isolation of human gDNA
- ↳ PCR with oligos for enhancers
  - ↳ Precipitation and Digestion of the enhancer sequences with restriction enzymes
  - ↳ Gel Purification
  - ↳ Digestion of the plasmid with the corresponding restriction enzyme
  - ↳ Ligation
  - ↳ Transformation

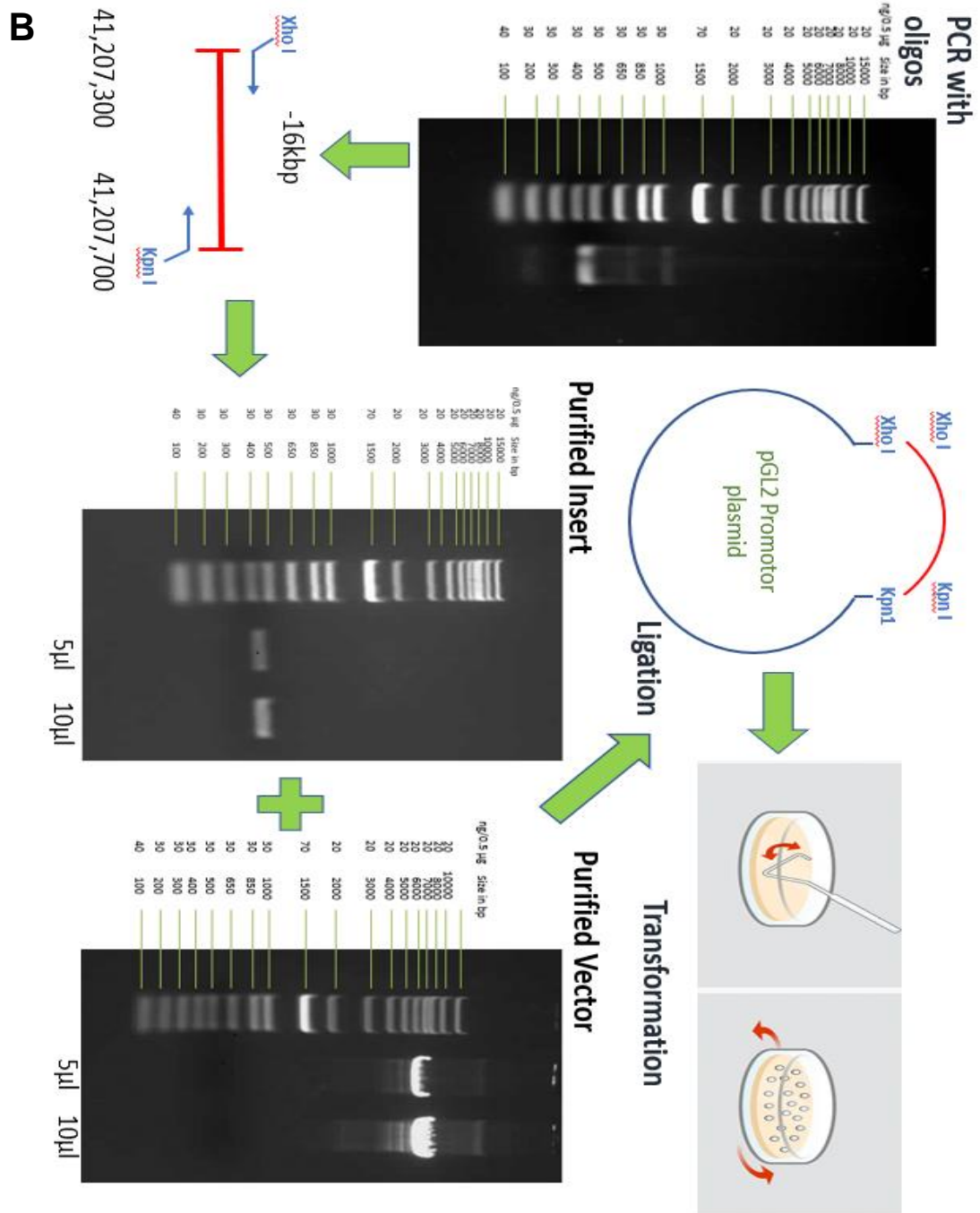


**Figure 4.8:** A) Flow diagram of steps involved in the cloning process. B) The cloning procedure of -16 kb enhancer which would serve as the control as it does not contain any putative ATF2 binding site. The named PCR with oligos, purified insert and purified vector represents images of agarose gel electrophoresis of PCR products performed at various stages of the cloning process.

### 3.4.1 PREPARATION OF pGL2-PROMOTER FOR CLONING

The pGL2-Promoter vector was chosen as cloning plasmid for the *DLL4* enhancers as it contains the luciferase gene as reporter, and hence luciferase activity could be measured to quantitatively determine the functionality of the putative binding sites for ATF2 found on the *DLL4* enhancers/promoter. Luciferase expression on pGL2-Promoter is controlled by the SV40 minimal promoter placed upstream of the Luciferase cDNA (Figure 4.8).

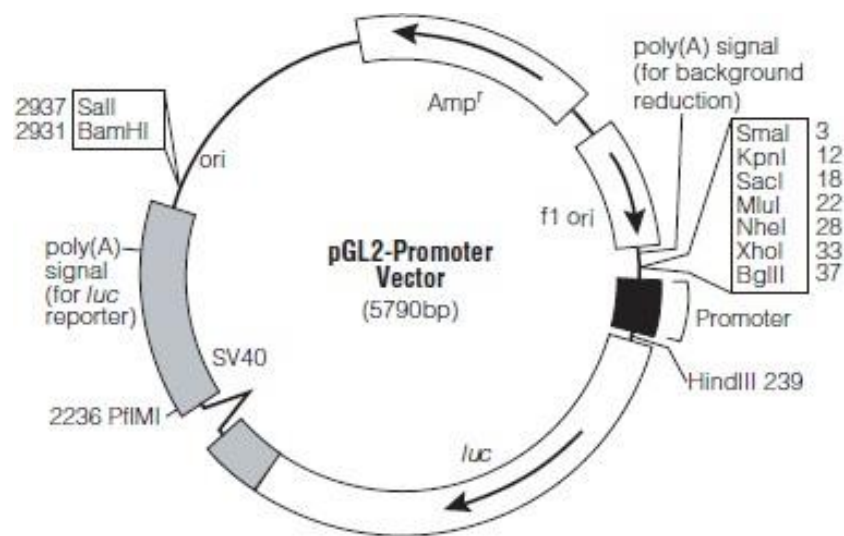


**Figure 4.9: pGL2 promoter vector image obtained from the 'Promega pGL2 Luciferase reporter vectors manual'.**

Furthermore, the design of pGL2-Promoter containing restriction sites both upstream and downstream of the SV40 minimal promoter, allows insertion of the *DLL4* enhancers either upstream or downstream of the promoter, resembling the real position of these enhancers in the *DLL4* locus. Finally, pGL2 also contains a gene that confers resistance to ampicillin, that can be used for selection of transformed colonies.

As the oligos used for PCR amplification of the enhancers were designed with flanking restriction enzymes *Xho*I and *Kpn*I to facilitate the cloning, the pGL2-Promoter vector was digested with restriction enzymes *Xho*I and *Kpn*I. The digestion reaction was subjected to DNA electrophoresis in a 0.7% agarose gel

to separate the lineal digested vector from uncut plasmids and purified from the gel. Successful purification was confirmed by DNA gel electrophoresis. As it can be seen in Figure 4.9, a band corresponding to the size of lineal pGL2-Promoter (6,790 bp) was detected.

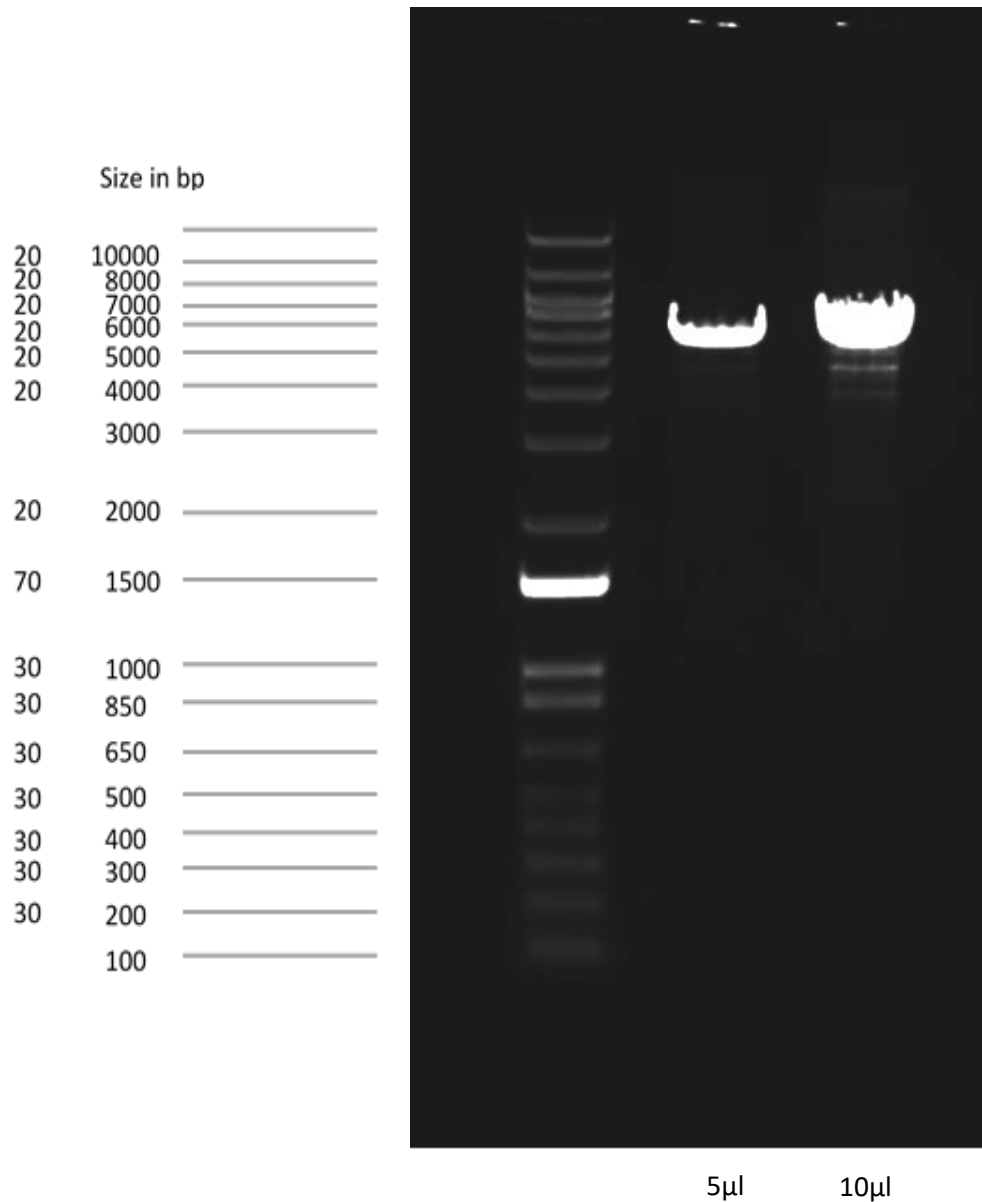


**Figure 4.10: Agarose gel electrophoresis of the digested pGL2 promotor vector.** 5 $\mu$ l and 10 $\mu$ l of pGL2 promotor vector in the second and third well respectively digested with XhoI and KpnI. This is done using 0.7% agarose gel containing ethidium bromide. 1 Kb DNA ladder (Invitrogen) was used as marker to estimate length of amplified fragments.

## **4.4.2 OPTIMISATION OF PCR REACTIONS TO AMPLIFY *DLL4* ENHANCER REGIONS**

### ***Amplification and cloning of the -16 Kb enhancer***

To clone the -16 Kb enhancer, a PCR was performed using a human genomic DNA template isolated from 2262 PNT, a prostate cell line. To get accurate amplification, Super Fi polymerase master mix (Invitrogen) was used, as Super Fi DNA polymerase has proof reading ability and that minimizes the risk of mutation during PCR amplification. On the first attempt, the gel electrophoresis analyses of the PCR reaction showed an intense background suggesting unspecific amplification. This could be due to the high content of GC islands present on the sequence of the -16Kb *DLL4* enhancer region. Hence, the PCR reaction was repeated using a GC enhancer buffer (Invitrogen) to improve denaturation of this region and thus facilitate the binding of forward and reverse oligonucleotides to the specific region to be amplified. As shown in Figure 4.10, agarose gel electrophoresis of the PCR performed following this strategy, showed a major amplification product of around 400 bp that corresponds to the expected size of the *DLL4* -16 Kb enhancer.

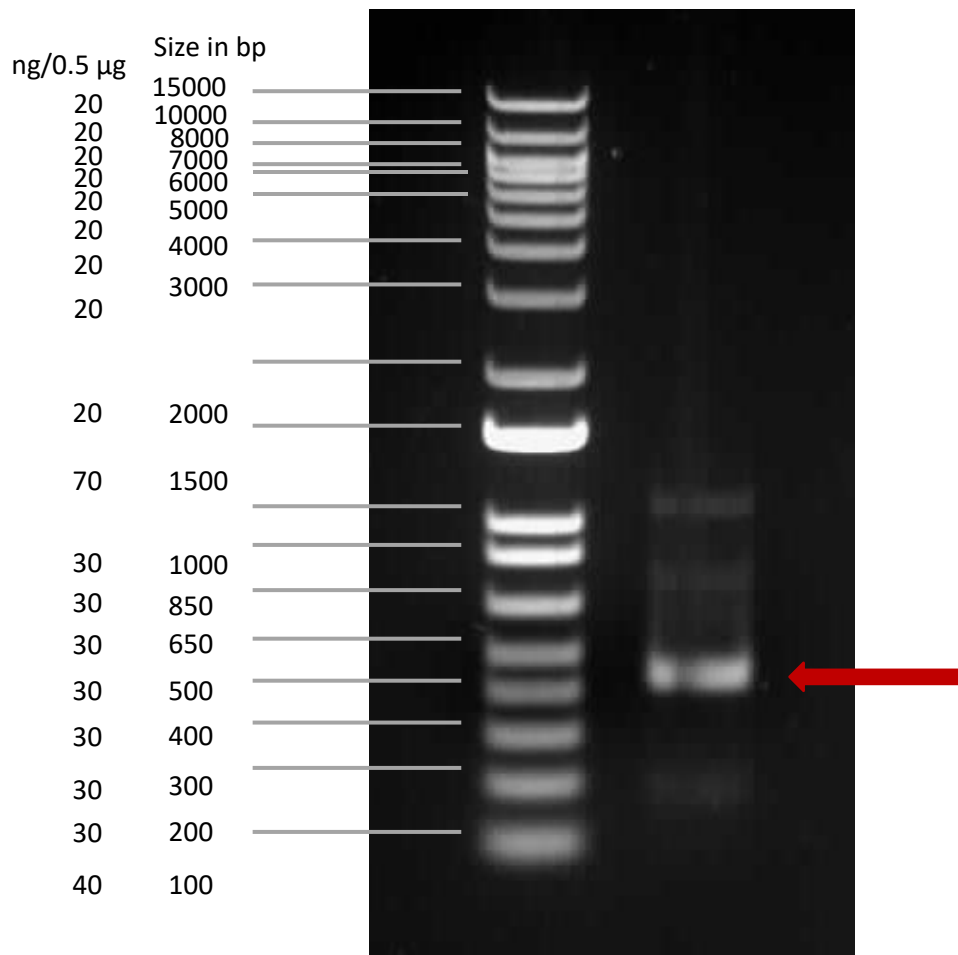


**Figure 4.11: Agarose gel electrophoresis of the PCR product of -16 Kb enhancer insert.** - 16 kb enhancer present in *DLL4* locus is 400bp in length. Figure shows a representative 1% agarose gel electrophoresis analyses of PCR amplification products using oligos CTTGCGGTACCCCTGGGGCTTCTCTCAAGCTG (forward primer) and CTTGCGCTCGAGAGCAGCCAGGGTGAGGCCGCC (reverse primer). The red arrow indicates the -16 kb enhancer which is adjacent to the 400 bp band indicated in the marker 1Kb DNA ladder (Invitrogen)

The amplified PCR reaction was subjected to digestion with restriction enzymes *XhoI* and *KpnI*, and the digested 400 bp band corresponding to the fragment of the -16 Kb *DLL4* enhancer was purified by gel electrophoresis. This fragment was then ligated in a 3:1 molar ratio reaction in the *XhoI*-*KpnI* digested pGL2-Promoter vector (Figure 4.9). To set up the ligation reaction in a 3:1 molar ratio the following formula was used:

$$\text{Required insert mass} = \left[ \frac{(\text{Amount of vector}) * (\text{Size of insert})}{(\text{Size of vector})} \right] * \left( \frac{3}{1} \right)$$

Competent bacteria were transformed with the ligation reaction and subsequently plated on LB-agar plates containing ampicillin. No colonies were present after incubation of plates for 24 hours, indicating that the cloning was unsuccessful.

### ***Amplification of the -12 Kb DLL4 enhancer***

To amplify the -12 Kb enhancer, different temperatures for the annealing step in the PCR reaction were tested, and finally a temperature of oligonucleotides annealing at 51°C was determined optimal for the specific amplification of -12kb enhancer which is 1500 bp in length (Figure 4.11). Unfortunately, at this point, laboratory lockdown due to the COVID-19 pandemic did not allow the continuation with the subsequent steps to clone this fragment into the digested pGL2-Promoter vector.

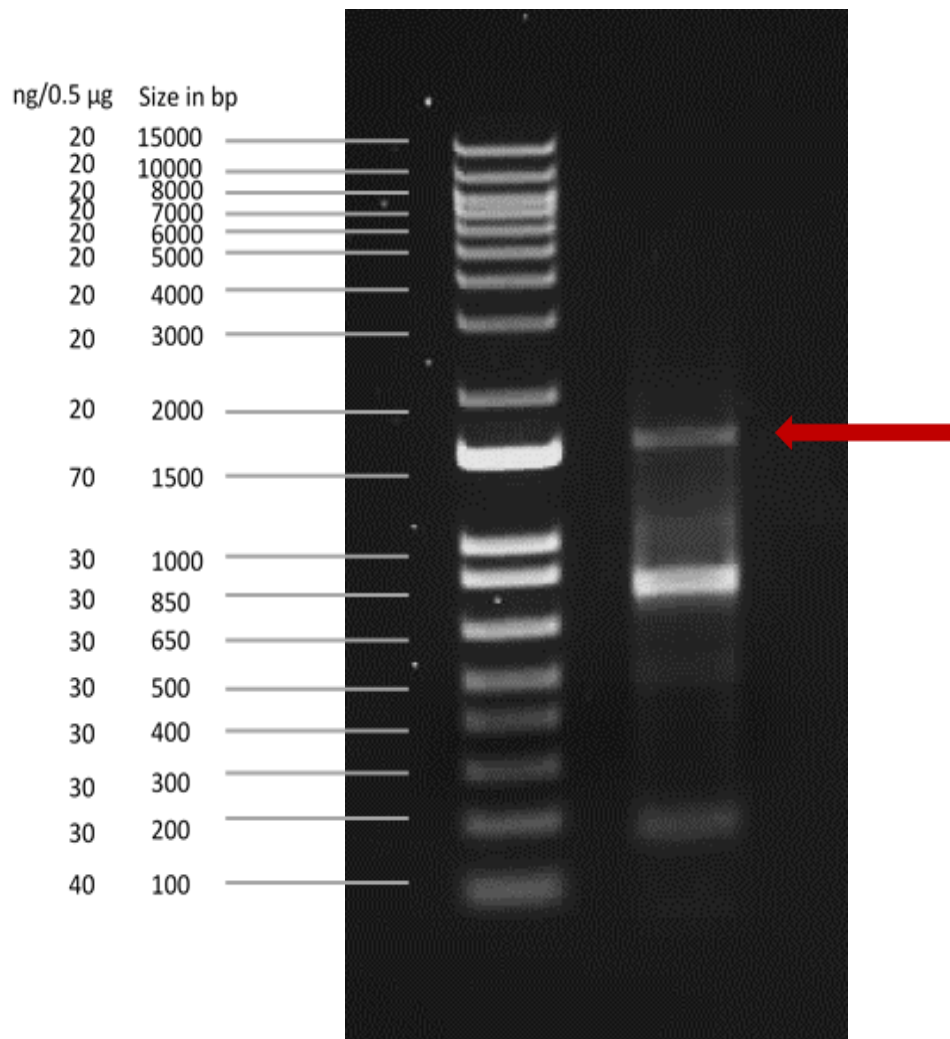


**Figure 4.12: Agarose gel electrophoresis of the PCR product of -12 kb enhancer insert** -12 kb enhancer present in *DLL4* locus is 1500bp in length. Figure shows a representative 1% agarose gel electrophoresis analyses of PCR amplification products using oligos CTTTCGCGGTACCCCTGGGGCTTCTCTCAAGCTG (forward primer) and CTTTCGCCTCGAGAGCAGCCAGGGTGAGGCCGCC (reverse primer). The red arrow indicates the -12 kb enhancer which is adjacent to the 1500 bp band indicated in the marker 1Kb DNA ladder (Invitrogen)

## 4.5 EFFECT OF ATF2 SILENCING ON GENES DOWNSTREAM TO *DLL4*

Previous experiments conducted in our laboratory indicated that knockdown of ATF2 significantly increases *DLL4* gene expression (Figure 4.3). *DLL4* has been reported to influence the expression of various downstream targets like *HEY1*,

*ID1*, *NRARP* (Phng LK, 2009) etc. which play a major role in angiogenesis (Fischer A, 2004; Volpert OV, 2003). To analyse the effect of ATF2 silencing on the expression of DLL4-target genes, ATF2 gene expression was knocked down in HUVEC by transfection of small interference RNA (siRNA) as previously shown (Figure 4.2).

qPCR analysis of *HEY1*, *ID1* and *NRARP* gene expression in cells lacking ATF2 did not show any differences with the expression of these genes in control (siNT-transfected) cells (Figure 4.12-4.14).

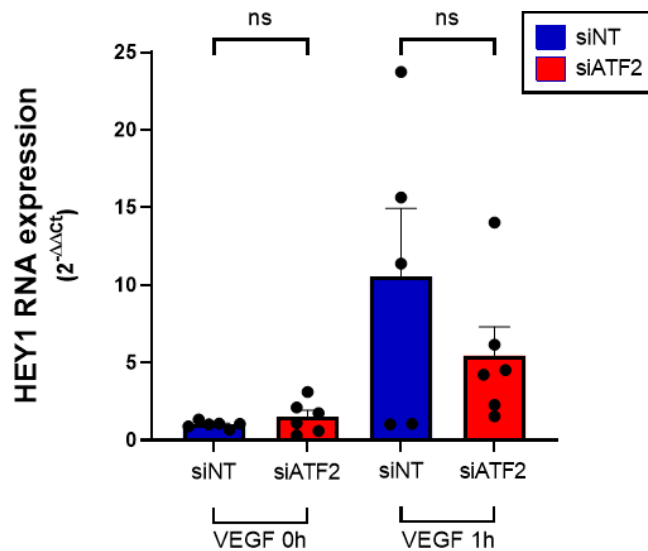


**Figure 4.13: Functional suppression of ATF2 results in no significant change in HEY1 mRNA abundance in either in the control or VEGF stimulated conditions endothelial cells.** HUVEC were transfected with small interference RNA for ATF2 RNA (siATF2) or small interference RNA that does not target any genes (siNT). Transfected cells were left unstimulated (control) or stimulated with VEGF (25 ng/mL) for 1 hour. qPCR analysis of *Hey1* RNA expression is shown. Values are expressed using the  $2^{-\Delta\Delta C_t}$  method referred to unstimulated HUVEC transfected with siNT. Histograms represent mean  $\pm$  SEM (n=6). Differences in gene expression were evaluated using Two-Way ANOVA with Tukey's multiple comparisons post-hoc test. Ns = non-significant

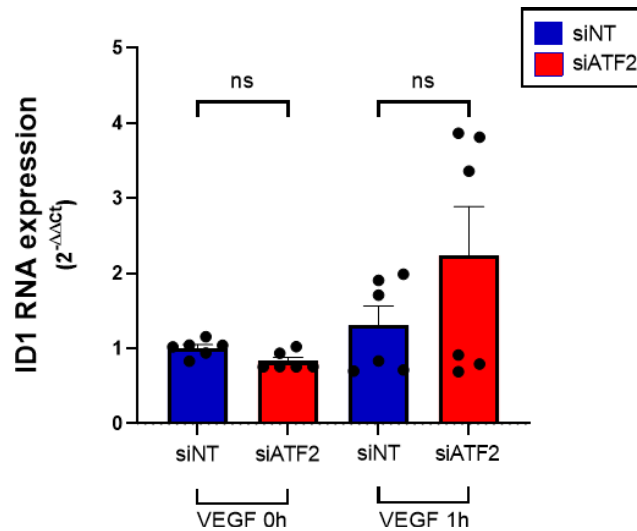


**Figure 4.14: Functional suppression of ATF2 results in no significant change in *ID1* mRNA abundance in either the control or VEGF stimulated conditions in endothelial cells.** HUVEC were transfected with small interference RNA for ATF2 RNA (siATF2) or small interference RNA that does not target any genes (siINT). Transfected cells were left unstimulated (control) or stimulated with VEGF (25 ng/mL) for 1 hour. qPCR analysis of *ID1* RNA expression is shown. Values are expressed using the  $2^{-\Delta\Delta C_t}$  method referred to unstimulated HUVEC transfected with siINT. Histograms represent mean  $\pm$  SEM (n=6). Differences in gene expression were evaluated using Two-Way ANOVA with Tukey's multiple comparisons post-hoc test. Ns = non-significant

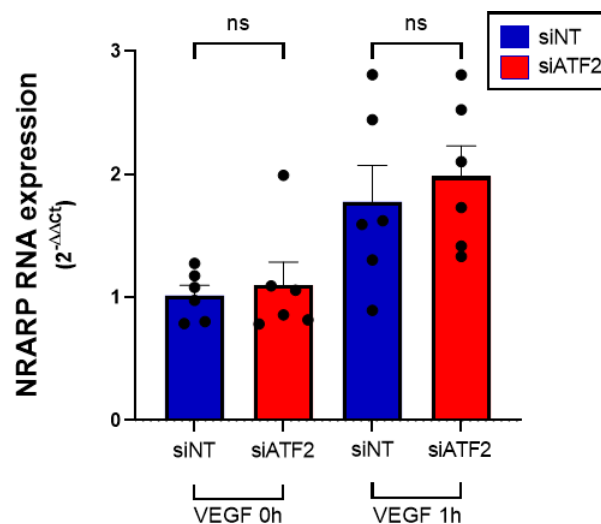


**Figure 4.15: Functional suppression of ATF2 results in no significant change in *NRARP* mRNA abundance in either the control or VEGF stimulated conditions in endothelial cells.** HUVEC were transfected with small interference RNA for ATF2 protein (siATF2) or small interference RNA that does not target any genes (siINT). Transfected cells were left unstimulated (control) or stimulated with VEGF (25 ng/mL) for 1 hour. qPCR analysis of *NRARP* RNA expression is shown. Values are expressed using the  $2^{-\Delta\Delta C_t}$  method referred to unstimulated HUVEC transfected with siINT. Histograms represent mean  $\pm$  SEM (n=6). Differences in gene expression were evaluated using Two-Way ANOVA with Tukey's multiple comparisons post-hoc test. Ns = non-significant

Other important regulators of VEGF-induced angiogenesis are the VEGF receptors VEGFR1, VEGFR2, and NRP1 which are regulated by DLL4 via a feedback loop (Potente M, 2011). Thus, the next step was to analyse whether ATF2 silencing had any effect on the expression of these genes. Expression of *VEGFR1* and *VEGFR2* increased significantly after knockdown of ATF2 (Figure 4.15, Figure 4.16). Interestingly, increase in the expression of these genes was independent of VEGF stimulation. Conversely, expression of the neuropilin receptor (NRP1), that also binds VEGF and whose expression in endothelial cells is regulated by DLL4, was not affected by ATF2 silencing (Figure 4.17).

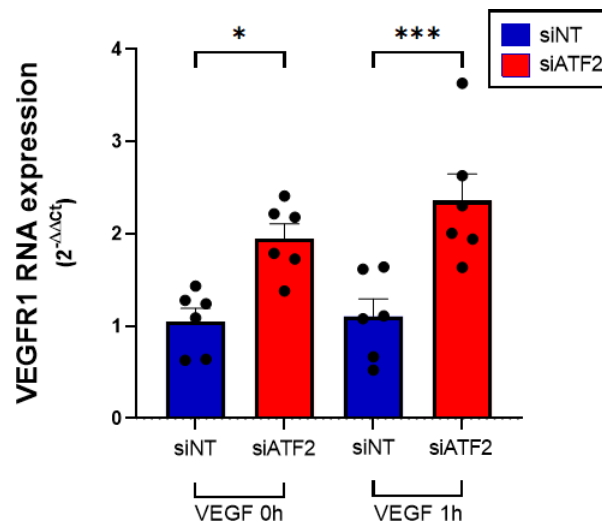


**Figure 4.16: Functional suppression of ATF2 results to significant increase of *VEGFR1* mRNA abundance in endothelial cells independent of VEGF stimulation.** HUVEC were transfected with small interference RNA for ATF2 protein (siATF2) or small interference RNA that does not target any genes (siNT). Transfected cells were left unstimulated (control) or stimulated with VEGF (25 ng/mL) for 1 hour. qPCR analysis of *VEGFR1* RNA expression is shown. Values are expressed using the  $2^{-\Delta\Delta C_t}$  method referred to unstimulated HUVEC transfected with siNT. Histograms represent mean  $\pm$  SEM (n=6). Differences in gene expression were evaluated using Two-Way ANOVA with Tukey's multiple comparisons post-hoc test. \*- $p < 0.05$  and \*\*- $p < 0.01$  indicates statistical significance when comparing cells transfected with siNT or siATF2, and stimulated with VEGF for upto 1 hour.

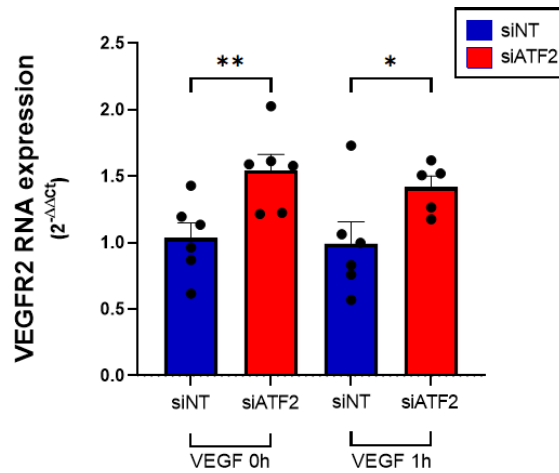


**Figure 4.17: Functional suppression of ATF2 results to significant increase of VEGFR2 mRNA abundance in endothelial cells independent of VEGF stimulation.** HUVEC were transfected with small interference RNA for ATF2 protein (siATF2) or small interference RNA that does not target any genes (siNT). Transfected cells were left unstimulated (control) or stimulated with VEGF (25 ng/mL) for 1 hour. qPCR analysis of *VEGFR2* RNA expression is shown. Values are expressed using the  $2^{-\Delta\Delta C_t}$  method referred to unstimulated HUVEC transfected with siNT. Histograms represent mean  $\pm$  SEM (n=6). Differences in gene expression were evaluated using Two-Way ANOVA with Tukey's multiple comparisons post-hoc test. \*- $p < 0.05$  and \*\*- $p < 0.01$  indicates statistical significance when comparing cells transfected with siNT or siATF2, and stimulated with VEGF of upto 1 hour.

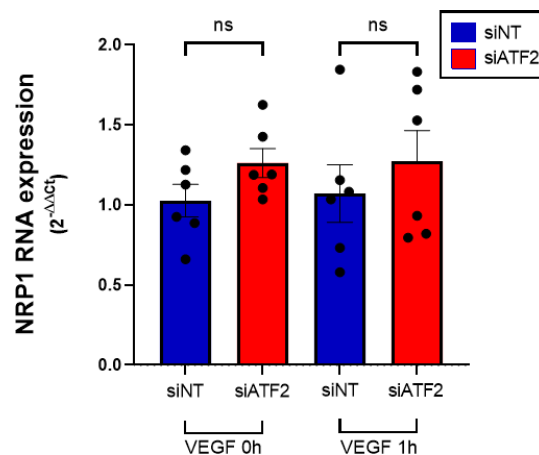


**Figure 4.18: Functional suppression of ATF2 results in no significant changes in NRP1 mRNA abundance in either the control or VEGF stimulated conditions in endothelial cells.** HUVEC were transfected with small interference RNA for ATF2 protein (siATF2) or small interference RNA that does not target any genes (siNT). Transfected cells were left unstimulated (control) or stimulated with VEGF (25 ng/mL) for 1 hour. qPCR analysis of *NRP1* RNA expression is shown. Values are expressed using the  $2^{-\Delta\Delta C_t}$  method referred to unstimulated HUVEC transfected with siNT. Histograms represent mean  $\pm$  SEM (n=6). Differences in gene expression were evaluated using Two-Way ANOVA with Tukey's multiple comparisons post-hoc test. Ns = non-significant

Additionally, investigation was conducted to demonstrate the effect of ATF2 silencing on the expression of other genes characterised as important regulators of angiogenesis, such as LRP1 (a negative regulator of angiogenesis) (Strickland D.K. et al; 2016) and Jag1 (a Notch ligand present in stalk cells). Our results (Figure 4.18) show that knockdown of ATF2 increases expression of JAG1 gene but only in cells stimulated with VEGF for 1 hour. In the case of *LRP1* expression, no changes were detected after ATF2 silencing (Figure 4.19).

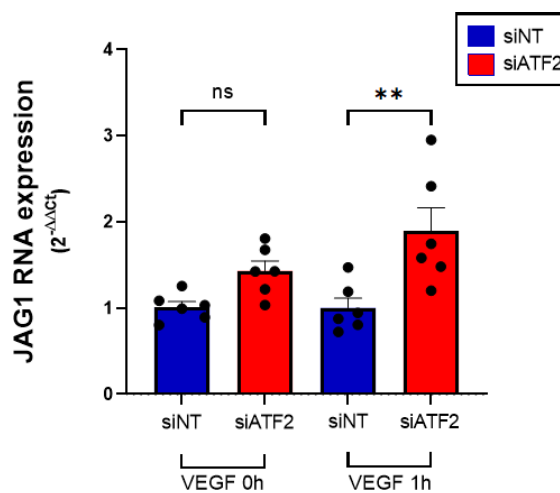


**Figure 4.19: Functional suppression of ATF2 results in a significant increase in the VEGF stimulated JAG1 mRNA abundance in endothelial cells.** HUVEC were transfected with small interference RNA for ATF2 protein (siATF2) or small interference RNA that does not target any genes (siINT). Transfected cells were left unstimulated (control) or stimulated with VEGF (25 ng/mL) for 1 hour. qPCR analysis of JAG1 RNA expression is shown. Values are expressed using the  $2^{-\Delta\Delta C_t}$  method referred to unstimulated HUVEC transfected with siINT. Histograms represent mean  $\pm$  SEM (n=6). Differences in gene expression were evaluated using Two-Way ANOVA with Tukey's multiple comparisons post-hoc test. \*\* $p < 0.01$  indicates statistical significance when comparing cells transfected with siINT or siATF2 and stimulated with VEGF of upto 1 hour. Ns = non-significant

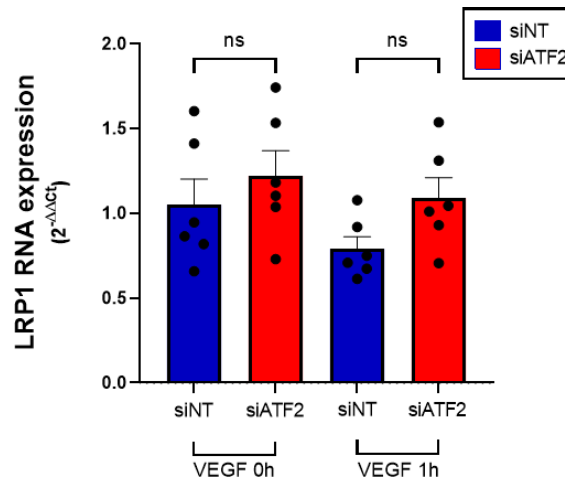


**Figure 4.20: Functional suppression of ATF2 results in no significant change in *LRP1* mRNA abundance in either the control or VEGF stimulated conditions in endothelial cells.** HUVEC were transfected with small interference RNA for ATF2 protein (siATF2) or small interference RNA that does not target any genes (siNT). Transfected cells were left unstimulated (control) or stimulated with VEGF (25 ng/mL) for 1 hour. qPCR analysis of *LRP1* RNA expression is shown. Values are expressed using the  $2^{-\Delta\Delta C_t}$  method referred to unstimulated HUVEC transfected with siNT. Histograms represent mean  $\pm$  SEM (n=6). Differences in gene expression were evaluated using Two-Way ANOVA with Tukey's multiple comparisons post-hoc test. Ns = non-significant

#### 4.6 EFFECT OF BLOCKAGE OF ATF2 FUNCTIONALITY ON THE EXPRESSION OF DOWNSTREAM TARGETS OF DLL4

To further substantiate the studies presented in the previous section where the role of ATF2 in the expression of targets of DLL4 was analysed after ATF2 silencing using siRNA, the analysis of the above genes was repeated by suppressing the function of ATF2, achieved by overexpression of the dominant negative mutant ATF2(AA).

In contrast to the results observed with siRNA mediated ATF2 silencing, overexpression of the mutated ATF2 protein resulted in a significant increase in *Hey1* and *NRARP* expression (Figure 4.20, Figure 4.22). However, no changes were observed in the expression of *ID1* in agreement with the results observed in the silencing experiments (Figure 4.21).

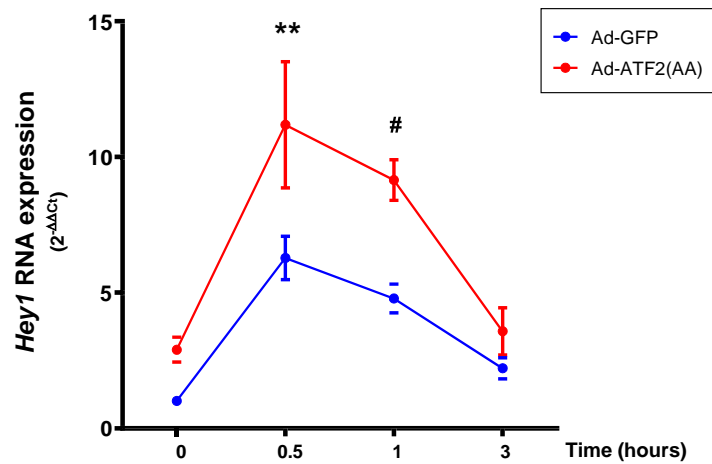


**Figure 4.21: Functional suppression of ATF2 leads to an increase in the VEGF-induced upregulation of *Hey1* in endothelial cells.** HUVEC were infected with Adenovirus containing a mutated ATF2 protein (Ad-ATF2AA) or green fluorescence protein which will contain wild type ATF2 protein (Ad-GFP). Infected cells were left unstimulated (control) or stimulated with VEGF (25 ng/mL) for various time intervals. qPCR analysis of *Hey1* RNA expression is shown. Values are expressed using the  $2^{-\Delta\Delta C_t}$  method referred to unstimulated HUVEC infected with Ad-GFP. Histograms represent mean  $\pm$  SEM (n=6). Differences in gene expression were evaluated using Two-Way ANOVA with Tukey's multiple comparisons post-hoc test. \*\*- $p < 0.01$  and #- $p < 0.05$  indicates statistical significance when comparing cells transfected with Ad-GFP or Ad-ATF2AA, and stimulated with VEGF for up to 3 hours.

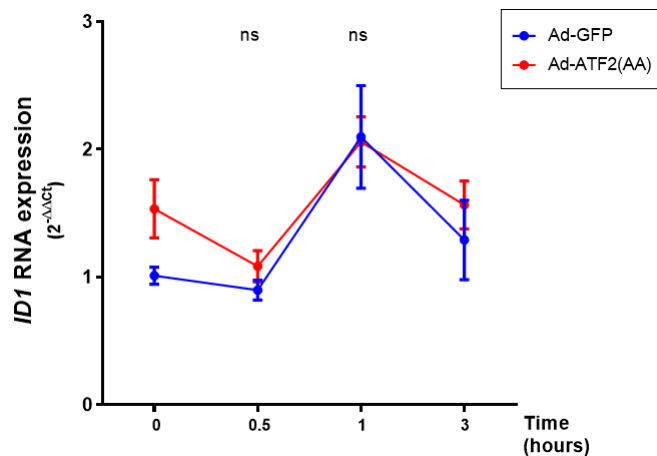


**Figure 4.22: Functional suppression of ATF2 does not alter *ID1* mRNA abundance in endothelial cells irrespective of VEGF stimulation.** HUVEC were infected with Adenovirus containing a mutated ATF2 protein (Ad-ATF2AA) or green fluorescence protein which will contain wild type ATF2 protein (Ad-GFP). Infected cells were left unstimulated (control) or stimulated with VEGF (25 ng/mL) for various time intervals. qPCR analysis of *ID1* RNA expression is shown. Values are expressed using the  $2^{-\Delta\Delta C_t}$  method referred to unstimulated HUVEC infected with Ad-GFP. Histograms represent mean  $\pm$  SEM (n=6). Differences in gene expression were evaluated using Two-Way ANOVA with Tukey's multiple comparisons post-hoc test. Ns = non-significant

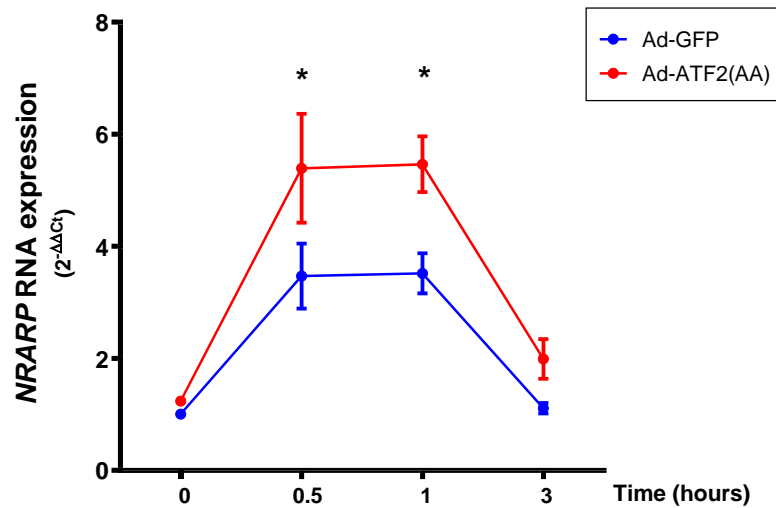


**Figure 4.23: Functional suppression of ATF2 leads to an increase in the VEGF-induced upregulation of *NRARP* in endothelial cells.** HUVEC were infected with Adenovirus containing a mutated ATF2 protein (Ad-ATF2AA) or green fluorescence protein which will contain wild type ATF2 protein (Ad-GFP). Infected cells were left unstimulated (control) or stimulated with VEGF (25 ng/mL) for various time intervals. qPCR analysis of *NRARP* RNA expression is shown. Values are expressed using the  $2^{-\Delta\Delta C_t}$  method referred to unstimulated HUVEC infected with Ad-GFP. Histograms represent mean  $\pm$  SEM (n=6). Differences in gene expression were evaluated using One-Way ANOVA with Tukey's multiple comparisons post-hoc test. \* $p < 0.05$  indicates statistical significance when comparing cells transfected with Ad-GFP or Ad-ATF2AA and stimulated with VEGF of upto 3 hours.

Silencing experiments revealed an increase in VEGFR1 and VEGFR2 expression after the knockdown of ATF2 expression in endothelial cells (Figure 4.15, Figure 4.16), however, overexpression of ATF2(AA) did not lead to any changes in the expression of the VEGF receptors, either in basal or VEGF-stimulated conditions (Figure 4.23, Figure 4.24). As observed in silencing experiments, NRP1 gene expression remains unaltered (Figure 4.25).

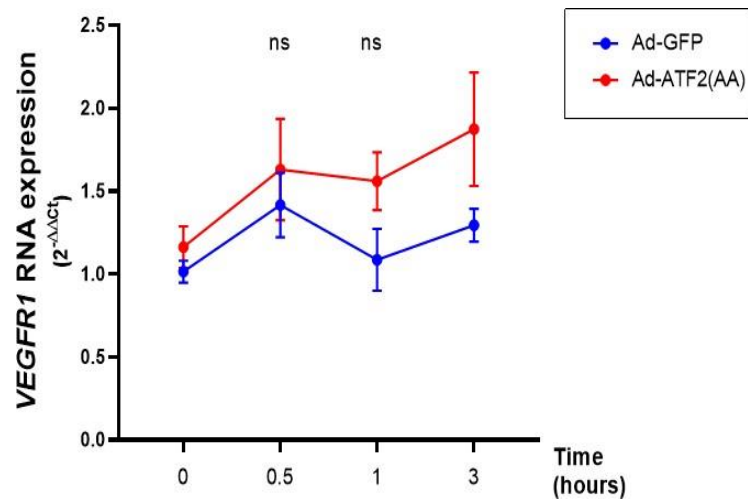


**Figure 4.24: Functional suppression of ATF2 does not alter the *VEGFR1* mRNA abundance in endothelial cells irrespective of VEGF stimulation.** HUVEC were infected with Adenovirus containing a mutated ATF2 protein (Ad-ATF2AA) or green fluorescence protein which will contain wild type ATF2 protein (Ad-GFP). Infected cells were left unstimulated (control) or stimulated with VEGF (25 ng/mL) for various time intervals. qPCR analysis of *VEGFR1* RNA expression is shown. Values are expressed using the  $2^{-\Delta\Delta C_t}$  method referred to unstimulated HUVEC infected with Ad-GFP. Histograms represent mean  $\pm$  SEM (n=6). Differences in gene expression were evaluated using Two-Way ANOVA with Tukey's multiple comparisons post-hoc test. Ns = non-significant

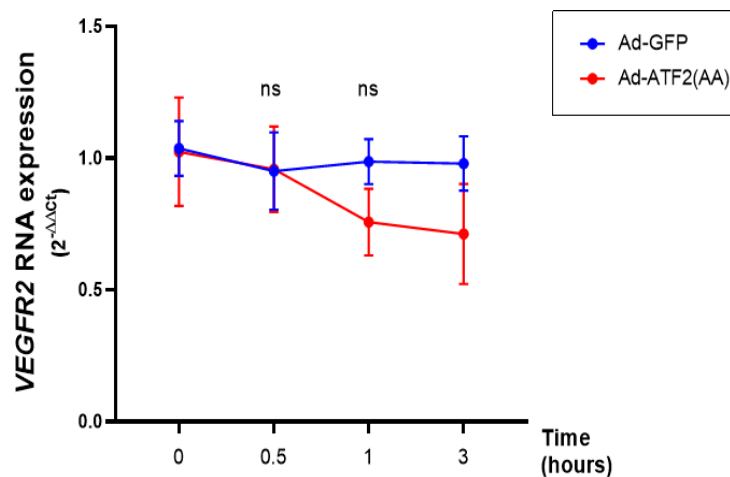


**Figure 4.25: Functional suppression of ATF2 does not alter the *VEGFR2* mRNA abundance in endothelial cells irrespective of VEGF stimulation.** HUVEC were infected with Adenovirus containing a mutated ATF2 protein (Ad-ATF2AA) or green fluorescence protein which will contain wild type ATF2 protein (Ad-GFP). Infected cells were left unstimulated (control) or stimulated with VEGF (25 ng/mL) for various time intervals. qPCR analysis of *VEGFR2* RNA expression is shown. Values are expressed using the  $2^{-\Delta\Delta C_t}$  method referred to unstimulated HUVEC infected with Ad-GFP. Histograms represent mean  $\pm$  SEM (n=6). Differences in gene expression were evaluated using Two-Way ANOVA with Tukey's multiple comparisons post-hoc test. Ns = non-significant

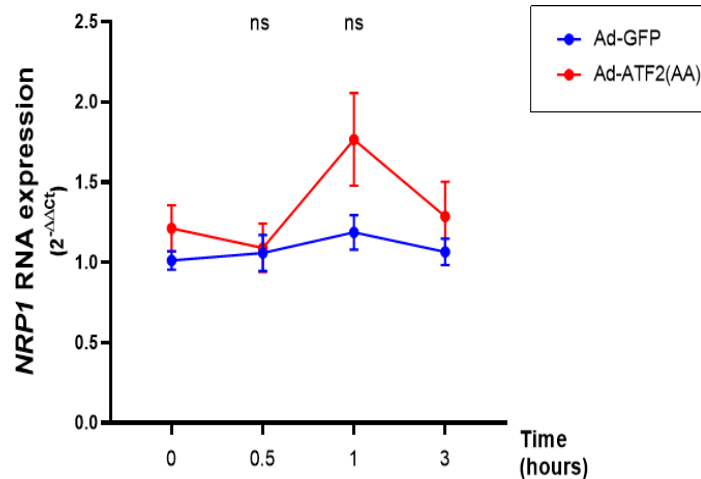


**Figure 4.26: Functional suppression of ATF2 does not alter the *NRP1* mRNA abundance in endothelial cells irrespective of VEGF stimulation.** HUVEC were infected with Adenovirus containing a mutated ATF2 protein (Ad-ATF2AA) or green fluorescence protein which will contain wild type ATF2 protein (Ad-GFP). Infected cells were left unstimulated (control) or stimulated with VEGF (25 ng/mL) for various time intervals. qPCR analysis of *NRP1* RNA expression is shown. Values are expressed using the  $2^{-\Delta\Delta C_t}$  method referred to unstimulated HUVEC infected with Ad-GFP. Histograms represent mean  $\pm$  SEM (n=6). Differences in gene expression were evaluated using Two-Way ANOVA with Tukey's multiple comparisons post-hoc test. Ns = non-significant

Finally, analysis of the expression of *Jag1* and *LRP1* in cells containing ATF2(AA) did not show any significant difference to control cells containing GFP (Figure 4.26, Figure 4.27). Although, in agreement with the results observed in ATF2-silenced cells, a clear tendency to express higher levels of *Jag1* was observed in cells infected with Ad-ATF2(AA).

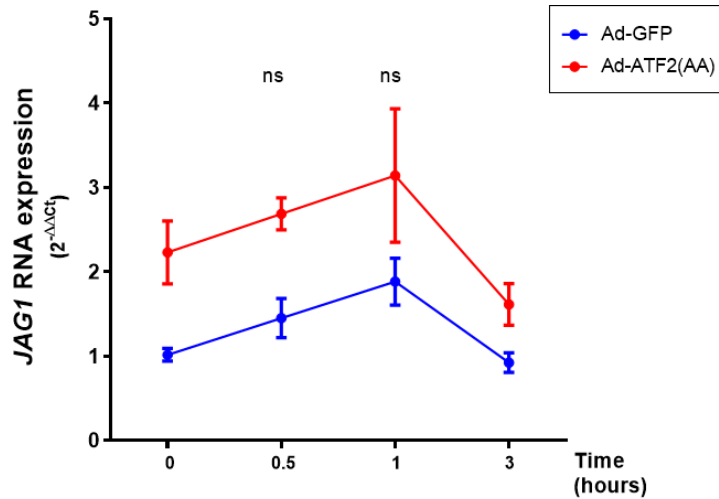


**Figure 4.27: Functional suppression of ATF2 does not alter the VEGF-induced upregulation of *JAG1* in endothelial cells.** HUVEC were infected with Adenovirus containing a mutated ATF2 protein (Ad-ATF2AA) or green fluorescence protein which will contain wild type ATF2 protein (Ad-GFP). Infected cells were left unstimulated (control) or stimulated with VEGF (25 ng/mL) for various time intervals. qPCR analysis of *JAG1* RNA expression is shown. Values are expressed using the  $2^{-\Delta\Delta C_t}$  method referred to unstimulated HUVEC infected with Ad-GFP. Histograms represent mean  $\pm$  SEM (n=6). Differences in gene expression were evaluated using Two-Way ANOVA with Tukey's multiple comparisons post-hoc test. Ns = non-significant

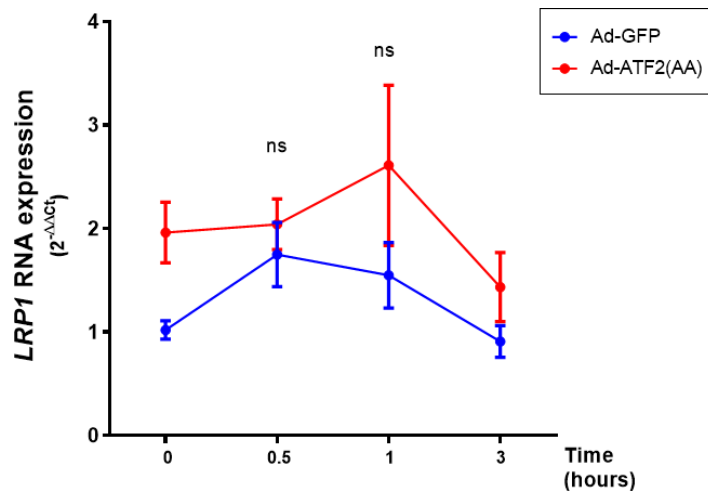


**Figure 4.28: Functional suppression of ATF2 does not alter the *LRP1* mRNA abundance in endothelial cells irrespective of VEGF stimulation.** HUVEC were infected with Adenovirus containing a mutated ATF2 protein (Ad-ATF2AA) or green fluorescence protein which will contain wild type ATF2 protein (Ad-GFP). Infected cells were left unstimulated (control) or stimulated with VEGF (25 ng/mL) for various time intervals. qPCR analysis of *LRP1* RNA expression is shown. Values are expressed using the  $2^{-\Delta\Delta C_t}$  method referred to unstimulated HUVEC infected with Ad-GFP. Histograms represent mean  $\pm$  SEM (n=6). Differences in gene expression were evaluated using Two-Way ANOVA with Tukey's multiple comparisons post-hoc test. Ns = non-significant

## 4.7 GENOTYPING OF THE MICE EAR SNIP SAMPLES

One of the aims of the project was to generate an ATF2 KO mouse to study the effects of ATF2 in in vivo angiogenesis. As it has been reported that ATF2 global KO mice die during birth due to meconium aspiration syndrome (Maekawa et al, 1999), one objective of this work was to develop a tamoxifen-inducible, endothelial-specific ATF2 knockout, by crossing ATF2<sup>flox/flox</sup> mice (Breitwieser et al, 2007) with transgenic mice expressing Cre recombinase under the control of the Vascular Endothelial Cadherin promoter and with activity inducible by treatment with tamoxifen (Tg(Cdh5-cre/ERT2)1Rha). Two breeder couples of ATF2<sup>flox/flox</sup> mice were kindly donated by Dr Breitwieser (Cancer Research UK, Manchester Institute, UK) to the laboratory of our collaborator Prof Elizabeth Cartwright (University of Manchester, UK). Crossing of these breeders did not produce any offspring so it was decided to cross one of the ATF2<sup>flox/flox</sup> breeders with an ATF2 wild type mouse as that strategy usually restores the breeding capacity of mice after transportation. This crossing would generate an offspring of ATF2<sup>WT/flox</sup> mice. Offspring from this crossing was genotyped using DNA isolated from ear snips by PCR as described (Breitwieser et al, 2007). As expected, all samples contained the PCR products amplified from the wild type allele (195 bp) and the floxed allele (230 bp) (Figure 4.29) confirming the ATF2<sup>WT/flox</sup> genotype of all animals.

Subsequently, crossing of two heterozygous mice would yield ATF2<sup>flox/flox</sup> mice as part of the offspring. Due to the pandemic, as the laboratories had to be temporarily closed, our collaborators were unable to maintain the developed ATF2<sup>WT/flox</sup> mice. Hence, it was necessary to store frozen sperm isolated from the heterozygous mice to generate ATF2<sup>flox/flox</sup> breeders later.

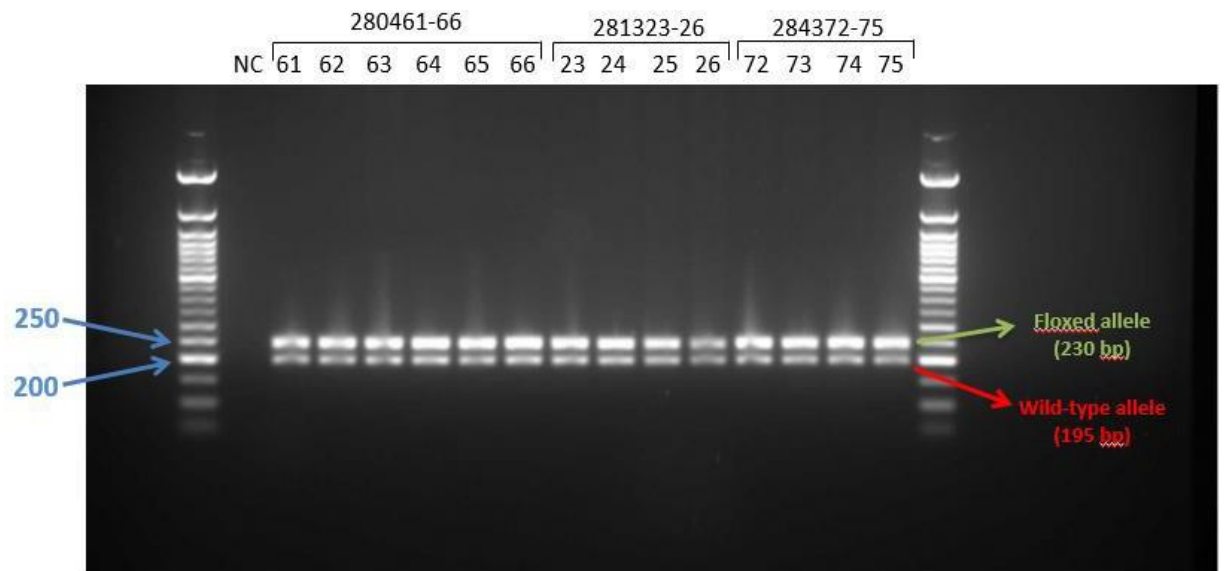


**Figure 4.29: Agarose gel electrophoresis performed using the PCR products obtained from mice ear snips.** The PCR product of the floxed allele (green arrow) is 230 bp in length and the PCR product of the wild type allele (red arrow) is 195 bp in length. NC represents a PCR assay performed without any DNA template (negative control).

## **5. DISCUSSION**

VEGF proangiogenic factor has been proved to activate various cellular pathways implicated in the pathophysiology of angiogenesis. Anti-VEGF therapy has been developed to treat human diseases that are caused with excessive angiogenesis, such as tumour angiogenesis. Unfortunately, blocking VEGF with the current anti-VEGF drugs clinically available induces the release of other pro-angiogenic factors like bFGF, HGF, EGF, etc from the tumoral cells, promoting the regrowth of the tumour (Cascone T. et al., 2011; Casanovas O. et al., 2005; Shojaei F. et al., 2010; Huang Z. et al., 2004). Hence there is an urgent need to identify a molecular target that would be activated by all proangiogenic factors (Vasudev N.S. et al., 2014). Targeting such a molecule would be an efficient way to combat the action of all pro-angiogenic factors and thus reduce tumour angiogenesis. Unpublished data obtained in our laboratory show that ATF2 could be a possible target as it is shown to be activated by a number of proangiogenic factors other than VEGF (section 1.7, figure 1.6). Activation of ATF2 molecule requires phosphorylation at the Thr69 and Thr71 residue by two independent pathways to form a heterodimerised transcription factor complex (Lau E, 2012; Ouwens D.M., 2002) and hence influence the expression of angiogenic related genes (Penix L.A. et al., 1996; Song H., 2006; Sato N., 1990). Hence, it was decided to further analyse the role of ATF2 in angiogenesis. Here, it was demonstrated that ATF2 acts as a negative regulator of *DLL4* gene expression in endothelial cells.

Previous published data demonstrates that ATF2 can either induce or repress the expression of target genes depending on the association to different co-activators. In this sense, a transcription factor complex containing ATF2 has shown to induce the expression of *E-Selectin*, a cell-surface protein that is essential in endothelial-leukocyte adhesion (Read M.A. et al., 1997; Oh I. et al., 2007). On the contrary, ATF2 is known to interact with JDP2 or JunD to form a

transcription factor complex and downregulate the expression of some genes like *c-JUN* and *Cdk4* respectively (Jin et al., 2002; Xiao L, 2010) which are also involved in angiogenesis (Rostama B, 2015). In fact, it has been hypothesised that inhibition of *c-jun* gene expression could be observed when a transcription factor complex containing ATF2, JDP2 and HDAC3 binds to the *c-jun* promoter containing a region called the differentiation response element, whereas in the presence of retinoic acid, p300 protein replaces HDAC3 and JDP2, forming a different transcription factor complex and resulting in the activation of *c-jun* gene expression (Jin C, 2002) (Figure 5.1). Due to the dual function of activated ATF2 molecule, it is not surprising that suppression of ATF2 function in endothelial cells results in enhancement of *DLL4* gene expression (Figure 2.3 and 4.3).

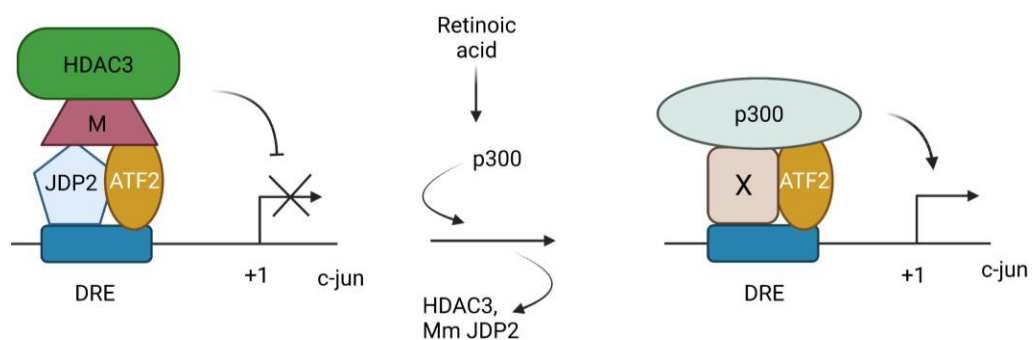


**Figure 5.1: Hypothetical model of the regulation of *c-jun* gene expression by transcription factor complex containing activated ATF2. Modified from Jin C et al (2002).** The yellow molecule in the transcription factor complex represents the ATF2 protein and the transcription factor complex binds to the blue sequence, the differentiation response element in the *c-jun* promoter. In the presence of retinoic acid, the other cofactors of the transcription factor complex dissociate from the ATF2 protein and bind p300 to activate *c-jun* gene expression.

This suggests that ATF2 acts as a negative regulator of *DLL4* gene expression in physiological conditions. However, the mechanism of *DLL4* repression by ATF2 is still unclear.

The negative regulatory effect of ATF2 on the *DLL4* locus could be hypothesised to be the direct binding of ATF2 to the regulatory regions of *DLL4* gene, or by the

indirect effect of ATF2 that activates a repressor of *DLL4*, and the repressor protein in turn binds to the *DLL4* regulatory regions, reducing the expression of the gene (section 3.2, figure 3.4). Alternatively, ATF2 could activate the expression of a miRNA which targets the 3' untranslated region of the *DLL4*, thus reducing its gene expression. In a paper published by Howe GA (2017), they suggest a mechanism of the effect of miR-30b on *TGFβ2* via the activation of ATF2. Interestingly, miR-30b targets the ATF2 co-repressor JDP2, decreasing the RNA levels for this protein. The miR-30b mediated suppression of JDP2 allows ATF2 to interact with other co-activators, resulting in the induction of *TGFβ2*. Future experiments will have to address whether ATF2 interaction with JDP2 (or other corepressors) is implicated in *DLL4* regulation. Another example where ATF2 was identified to have a negative regulatory effect on gene expression is on the *IFNβ1*. In this case, ChIP (Chromatin ImmunoPrecipitation) experiments showed that ATF2 directly binds to the *IFNβ1* promoter region. Moreover, cloning of the region containing putative ATF2 binding sites in a luciferase-based reporter plasmid, established the functionality of identified interactions between ATF2 and the *IFNβ1* promoter (Lau E, 2015).

In this work, a bioinformatic analysis was conducted to identify potential ATF2 binding sites in the super enhancer or promoter regions of the *DLL4* locus (Shah, A., 2017). 12 highly conserved putative binding sites for ATF2 were identified on the -12 kb enhancer, +14 kb enhancer and on the *DLL4* promoter (section 3.3, figure 3.6). ChIP and cloning of the predicted ATF2 binding sites into luciferase gene reporter vectors were planned in this MPhil project to determine the functional significance of these sites in the *DLL4* locus. Unfortunately, time constrictions due to COVID-19 lockdown of laboratories did not allow completion of this part of the project.

Activation of endothelial VEGFR2 by VEGF upregulates the expression of DLL4 which further binds to the Notch receptor present on the stalk cell, activating the Notch-signalling pathway, and resulting in changes in the expression of DLL4-target genes (Phng LK, 2009). The effect of ATF2 suppression on *DLL4* expression prompted the study of the consequences of ATF2 suppression on the expression of DLL4-target genes.

Expression of the DLL4-target genes *HEY1* and *NRARP* in control cells was transiently upregulated by stimulation with VEGF, reaching a peak at 30 minutes and 1 hour post-stimulation (Figure 4.20 and 4.22). These results are in agreement with the same kinetic of upregulation found by other authors for *DLL4* and *HEY1* expression in endothelial cells treated with VEGF (Adam M.G. et al., 2013). *HEY1* (Figure 4.20) and *NRARP* (Figure 4.22) gene expression increased in cells infected with Ad-ATF2AA but only after stimulation with VEGF. Expression of *ID1* was not affected by functional suppression of ATF2.

In addition to these genes, changes in the expression of *VEGFR1*, *VEGFR2*, *NRP1*, *JAG1*, and *LRP1* were also analysed. Activation of Notch signalling through DLL4 binding has been reported to inhibit *VEGFR1* and *NRP1* gene expression in the stalk cells. This feedback loop is essential to maintain tip cell selection (Potente M. et al., 2011). *JAG1* ligand is present in the stalk cells and helps in maintaining differential Notch activity by inhibiting *DLL4* gene expression (Potente M. et al., 2011). Furthermore, *LRP1* has been proved to interact with Delta and Jag ligands, thus influencing and inhibiting tumour angiogenesis (Bian W. et al., 2021). PCR for all the above-mentioned genes did not show any significant changes in gene expression due to the functional suppression of ATF2 either in control or VEGF-stimulated conditions. The absence of change in gene expression could be due to the *NRARP* gene regulating the Notch signalling

pathway via a feedback loop (Lamar E, 2001). The *NRARP* gene is known to be activated by the Notch signalling pathway but in this paper, they demonstrate that an overexpression of *Nrarp* in *Xeopus* embryos, leads to a downregulation of notch target genes. Hence, it could be assumed that NRARP influences the gene expression of other angiogenic related genes in our *in vitro* conditions.

Apart from overexpressing a mutant form of the ATF2 protein, a parallel set of experiments was performed suppressing the expression of ATF2 in HUVEC cells by siRNA-mediated knockdown. Small interference RNA Non-target (siNT) transfected cells were used as a control. Under these conditions, expression of DLL4-target genes *HEY1*, *ID1* and *NRARP* remained unchanged whereas the *VEGFR1*, *VEGFR2* and *JAG1* gene expression were significantly increased. The difference in gene expression of the Notch ligands and other angiogenic related genes when the ATF2 mutant is overexpressed and when wild type ATF2 is knockdown could be due to various reasons which requires further investigation. One of my assumptions for the difference in the gene expression of angiogenic related genes as observed above was the action of ATF7, another member of the ATF family of transcription factors that recognise the same DNA binding domain as ATF2. Due to this fact, it is thought that ATF2 and ATF7 can play redundant functions (Breitwieser W et al 2007). When the *ATF2* gene is silenced by siRNA, there are no significant changes in the expression of the downstream targets of DLL4. However, overexpression of a mutant form of ATF2 resulted in increased expression of *HEY1* and *NRARP* genes. I decided to check the expression of the homologous variant, ATF7, in cells transfected with siRNA targeting ATF2. Figure 5.2 below shows that the small interference RNA targeting ATF2 does not affect the expression of ATF7. It can be hypothesised that ATF7 can compensate for

the absence of ATF2 in the experiments conducted using siRNA-mediated suppression, and hence no changes in the expression of *HEY1* and *NRARP* were observed. The ATF2(AA) mutant still maintains an intact DNA binding domain and thus it is expected to occupy the binding sites and block binding of both ATF2 and ATF7, thus causing changes in the expression of *HEY1* and *NRARP*. In the case of *DLL4*, same result can be observed using either ATF2(AA) or siRNA-mediated knockdown of ATF2 suggesting that there is no redundancy between ATF2 and ATF7 in the regulation of *DLL4* gene expression.

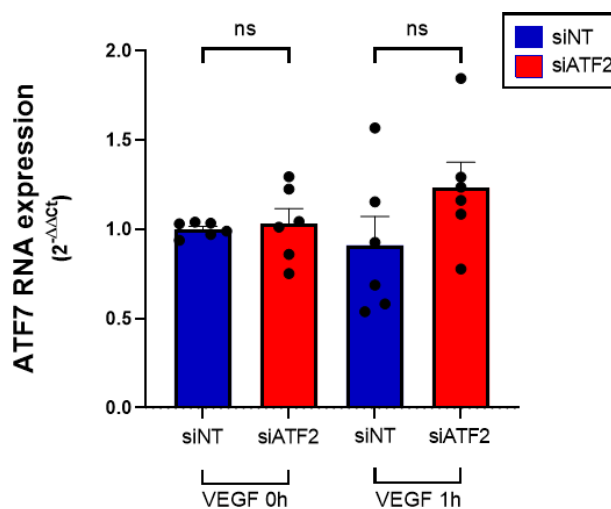


**Figure 5.2: Functional suppression of ATF2 results in no significant change in ATF7 mRNA abundance in either the control or VEGF stimulated conditions in endothelial cells.** HUVEC were transfected with small interference RNA for ATF2 protein (siATF2) or small interference RNA that does not target any genes (siINT). Transfected cells were left unstimulated (control) or stimulated with VEGF (25 ng/mL) for 1 hour. qPCR analysis of *ATF7* RNA expression is shown. Values are expressed using the  $2^{-\Delta\Delta C_t}$  method referred to unstimulated HUVEC transfected with siINT. Histograms represent mean  $\pm$  SEM (n=6). Differences in gene expression were evaluated using Two-Way ANOVA with Tukey's multiple comparisons post-hoc test. Ns = non-significant

Altogether, these results indicate that some genes are specifically regulated by ATF2, whereas others can be regulated by both ATF2 and ATF7 in a redundant manner. Concurrently, a double knockout mouse where ATF2 and ATF7 were deleted, led to the death of the mice embryo (Breitwieser W et al., 2007). A single deletion of *ATF2* resulted in post-natal death due to meconium aspiration syndrome (Maekawa T. et al., 1999) and single deletion of *ATF7* led to adult

animals with abnormal response to social stress (Maekawa T. et al., 2010). One of the genes identified as exclusively regulated by ATF2, and not ATF7, is *E-Selectin*. *In vivo* studies under LPS treated conditions indicate that in the mice containing a germline mutation of ATF2 gene produced decreased E-Selectin expression where the VCAM1 (lacking ATF2 binding site) gene expression was assessed as a control and was not affected (Reimold A.M. et al, 1996). This proves ATF2 to have a positive regulatory effect on an angiogenic related *E-Selectin* gene expression. To verify that the effect exerted by ATF2(AA) on the expression of DLL4 and its downstream targets was owing to the absence of functional ATF2 and not due to an artifact of the viral infection, a PCR was performed for the *E-Selectin* gene where the cells were infected with Ad-ATF2(AA). As expected in this case ATF2(AA) significantly attenuated *E-Selectin* gene expression (Figure 5.3) confirming the positive role of ATF2 on the expression of this gene.

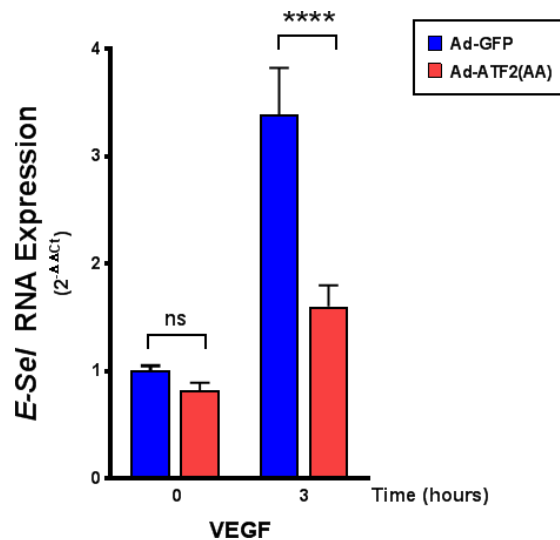


**Figure 5.3: Functional suppression of ATF2 leads to a decrease in *E-Selectin* mRNA abundance in VEGF stimulated conditions in endothelial cells.** HUVEC were infected with Adenovirus containing a mutated ATF2 protein (Ad-ATF2AA) or green fluorescence protein which will contain wild type ATF2 protein (Ad-GFP). Infected cells were left unstimulated (control) or stimulated with VEGF (25 ng/mL) for 3 hours. qPCR analysis of *E-Selectin* RNA expression is shown. Values are expressed using the  $2^{-\Delta\Delta C_t}$  method referred to unstimulated HUVEC infected with Ad- GFP. Histograms represent mean  $\pm$  SEM (n=9). Differences in gene expression were evaluated using Two-Way ANOVA with Tukey's multiple comparisons post-hoc test. \*\*\*\* $p < 0.0001$  indicates statistical significance when comparing cells transfected with Ad-GFP or Ad-ATF2AA and stimulated with VEGF for 3 hours. Ns = non-significant

Another aspect of this project was to increase the population of  $ATF2^{flox/flox}$  mice. As I have mentioned before, previous work by Toshio Maekawa (Maekawa T., 1999) to develop *ATF2*-deficient global knockout mice resulted in the death of the mice at birth due to meconium aspiration syndrome. Future work with the increased population of  $ATF2^{flox/flox}$  mice would be crossing the *ATF2* floxed mice with a tamoxifen inducible Cre recombinase mice (*Cdh5*(PAC)-CreERT2) where the Cre recombinase is controlled by the vascular endothelial cadherin promoter and hence can be activated only in endothelial cells. The tamoxifen can be administered after birth, thus creating endothelial-specific *ATF2* knockout mice which can be used as an *in vivo* model to study the effect of *ATF2* on angiogenesis. Unfortunately, restrictions on animal maintenance during COVID prevented the breeding of this colony, so this part of the project could not be completed.

## **6. CONCLUSIONS**

- ATF2 transcription factor has 12 putative binding sites on the regulatory regions of *DLL4*. These predicted binding sites are present either in -12 Kb enhancer, +14 Kb enhancer or on the *DLL4* promoter.
- ATF2 transcription factor has a negative regulatory effect on *DLL4* gene expression, both in the basal and VEGF stimulated conditions.
- The *DLL4*-target genes *HEY1* and *NRARP* were upregulated when a mutant ATF2 was overexpressed, but the expression of these downstream targets of *DLL4* remained unchanged when ATF2 was silenced by small interference RNA. This suggests that ATF2 and ATF7 have redundant functions in the expression of these genes.
- Upregulation of angiogenesis inhibitors *DLL4*, *HEY1* and *NRARP* in response to functional suppression of ATF2 might be one of the causes of the decrease in angiogenesis previously observed in cells lacking ATF2.
- Other genes related to angiogenesis like *JAG1*, *VEGFR1*, *VEGFR2* were differentially expressed depending on the functional suppression of ATF2 by siRNA or the overexpression of mutant ATF2(AA).

## REFERENCES

- Adam, M. G., Berger, C., Feldner, A., Yang, W. J., Wüstehube-Lausch, J., Herberich, S. E., Pinder, M., Gesierich, S., Hammes, H. P., Augustin, H. G., & Fischer, A. (2013). Synoptojanin-2 binding protein stabilizes the Notch ligands DLL1 and DLL4 and inhibits sprouting angiogenesis. *Circulation research*, *113*(11), 1206–1218.
- Adams, R. H., & Alitalo, K. (2007). Molecular regulation of angiogenesis and lymphangiogenesis. *Nature reviews. Molecular cell biology*, *8*(6), 464–478.
- Anversa, P., Cheng, W., Liu, Y., Leri, A., Redaelli, G., & Kajstura, J. (1998). Apoptosis and myocardial infarction. *Basic research in cardiology*, *93 Suppl 3*, 8–12.
- Armesilla, A. L., Lorenzo, E., Gómez del Arco, P., Martínez-Martínez, S., Alfranca, A., & Redondo, J. M. (1999). Vascular endothelial growth factor activates nuclear factor of activated T cells in human endothelial cells: a role for tissue factor gene expression. *Molecular and cellular biology*, *19*(3), 2032–2043.
- Arroyo, A. G., & Iruela-Arispe, M. L. (2010). Extracellular matrix, inflammation, and the angiogenic response. *Cardiovascular research*, *86*(2), 226–235.
- Baggott RR, Alfranca A, López-Maderuelo D, Mohamed TM, Escolano A, Oller J, Ornes BC, Kurusamy S, Rowther FB, Brown JE, Oceandy D, Cartwright EJ, Wang W, Gómez-del Arco P, Martínez-Martínez S, Neyses L, Redondo JM, Armesilla AL. Plasma membrane calcium ATPase isoform 4 inhibits vascular endothelial growth factor-mediated angiogenesis through interaction with calcineurin. *Arterioscler Thromb Vasc Biol*. 2014 Oct;*34*(10):2310-20.
- Bagri, A., Kouros-Mehr, H., Leong, K. G., & Plowman, G. D. (2010). Use of anti-VEGF adjuvant therapy in cancer: challenges and rationale. *Trends in molecular medicine*, *16*(3), 122–132.
- Bentley, K., Mariggi, G., Gerhardt, H., & Bates, P. A. (2009). Tipping the balance: robustness of tip cell selection, migration and fusion in angiogenesis. *PLoS computational biology*, *5*(10), e1000549.
- Bergers, G., & Hanahan, D. (2008). Modes of resistance to anti-angiogenic therapy. *Nature reviews. Cancer*, *8*(8), 592–603.
- Bian, W., Tang, M., Jiang, H., Xu, W., Hao, W., Sui, Y., Hou, Y., Nie, L., Zhang, H., Wang, C., Li, N., Wang, J., Qin, J., Wu, L., Ma, X., Chen, J., Wang, W., & Li, X. (2021). Low-density-lipoprotein-receptor-related protein 1 mediates Notch pathway activation. *Developmental cell*, *56*(20), 2902–2919.e8.
- Botrel, T., Clark, L., Paladini, L., & Clark, O. (2016). Efficacy and safety of

bevacizumab plus chemotherapy compared to chemotherapy alone in previously untreated advanced or metastatic colorectal cancer: a systematic review and meta-analysis. *BMC cancer*, 16(1), 677.

Breitwieser, W., Lyons, S., Flenniken, A. M., Ashton, G., Bruder, G., Willington, M., Lacaud, G., Kouskoff, V., & Jones, N. (2007). Feedback regulation of p38 activity via ATF2 is essential for survival of embryonic liver cells. *Genes & development*, 21(16), 2069–2082.

Butler, J. M., Kobayashi, H., & Rafii, S. (2010). Instructive role of the vascular niche in promoting tumour growth and tissue repair by angiocrine factors. *Nature reviews. Cancer*, 10(2), 138–146.

Carmeliet P. (2003). Angiogenesis in health and disease. *Nature medicine*, 9(6), 653–660.

Carmeliet, P., & Jain, R. K. (2011). Molecular mechanisms and clinical applications of angiogenesis. *Nature*, 473(7347), 298–307.

Casanovas, O., Hicklin, D. J., Bergers, G., & Hanahan, D. (2005). Drug resistance by evasion of antiangiogenic targeting of VEGF signaling in late-stage pancreatic islet tumors. *Cancer cell*, 8(4), 299–309.

Cascone, T., Herynk, M. H., Xu, L., Du, Z., Kadara, H., Nilsson, M. B., Oborn, C. J., Park, Y. Y., Erez, B., Jacoby, J. J., Lee, J. S., Lin, H. Y., Ciardiello, F., Herbst, R. S., Langley, R. R., & Heymach, J. V. (2011). Upregulated stromal EGFR and vascular remodeling in mouse xenograft models of angiogenesis inhibitor-resistant human lung adenocarcinoma. *The Journal of clinical investigation*, 121(4), 1313–1328.

Cébe-Suarez, S., Zehnder-Fjällman, A., & Ballmer-Hofer, K. (2006). The role of VEGF receptors in angiogenesis; complex partnerships. *Cellular and molecular life sciences : CMLS*, 63(5), 601–615.

Chappell, J. C., & Bautch, V. L. (2010). Vascular development: genetic mechanisms and links to vascular disease. *Current topics in developmental biology*, 90, 43–72.

Claesson-Welsh, L., & Welsh, M. (2013). VEGFA and tumour angiogenesis. *Journal of internal medicine*, 273(2), 114–127.

Crawford, Y., & Ferrara, N. (2009). VEGF inhibition: insights from preclinical and clinical studies. *Cell and tissue research*, 335(1), 261–269.

De Smet, F., Segura, I., De Bock, K., Hohensinner, P. J., & Carmeliet, P. (2009). Mechanisms of vessel branching: filopodia on endothelial tip cells lead the way. *Arteriosclerosis, thrombosis, and vascular biology*, 29(5), 639–649.

Desch, M., Hackmayer, G., & Todorov, V. T. (2012). Identification of ATF2 as a

transcriptional regulator of renin gene. *Biological chemistry*, 393(1-2), 93–100.

Eble, J. A., & Niland, S. (2009). The extracellular matrix of blood vessels. *Current pharmaceutical design*, 15(12), 1385–1400.

Ebos, J. M., & Kerbel, R. S. (2011). Antiangiogenic therapy: impact on invasion, disease progression, and metastasis. *Nature reviews. Clinical oncology*, 8(4), 210–221.

Fearnley, G. W., Odell, A. F., Latham, A. M., Mughal, N. A., Bruns, A. F., Burgoyne, N. J., Homer-Vanniasinkam, S., Zachary, I. C., Hollstein, M. C., Wheatcroft, S. B., & Ponnambalam, S. (2014). VEGF-A isoforms differentially regulate ATF-2-dependent VCAM-1 gene expression and endothelial-leukocyte interactions. *Molecular biology of the cell*, 25(16), 2509–2521.

Ferrara N. (2010). Pathways mediating VEGF-independent tumor angiogenesis. *Cytokine & growth factor reviews*, 21(1), 21–26.

Ferrara, N., Carver-Moore, K., Chen, H., Dowd, M., Lu, L., O'Shea, K. S., Powell-Braxton, L., Hillan, K. J., & Moore, M. W. (1996). Heterozygous embryonic lethality induced by targeted inactivation of the VEGF gene. *Nature*, 380(6573), 439–442.

Ferrara, N., Gerber, H. P., & LeCouter, J. (2003). The biology of VEGF and its receptors. *Nature medicine*, 9(6), 669–676.

Fischer, A., Schumacher, N., Maier, M., Sendtner, M., & Gessler, M. (2004). The Notch target genes *Hey1* and *Hey2* are required for embryonic vascular development. *Genes & development*, 18(8), 901–911.

Fischer, C., Mazzone, M., Jonckx, B., & Carmeliet, P. (2008). FLT1 and its ligands VEGFB and PlGF: drug targets for anti-angiogenic therapy?. *Nature reviews. Cancer*, 8(12), 942–956.

Forster, J. C., Harriss-Phillips, W. M., Douglass, M. J., & Bezak, E. (2017). A review of the development of tumor vasculature and its effects on the tumor microenvironment. *Hypoxia (Auckland, N.Z.)*, 5, 21–32.

Fraisl, P., Mazzone, M., Schmidt, T., & Carmeliet, P. (2009). Regulation of angiogenesis by oxygen and metabolism. *Developmental cell*, 16(2), 167–179.

Gozdecka, M., Lyons, S., Kondo, S., Taylor, J., Li, Y., Walczynski, J., Thiel, G., Breitwieser, W., & Jones, N. (2014). JNK suppresses tumor formation via a gene-expression program mediated by ATF2. *Cell reports*, 9(4), 1361–1374.

Gridelli, C., Maione, P., Del Gaizo, F., Colantuoni, G., Guerriero, C., Ferrara, C., Nicoletta, D., Comunale, D., De Vita, A., & Rossi, A. (2007). Sorafenib and sunitinib in the treatment of advanced non-small cell lung cancer. *The oncologist*, 12(2), 191–

200.

Harper, S. J., & Bates, D. O. (2008). VEGF-A splicing: the key to anti-angiogenic therapeutics?. *Nature reviews. Cancer*, *8*(11), 880–887.

Harris, V. K., Coticchia, C. M., Kagan, B. L., Ahmad, S., Wellstein, A., & Riegel, A. T. (2000). Induction of the angiogenic modulator fibroblast growth factor-binding protein by epidermal growth factor is mediated through both MEK/ERK and p38 signal transduction pathways. *The Journal of biological chemistry*, *275*(15), 10802–10811.

Herbert, S. P., & Stainier, D. Y. (2011). Molecular control of endothelial cell behaviour during blood vessel morphogenesis. *Nature reviews. Molecular cell biology*, *12*(9), 551–564.

Herbert, S. P., Huisken, J., Kim, T. N., Feldman, M. E., Houseman, B. T., Wang, R. A., Shokat, K. M., & Stainier, D. Y. (2009). Arterial-venous segregation by selective cell sprouting: an alternative mode of blood vessel formation. *Science (New York, N.Y.)*, *326*(5950), 294–298.

Howe, G. A., Kazda, K., & Addison, C. L. (2017). MicroRNA-30b controls endothelial cell capillary morphogenesis through regulation of transforming growth factor beta 2. *PloS one*, *12*(10), e0185619.

Hsu, C. C., & Hu, C. D. (2012). Critical role of N-terminal end-localized nuclear export signal in regulation of activating transcription factor 2 (ATF2) subcellular localization and transcriptional activity. *The Journal of biological chemistry*, *287*(11), 8621–8632.

Huang, H., Bhat, A., Woodnutt, G., & Lappe, R. (2010). Targeting the ANGPT-TIE2 pathway in malignancy. *Nature reviews. Cancer*, *10*(8), 575–585.

Huang, Z., & Bao, S. D. (2004). Roles of main pro- and anti-angiogenic factors in tumor angiogenesis. *World journal of gastroenterology*, *10*(4), 463–470.

Iruela-Arispe, M. L., & Davis, G. E. (2009). Cellular and molecular mechanisms of vascular lumen formation. *Developmental cell*, *16*(2), 222–231.

Jacobs J. (2007). Combating cardiovascular disease with angiogenic therapy. *Drug discovery today*, *12*(23-24), 1040–1045.

Jain R. K. (2003). Molecular regulation of vessel maturation. *Nature medicine*, *9*(6), 685–693.

Jin, C., Li, H., Murata, T., Sun, K., Horikoshi, M., Chiu, R., & Yokoyama, K. K. (2002). JDP2, a repressor of AP-1, recruits a histone deacetylase 3 complex to inhibit the retinoic acid-induced differentiation of F9 cells. *Molecular and cellular biology*, *22*(13), 4815–4826.

Kim, S. J., Wagner, S., Liu, F., O'Reilly, M. A., Robbins, P. D., & Green, M. R. (1992).

Retinoblastoma gene product activates expression of the human TGF-beta 2 gene through transcription factor ATF-2. *Nature*, 358(6384), 331–334.

Koerselman, J., van der Graaf, Y., de Jaegere, P. P., & Grobbee, D. E. (2003). Coronary collaterals: an important and underexposed aspect of coronary artery disease. *Circulation*, 107(19), 2507–2511.

Krebs, L. T., Shutter, J. R., Tanigaki, K., Honjo, T., Stark, K. L., & Gridley, T. (2004). Haploinsufficient lethality and formation of arteriovenous malformations in Notch pathway mutants. *Genes & development*, 18(20), 2469–2473.

Kuhnert, F., Kirshner, J. R., & Thurston, G. (2011). Dll4-Notch signaling as a therapeutic target in tumor angiogenesis. *Vascular cell*, 3(1), 20.

Lamar, E., Deblandre, G., Wettstein, D., Gawantka, V., Pollet, N., Niehrs, C., & Kintner, C. (2001). Nrarp is a novel intracellular component of the Notch signaling pathway. *Genes & development*, 15(15), 1885–1899.

Lau, E., & Ronai, Z. A. (2012). ATF2 - at the crossroad of nuclear and cytosolic functions. *Journal of cell science*, 125(Pt 12), 2815–2824.

Lau, E., Kluger, H., Varsano, T., Lee, K., Scheffler, I., Rimm, D. L., Ideker, T., & Ronai, Z. A. (2012). PKC $\epsilon$  promotes oncogenic functions of ATF2 in the nucleus while blocking its apoptotic function at mitochondria. *Cell*, 148(3), 543–555.

Lau, E., Sedy, J., Sander, C., Shaw, M. A., Feng, Y., Scortegagna, M., Claps, G., Robinson, S., Cheng, P., Srivas, R., Soonthornvacharin, S., Ideker, T., Bosenberg, M., Gonzalez, R., Robinson, W., Chanda, S. K., Ware, C., Dummer, R., Hoon, D., Kirkwood, J. M., ... Ronai, Z. A. (2015). Transcriptional repression of IFN $\beta$ 1 by ATF2 confers melanoma resistance to therapy. *Oncogene*, 34(46), 5739–5748.

Liu, C. H., Wang, Z., Sun, Y., & Chen, J. (2017). Animal models of ocular angiogenesis: from development to pathologies. *FASEB journal : official publication of the Federation of American Societies for Experimental Biology*, 31(11), 4665–4681.

Lugano, R., Ramachandran, M., & Dimberg, A. (2020). Tumor angiogenesis: causes, consequences, challenges and opportunities. *Cellular and molecular life sciences : CMLS*, 77(9), 1745–1770. <https://doi.org/10.1007/s00018-019-03351-7>

Maekawa, T., Bernier, F., Sato, M., Nomura, S., Singh, M., Inoue, Y., Tokunaga, T., Imai, H., Yokoyama, M., Reimold, A., Glimcher, L. H., & Ishii, S. (1999). Mouse ATF-2 null mutants display features of a severe type of meconium aspiration syndrome. *The Journal of biological chemistry*, 274(25), 17813–17819.

Maekawa, T., Kim, S., Nakai, D., Makino, C., Takagi, T., Ogura, H., Yamada, K., Chatton, B., & Ishii, S. (2010). Social isolation stress induces ATF-7 phosphorylation

and impairs silencing of the 5-HT 5B receptor gene. *The EMBO journal*, 29(1), 196–208.

Melincovici, C. S., Boşca, A. B., Şuşman, S., Mărginean, M., Mişu, C., Istrate, M., Moldovan, I. M., Roman, A. L., & Mişu, C. M. (2018). Vascular endothelial growth factor (VEGF) - key factor in normal and pathological angiogenesis. *Romanian journal of morphology and embryology = Revue roumaine de morphologie et embryologie*, 59(2), 455–467.

Miles, D., Harbeck, N., Escudier, B., Hurwitz, H., Saltz, L., Van Cutsem, E., Cassidy, J., Mueller, B., & Sirzén, F. (2011). Disease course patterns after discontinuation of bevacizumab: pooled analysis of randomized phase III trials. *Journal of clinical oncology : official journal of the American Society of Clinical Oncology*, 29(1), 83–88.

Noguera-Troise, I., Daly, C., Papadopoulos, N. J., Coetzee, S., Boland, P., Gale, N. W., Lin, H. C., Yancopoulos, G. D., & Thurston, G. (2006). Blockade of DLL4 inhibits tumour growth by promoting non-productive angiogenesis. *Nature*, 444(7122), 1032–1037.

Oh, I. Y., Yoon, C. H., Hur, J., Kim, J. H., Kim, T. Y., Lee, C. S., Park, K. W., Chae, I. H., Oh, B. H., Park, Y. B., & Kim, H. S. (2007). Involvement of E-selectin in recruitment of endothelial progenitor cells and angiogenesis in ischemic muscle. *Blood*, 110(12), 3891–3899.

Olivetti, G., Quaini, F., Sala, R., Lagrasta, C., Corradi, D., Bonacina, E., Gambert, S. R., Cigola, E., & Anversa, P. (1996). Acute myocardial infarction in humans is associated with activation of programmed myocyte cell death in the surviving portion of the heart. *Journal of molecular and cellular cardiology*, 28(9), 2005–2016.

Ouwens, D. M., de Ruiter, N. D., van der Zon, G. C., Carter, A. P., Schouten, J., van der Burgt, C., Kooistra, K., Bos, J. L., Maassen, J. A., & van Dam, H. (2002). Growth factors can activate ATF2 via a two-step mechanism: phosphorylation of Thr71 through the Ras-MEK-ERK pathway and of Thr69 through RalGDS-Src-p38. *The EMBO journal*, 21(14), 3782–3793.

Pandya, N. M., Dhalla, N. S., & Santani, D. D. (2006). Angiogenesis--a new target for future therapy. *Vascular pharmacology*, 44(5), 265–274.

Papavassiliou, A. G., Treier, M., & Bohmann, D. (1995). Intramolecular signal transduction in c-Jun. *The EMBO journal*, 14(9), 2014–2019.

Penix, L. A., Sweetser, M. T., Weaver, W. M., Hoeffler, J. P., Kerppola, T. K., & Wilson, C. B. (1996). The proximal regulatory element of the interferon-gamma promoter mediates selective expression in T cells. *The Journal of biological*

*chemistry*, 271(50), 31964–31972.

Phng, L. K., Potente, M., Leslie, J. D., Babbage, J., Nyqvist, D., Lobov, I., Ondr, J. K., Rao, S., Lang, R. A., Thurston, G., & Gerhardt, H. (2009). Nrarp coordinates endothelial Notch and Wnt signaling to control vessel density in angiogenesis. *Developmental cell*, 16(1), 70–82.

Potente, M., Gerhardt, H., & Carmeliet, P. (2011). Basic and therapeutic aspects of angiogenesis. *Cell*, 146(6), 873–887.

Quintero-Fabián, S., Arreola, R., Becerril-Villanueva, E., Torres-Romero, J. C., Arana-Argáez, V., Lara-Riegos, J., Ramírez-Camacho, M. A., & Alvarez-Sánchez, M. E. (2019). Role of Matrix Metalloproteinases in Angiogenesis and Cancer. *Frontiers in oncology*, 9, 1370.

Rajabi, M., & Mousa, S. A. (2017). The Role of Angiogenesis in Cancer Treatment. *Biomedicines*, 5(2), 34.

Rao, A., Luo, C., & Hogan, P. G. (1997). Transcription factors of the NFAT family: regulation and function. *Annual review of immunology*, 15, 707–747.

Read, M. A., Whitley, M. Z., Gupta, S., Pierce, J. W., Best, J., Davis, R. J., & Collins, T. (1997). Tumor necrosis factor alpha-induced E-selectin expression is activated by the nuclear factor-kappaB and c-JUN N-terminal kinase/p38 mitogen-activated protein kinase pathways. *The Journal of biological chemistry*, 272(5), 2753–2761.

Reimold, A. M., Grusby, M. J., Kosaras, B., Fries, J. W., Mori, R., Maniwa, S., Clauss, I. M., Collins, T., Sidman, R. L., Glimcher, M. J., & Glimcher, L. H. (1996). Chondrodysplasia and neurological abnormalities in ATF-2-deficient mice. *Nature*, 379(6562), 262–265.

Ridgway, J., Zhang, G., Wu, Y., Stawicki, S., Liang, W. C., Chantry, Y., Kowalski, J., Watts, R. J., Callahan, C., Kasman, I., Singh, M., Chien, M., Tan, C., Hongo, J. A., de Sauvage, F., Plowman, G., & Yan, M. (2006). Inhibition of DLL4 signalling inhibits tumour growth by deregulating angiogenesis. *Nature*, 444(7122), 1083–1087.

Rostama, B., Turner, J. E., Seavey, G. T., Norton, C. R., Gridley, T., Vary, C. P., & Liaw, L. (2015). DLL4/Notch1 and BMP9 Interdependent Signaling Induces Human Endothelial Cell Quiescence via P27KIP1 and Thrombospondin-1. *Arteriosclerosis, thrombosis, and vascular biology*, 35(12), 2626–2637.

Sacilotto, N., Monteiro, R., Fritzsche, M., Becker, P. W., Sanchez-Del-Campo, L., Liu, K., Pinheiro, P., Ratnayaka, I., Davies, B., Goding, C. R., Patient, R., Bou-Gharios, G., & De Val, S. (2013). Analysis of DLL4 regulation reveals a combinatorial role for Sox and Notch in arterial development. *Proceedings of the National Academy of Sciences of the United States of America*, 110(29), 11893–11898.

- Sanalkumar, R., Indulekha, C. L., Divya, T. S., Divya, M. S., Anto, R. J., Vinod, B., Vidyanand, S., Jagatha, B., Venugopal, S., & James, J. (2010). ATF2 maintains a subset of neural progenitors through CBF1/Notch independent Hes-1 expression and synergistically activates the expression of Hes-1 in Notch-dependent neural progenitors. *Journal of neurochemistry*, *113*(4), 807–818.
- Sato, N., Nariuchi, H., Tsuruoka, N., Nishihara, T., Beitz, J. G., Calabresi, P., & Frackelton, A. R., Jr (1990). Actions of TNF and IFN-gamma on angiogenesis in vitro. *The Journal of investigative dermatology*, *95*(6 Suppl), 85S–89S.
- Shah, A. V., Birdsey, G. M., Peghaire, C., Pitulescu, M. E., Duffon, N. P., Yang, Y., Weinberg, I., Osuna Almagro, L., Payne, L., Mason, J. C., Gerhardt, H., Adams, R. H., & Randi, A. M. (2017). The endothelial transcription factor ERG mediates Angiopoietin-1-dependent control of Notch signalling and vascular stability. *Nature communications*, *8*, 16002.
- Shibuya M. (2011). Vascular Endothelial Growth Factor (VEGF) and Its Receptor (VEGFR) Signaling in Angiogenesis: A Crucial Target for Anti- and Pro-Angiogenic Therapies. *Genes & cancer*, *2*(12), 1097–1105.
- Shojaei, F., Lee, J. H., Simmons, B. H., Wong, A., Esparza, C. O., Plumlee, P. A., Feng, J., Stewart, A. E., Hu-Lowe, D. D., & Christensen, J. G. (2010). HGF/c-Met acts as an alternative angiogenic pathway in sunitinib-resistant tumors. *Cancer research*, *70*(24), 10090–10100.
- Song, H., Ki, S. H., Kim, S. G., & Moon, A. (2006). Activating transcription factor 2 mediates matrix metalloproteinase-2 transcriptional activation induced by p38 in breast epithelial cells. *Cancer research*, *66*(21), 10487–10496.
- Steinmüller, L., & Thiel, G. (2003). Regulation of gene transcription by a constitutively active mutant of activating transcription factor 2 (ATF2). *Biological chemistry*, *384*(4), 667–672.
- Strickland, D. K., & Muratoglu, S. C. (2016). LRP in Endothelial Cells: A Little Goes a Long Way. *Arteriosclerosis, thrombosis, and vascular biology*, *36*(2), 213–216.
- Sutton, M. G., & Sharpe, N. (2000). Left ventricular remodeling after myocardial infarction: pathophysiology and therapy. *Circulation*, *101*(25), 2981–2988.
- Takahashi, H., & Shibuya, M. (2005). The vascular endothelial growth factor (VEGF)/VEGF receptor system and its role under physiological and pathological conditions. *Clinical science (London, England : 1979)*, *109*(3), 227–241.
- Thiagarajan, H., Thiyagamoorthy, U., Shanmugham, I., Dharmalingam Nandagopal, G., & Kaliyaperumal, A. (2017). Angiogenic growth factors in myocardial infarction: a critical appraisal. *Heart failure reviews*, *22*(6), 665–683.

- van Dam, H., & Castellazzi, M. (2001). Distinct roles of Jun : Fos and Jun : ATF dimers in oncogenesis. *Oncogene*, *20*(19), 2453–2464.
- Vasudev, N. S., & Reynolds, A. R. (2014). Anti-angiogenic therapy for cancer: current progress, unresolved questions and future directions. *Angiogenesis*, *17*(3), 471–494.
- Volpert, O. V., Pili, R., Sikder, H. A., Nelius, T., Zaichuk, T., Morris, C., Shiflett, C. B., Devlin, M. K., Conant, K., & Alani, R. M. (2002). Id1 regulates angiogenesis through transcriptional repression of thrombospondin-1. *Cancer cell*, *2*(6), 473–483.
- Watson, G., Ronai, Z. A., & Lau, E. (2017). ATF2, a paradigm of the multifaceted regulation of transcription factors in biology and disease. *Pharmacological research*, *119*, 347–357.
- Weerkamp, F., Luis, T. C., Naber, B. A., Koster, E. E., Jeannotte, L., van Dongen, J. J., & Staal, F. J. (2006). Identification of Notch target genes in uncommitted T-cell progenitors: No direct induction of a T-cell specific gene program. *Leukemia*, *20*(11), 1967–1977.
- Xiao, L., Rao, J. N., Zou, T., Liu, L., Yu, T. X., Zhu, X. Y., Donahue, J. M., & Wang, J. Y. (2010). Induced ATF-2 represses CDK4 transcription through dimerization with JunD inhibiting intestinal epithelial cell growth after polyamine depletion. *American journal of physiology. Cell physiology*, *298*(5), C1226–C1234.
- Xu, L., Kanasaki, K., Kitada, M., & Koya, D. (2012). Diabetic angiopathy and angiogenic defects. *Fibrogenesis & tissue repair*, *5*(1), 13.
- Yamasaki, T., Takahashi, A., Pan, J., Yamaguchi, N., & Yokoyama, K. K. (2009). Phosphorylation of Activation Transcription Factor-2 at Serine 121 by Protein Kinase C Controls c-Jun-mediated Activation of Transcription. *The Journal of biological chemistry*, *284*(13), 8567–8581.
- Ylä-Herttua, S., Bridges, C., Katz, M. G., & Korpisalo, P. (2017). Angiogenic gene therapy in cardiovascular diseases: dream or vision?. *European heart journal*, *38*(18), 1365–1371.
- Zachary, I., & Morgan, R. D. (2011). Therapeutic angiogenesis for cardiovascular disease: biological context, challenges, prospects. *Heart (British Cardiac Society)*, *97*(3), 181–189.
- Zhang, J. Y., Jiang, H., Gao, W., Wu, J., Peng, K., Shi, Y. F., & Zhang, X. J. (2008). The JNK/AP1/ATF2 pathway is involved in H<sub>2</sub>O<sub>2</sub>-induced acetylcholinesterase expression during apoptosis. *Cellular and molecular life sciences : CMLS*, *65*(9), 1435–1445.